Princeton's Net-Zero America study

Annex B: Sensitivity of transition modeling results to input assumptions

Chuan Zhang, Eric Larson, Jesse Jenkins, Chris Greig, and Joshua Drossman
Andlinger Center for Energy and the Environment, Princeton University

20 August 2021

Contents

1 Introduction

One drawback of large-scale forward-looking energy system models like RIO, the energy-supply optimization model used in the Net Zero America study, lies in the representation of uncertainty. In particular, multi-decade projections for virtually every input variable (e.g. resource availability, technology costs and performance, fuel prices, inflation and costs of capital) carry significant uncertainties and no amount of analysis, *ex ante*, can eliminate these. To help address this shortcoming, this annex presents results of parametric sensitivity analyses around key RIO inputs. A total of 55 sensitivity cases are reported and discussed here. Table B1 groups these by general input category, e.g., natural gas prices or power generation capital costs, and summarizes the quantitative changes made in input values for each run. Shorthand case names in the table ending with "+" generally indicate that the sensitivity is with a higher value for the particular variable being investigated, while those ending with "-" generally indicate a lower value for the variable being investigated.

The sensitivity cases address many key uncertainties, but we readily acknowledge that the analysis is not comprehensive, and there are intrinsic shortcomings with such single-factor uncertainty analysis [1]. We also note that the sensitivity results shown here are from modeling at coarse geographic resolution (14 regions for the continental U.S.), and so provide high-level insights. Higher-resolution geospatial insights can be inferred from the sensitivity results but have not been quantified through downscaling of the sort detailed in the main Net-Zero America report. Taken as a whole, the sensitivity analysis provides some important insights regarding the robustness of conclusions drawn from the five net-zero scenarios detailed in our main report.

2 Orientation to sensitivity case results

2.1 Guide to sensitivity results

For each of the 14 groupings of sensitivity runs shown in Table B1, we report modeling results below in a set of graphs that give key insights into the impacts of different input assumptions. A core set of seven graphs showing aggregate national results are included for each set of sensitivities. In most cases, these seven are sufficient to show the most important changes (or lack of changes in some cases) resulting from different input assumptions. The core set of graphics are:

1. Net present value (billion 2018$) of the sum of annualized energy-supply system costs from 2020 – 2050. This is the objective function that the RIO model minimizes to find the energy-supply technology and resource mix that meets final-energy demands in each net zero pathway. Note that these represent energy-supply costs, but exclude costs of delivering energy, e.g., costs for distribution of electricity and of pipeline gas. These energy delivery costs, as well as all energy demand costs such as for vehicles or appliances, are calculated separately by the EnergyPathways model, as discussed in Annex A [2].
2. Annual electricity load (TWh/y) from 2020 to 2050. The load consists of 4 additive components: 1) final-electricity used across all sectors – the bulk of the load in most cases, 2) electricity used in industrial boilers that have hourly operating flexibility such that they run during hours when electricity-derived steam generation is less costly than fuel-fired steam generation, 3) electricity used for electrolysis units that similarly operate with hourly flexibility so that they produce hydrogen only when the cost of electricity is sufficiently low

to justify this, and 4) electricity used by direct air capture (DAC) units that are assumed to be able to operate with daily (not hourly) flexibility.
3. Annual electricity generation (TWh/y) by technology from 2020 to 2050.
4. Annual electricity generating capacity (GW) in place by technology from 2020 to 2050.
5. Average annual rate of capacity additions (GW/y) for wind and solar generators during each 5-year period from 2020 to 2050.
6. Average annual rate of capacity additions (GW/y) for thermal electricity generators during each 5-year period.
7. Snapshot of 2050 flows of H_2 (EJ/y), CO_2 (million tonnes/y), and biomass (EJ/y), including a) H_2 production and utilization by technology, b) amount of CO_2 captured by technology, utilized by technology, and geologically sequestered, and c) amount of biomass used by conversion technology.

For certain sensitivity groups, we include a few additional relevant graphics to supplement the core set. The additional graphics include

8. Annual CO_2 emissions (Gt/y) by fossil fuel source from 2020 to 2050, annual CO_2 sequestered underground (Gt/y), and the resulting annual net CO_2 emissions from the energy/industrial system.
9. Annual total inter-regional high-voltage electricity transmission capacity (GW) from 2020 to 2050. This is qualitatively indicative of the directional change in total high-voltage transmission capacity needed with changes in input assumptions, but does not correspond directly with the detailed quantitative transmission capacity estimates for the E+, E+RE-, and E+RE+ pathways described in the main Net Zero America study report because the downscaling analysis used a different approach to estimating transmission requirements.
10. Annual final-demand for fuel blends (EJ/y) by type of blend from 2020 to 2050. The RIO model allows for liquid and gaseous fuels and feedstocks to be made up of blends of fuels coming from different sources. For example, the "jet fuel blend" may include both petroleum-derived jet fuel and jet-fuel-equivalent synthesized by Fischer-Tropsch processing of H_2 and CO_2. This graphic shows both the total amount of each of eight blends and the distribution by source of the different components of each blend.
11. Average annual marginal fuel prices (2018 $/GJ) from 2020 to 2050 for the following fuel blends: diesel, pipeline gas, and hydrogen. These prices represent the cost of supplying one more unit of fuel. In the case of diesel and pipeline gas, the 2020 price is simply the price for petroleum-derived diesel and for natural gas as projected in the 2019 Annual Energy Outlook. In subsequent years, the price reflects either the cost of producing a zero-carbon drop-in replacement for fossil or of offsetting the carbon released from the fossil fuel when burned.

To facilitate comparisons, the graphics presented in this document show results from the sensitivity cases alongside the results for the corresponding original core net-zero scenario; 48 of the 55 sensitivity cases have been run to test input assumptions for the E+ scenario. The observant reader may note that results shown for the original core scenario in some of the graphics do not exactly match results shown for that scenario in the main Net-Zero America report. In particular, one may note differences in outputs relating to solar and wind generating capacity. These differences are generally small, and in any case do not qualitatively change

conclusions. The reason for these differences relates to the day binning method used in RIO, as explained in the following section.

Table B1. Modeling runs to test sensitivity of Net-Zero America study results to key input assumptions. Illustrative values for capital costs for fuels production technologies in this table are per kW_{HHV} of production capacity.

Group	Case no.	Shorthand name	Description of input changes
A. Land & non-CO_2 emissions	1	E+ Land+	Higher net (land sink + non-CO_2) emissions (2050 CO_2 emission cap for energy/industry changes from -0.17 to 0.27 Gt)
	2	E+ Land-	Lower net (land sink + non-CO_2) emissions (2050 CO_2 emission cap for energy/industry changes from -0.17 to -0.73 Gt)
B. Natural gas prices	3	E+ Gas+	Higher NG prices [AEO2020 'low oil and gas supply' case (e.g., 2050 Texas NG price changes from 3.53 to 6.56 USD/MMBtu)]
	4	E+ Gas-	Lower NG prices [AEO2020 'high oil and gas supply' case (e.g., 2050 Texas NG price changes from 3.53 to 2.54 USD/MMBtu)]
C. Power sector capital costs (non-nuclear)	5	E+ NGCC+	Higher NGCC-CCS capex (2050 capex changes from 1725 to 2589 $/kW)
	6	E+ NGCC-	Lower NGCC-CCS capex (2050 capex change from 1725 to 1380 $/kW)
	7	E+ Solar_Wind+	Higher solar/wind capex (e.g., 2050 NJ onshore wind TRG1 goes from 1723 to 2280 $/kW; PV TRG1 from 869 to 1144 $/kW)
	8	E+ Solar_Wind-	Lower solar/wind capex (e.g., 2050 NJ onshore wind TRG1 goes from 1723 to 1433 $/kW, PV TRG1 from 869 to 453 $/kW)
	9	E+ Trans+	Higher transmission cost (e.g., 2050 Mid-Atlantic<-->New York transmission cost doubles to 5642 $/kW)
D. Nuclear power capital costs and build rates	10	E+ Nu+	Higher nuclear capex (2050 capex changes from 5530 to 8295 $/kW)
	11	E+ Nu-	Lower nuclear capex (2050 capex changes from 5530 to 4423 $/kW)
	12	E+ NuRate-	E+ with constrained nuclear capacity built rate (10GW/year maximum from 2030)
	13	E+ Nu--	E+ with lowest nuclear capex (2050 capex changes from 5530 to 1800 $/kW)
	14	E+ Nu--Rate-	E+ with lowest nuclear capex (2050 capex 1800 $/kW) & constrained nuclear capacity built rate (10GW/y maximum from 2030)
	15	E+RE-NuRate-	E+RE- with constrained nuclear capacity built rate (10GW/year maximum from 2030)
	16	E+RE-Nu--	E+RE- with lowest nuclear capex (2050 capex 1800$/kW)
	17	E+RE-Nu--Rate--	E+RE- with lowest nuclear capex (2050 capex 1800$/kW) & most constrained nuclear built rate (0.36GW/y in 2025, 8GW/y in 2050)
E. Wind and transmission build rates	18	E+ TrRate-	Higher transmission capacity constraint (e.g. 2050 Mid-Atlantic<-->New York capacity limit 3830 MW instead of 19145 MW)
	19	E+ Wind-	GW wind installed capacity limits in 2050 (% of E+ capacity): onshore 50%; offshore-wind 100%, except 70% in Mid-Atlantic
	20	E+ Tr&Wind-	Constrained wind build rate + constrained transmission build rate (combines sensitivities 18 and 19)
F. H_2 turbines	21	E+ H2Turbine	Added constraint of only 100% H_2-firing of GTs allowed starting 2035.
G. Flexible load technologies	22	E+ EVflex0	No time shifting of EV charging or water heating loads
	23	E+ EVflex+	Increased flexibility in time-shifting loads (100% of EV load can shift; 40% of heat load can shift)
	24	E+ No Electrolysis	Disallows electrolysis, one of the hourly flexible loads
	25	E+ No Electrolysis No E-boiler	Disallows electrolysis and electric boilers, the two hourly flexible load technology options
	26	E+ Electrolysis-	Lower electrolysis capital costs (reaching 220$/kW in 2050)
	27	E+ Electroysis--	Lowest electrolysis capital costs (reaching 96$/kW in 2050)
H. Hydrogen production capital costs	28	E+ NoBioH_2	BECCS-H_2 technology not allowed
	29	E+ BioH_2+	Higher capex for bioconversion to H_2 with carbon capture (4050 $/kW in 2050 instead of 2700 $/kW)
	30	E+ BioH_2-	Lower capex for bioconversion to H_2 with carbon capture (2160 $/kW in 2050 instead of 2700 $/kW)
	31	E+ ATR+	Higher capex for ATR and SMR (both w/CCS) (from 814 to 1221 $/kW for ATR in 2050 and 826 to 1239 $/kW for SMR)
	32	E+ ATR-	Lower capex for ATR & SMR (both with CCS) (ATR: 814 → 651 $/kW in 2050; SMR: 826 → 660 $/kW)
I. Fuels production capital costs	33	E+ FTS+	Higher FTS/SNG capex (2050 SNG changes from 1155 to 1732 $/kW, FTS changes from 952 to 1428 $/kW)
	34	E+ FTS-	Lower FTS/SNG capex (2050 SNG changes from 1155 to 924 $/kW, FTS changes from 952 to 761 $/kW)
	35	E+ BioFT+	Higher biomass FT w/ccs capex (2050 capex changes from 3962 $/kW to 5948 $/kW)
	36	E+ BioFT-	Lower biomass FT w/ccs capex (2050 capex changes from 3962 $/kW to 3172 $/kW)
J. Direct air capture	37	E+ DAC-	Lower DAC capex (from $2,164 to $694 per tCO2/year, 2016$)
	38	E+ DAC eff+	Higher DAC electric efficiency (1 instead of 2 MWh/tCO2)
	39	E+ DAC- eff+	Lower DAC capex and higher efficiency (combines sensitivities 37 and 38)
K. Higher energy efficiency	40	E+ VMT-	15% lower VMT for light duty vehicles (cars/trucks) by 2050
	41	E+ Ieff+	3% per year increase in industrial output ($) per unit energy input (instead of 1.9% per year)
	42	E+ Beff+	1% per year building heating and cooling energy reduction due to greater shell efficiency improvements
	43	E+ EFF+	Combination of sensitivities 40, 41, and 42 (results in 2050 final energy demand ~25% below E+ level)

L. No new biomass	44	E+ B-	E+ but no additional lignocellulosic biomass beyond today's level
	45	E+ RE- B-	E+ RE- but no additional lignocellulosic biomass beyond today's level
M. High biomass supply	46	E+ B+	E+ RE+ with high biomass supply (24EJ per year from 13EJ per year)
	47	E- B+	E- with high biomass supply (24EJ per year from 13EJ per year) (This is one of the 5 core scenarios.)
	48	E+ RE+ B+	E+RE+ with high biomass supply (24EJ per year from 13EJ per year)
	49	E+ RE- B+	E+RE- with high biomass supply (24EJ per year from 13EJ per year)
	50	E- RE- B+	E-RE- with high biomass supply (24EJ per year from 13EJ per year)
N. CO_2 emissions trajectory	51	E+SlowStart	Energy/industry CO_2 emissions trajectory to 2030 follows 2005-2020 rate and then linearly declines to -0.17 Gt in 2050.
	52	E+S	Follows slow start emissions rate to 2030, then falls more rapidly to 2040, and then the decline rate slows to reach -0.17 Gt in 2050.
O. Higher social discount rate	53	E+ 7%	Social discounting @7% instead of 2%
	54	E- B+ 7%	Social discounting @7% instead of 2%
P. No CO_2 capture	55	E+NoCCUS	No CO_2 capture allowed. (No feasible model solution found with this constraint)

2.2 Day binning method in RIO

Day binning is a time-domain reduction technique used to improve computational tractability by selecting a set of sample days (24-hour periods) to represent the full variation in time series data (chiefly hourly wind and solar profiles and electricity demands). Like all time-domain reduction processes, selecting a subset of time-variant data changes values of parameters considered by the optimization model, and these changes introduce differences in outcomes relative to any other selection of sample days. In the case of our sensitivity analyses, the selection of different sample days across different versions of the otherwise-same set of inputs to a scenario may result in different outcomes between those scenarios.

As discussed in more detail in Annex A, RIO optimizes electricity sector operations (e.g. power generation, storage charging/discharging) for a subset of sample days, each of which is used to represent multiple days (in a full year) having similar time series profiles for demand and for wind and solar generation. Additionally, RIO tracks the state of charge (or energy storage level) of long duration storage, reservoir hydro resources, and fuels inventories at a daily level by assuming that changes in energy or fuel inventories across each sample day are representative of changes across all other days that are represented by that sample day. This method is intended to substantially reduce the computational burden of the optimization while capturing the impact of variability in wind, solar, electricity demand, and the role of energy and fuels storage across time without modeling the full 8,760 hours of operations in each modeled year.

The day clustering process is designed to identify days that represent a diverse set of potential system conditions, including variable renewable generation profiles and load shapes. Sample days are clustered based on a number of characteristics. These include different metrics describing each day in the data set, such as peak electricity load, net load (i.e., load less expected renewable generation), daily capacity factor (or average availability) for wind or solar, etc. The sampling process starts with a vector for each day that includes each of these features, with different assigned weighting factors. A clustering algorithm is then run so as to minimize the aggregate weighted error across all vectors to produce a desired number of representative days. The clustering process also identifies which cluster each day in the year belongs to, and then uses operational results from the representative day for that cluster to represent the change in long duration energy storage and fuels inventories in each day in the cluster. The newly created year of sample days can be validated by checking that metrics describing the original historical dataset match (within tolerable differences) those of the new set, mainly load duration curve and renewable capacity factors.

To help ensure that results from one of the core scenarios are internally consistent with any sensitivities run on that scenario, the core scenario and its sensitivity cases are run together in RIO. When there are multiple runs in one set of sensitivity cases, the clustering method first determines an average load profile across all runs, and then uses these in the clustering process. If one set of multiple runs has collective averages that are different from another set of multiple runs, the resulting day-binning results will also be different. Thus, the results for the core scenario may be different depending on which other scenarios it is grouped with when run in RIO. While there may be differences between results for a core scenario shown in this annex and the same scenario shown in the main Net-Zero America report, this does not impact the insights gained from comparisons with sensitivity cases because there is internal self-consistency across any give set of scenarios presented in this annex.

3 Sensitivity study results

3.1 Land sinks and non-CO_2 emissions

Greater uptake of carbon by soils and trees (i.e., stronger land sinks) and/or greater reductions in non-CO_2 greenhouse gas emissions (especially methane, nitrous oxides, and fluorocarbons) in 2050 than assumed in the E+ scenario mean that the energy/industrial system can have higher net CO_2 emissions than in E+ while still achieving net-zero greenhouse gas emissions economy wide in 2050. Conversely, a weaker land sink in 2050 and/or less progress than assumed in reducing non-CO_2 emission by 2050 would mean a tighter limit on net CO_2 emissions from the energy/industrial system. Two model runs tested the sensitivity of E+ results to the assumed land sink and non-CO_2 emissions (Table B1, Group A).

The original E+ scenario assumes that non-CO_2 emissions in 2050 are 1.02 $GtCO_{2eq}$/y (down from about 1.25 today [3]) and that the land sink absorbs 0.85 $GtCO_{2eq}$, leaving the energy/industrial system to deliver 0.17 $GtCO_2$/y of net negative emissions for there to be net-zero emissions economy wide by 2050. There is uncertainty about what the magnitude of the land since is today, but 0.7 $GtCO_{2eq}$/y is thought to be a reasonable estimate, and the expectation is that the natural land sink will weaken in the future to as low as 0.3 Gt/y by 2050 due to maturing of forest regrowth in the U.S. [4]. Thus, the E+ scenario assumes a concerted effort to enhance the natural land sink through agricultural and/or forest management measures of the type discussed in [5] and [6], respectively.

In the high land sink case (E+Land+), we assumed the mid-range of technical potential (1 Gt) from enhanced forest sink measures [6], plus the 0.3 Gt/y estimated 2050 natural sink. For the lower land sink, we assumed no enhanced sink, leaving only 0.3 Gt/y of natural sink in 2050. The resulting emissions allowed from the energy/industrial system in 2050 to meet the net-zero target are as in Table B2. Figure B1 – Figure B8 compare results of the original E+ case with the two sensitivity cases. (The last seven of these figures correspond to the first seven types of graphics described generically in Section 2.1.)

Table B2. Input assumptions that vary between cases in land sinks and non-CO_2 emissions sensitivities

Billion metric tCO2e in 2050	E+	E+ Land+	E+ Land-
Land sink	- 0.85	- 1.30	- 0.30
Non-CO2 emissions	1.02	1.02	1.02
Net emissions outside of energy/industry system	0.17	- 0.27	0.73
Allowed energy/industrial CO2 emissions in 2050	- 0.17	0.27	- 0.73

For E+Land+, when net emissions outside of the energy system are negative, the energy/industrial system is allowed greater emissions in 2050 than in E+. This results in greater natural gas use in 2050 and less underground CO_2 storage (Figure B1). For E+Land-, natural gas use is more constrained in 2050 than in E+, and CO_2 storage is higher.

The NPV of the sum of annual energy-supply system costs from 2020-2050 decreases by 2% for E+Land+ and increases by 3% in the E+Land- case, compared with E+ (Figure B2). Percentage-wise these appear to be small differences, but they represent hundreds of billions of dollars in

absolute terms and are, in fact, some of the biggest NPV differences observed across any of the sensitivities that we have run, pointing to the critical importance of the land sink and non-CO_2 emissions for achieving net-zero emissions. It should be noted that the objective function in RIO (Figure B2) does not include any costs for land sink enhancement or non-CO_2 abatement measures.

In the case of E+Land-, the higher demand for negative emissions from the energy/industrial system drives up cost because direct air capture (DAC) is the costliest and only mechanism available within the model for increasing negative emissions; the only other option – biomass conversion with CO_2 capture and storage – is already fully utilized in E+ and so will not be an option that can be enlarged in E+Land-. The greater use of DAC is also evident in its increased contribution to electricity demand (Figure B3). Final electricity demand shown in Figure B3 is modeled as fixed across scenarios, but the level of deployment of intermediate flexibly operable electricity-demand technologies (direct air capture, electrolysis, and electric boilers) can are optimized by RIO as it builds the least-cost energy-system. In E+Land-, RIO chooses to increase electrolysis (Figure B3) to generate more hydrogen than in E+ for use in making synthetic liquid fuels (Figure B8), a less costly option for liquid fuel supply than using petroleum-derived fuels whose emissions would need to be offset by additional DAC. The larger electricity demands created by electrolysis and DAC drive increased generation from solar and wind, greater utilization of battery storage, and some growth in natural gas generation with CO_2 capture (Figure B4). Total installed electricity supply capacity by 2050 is about 20% greater than in E+ (Figure B5), with the fastest annual capacity additions coming in the 2040s (Figure B6). By contrast, thermal generating capacity additions are not significantly different than in E+ across all years of the transition (Figure B7) because the increasing electricity demand from DAC and electrolysis are supplied through solar and wind, and the flexibility in DAC and electrolysis power match that of solar and wind as well. The greater need for negative emissions in in E+Land- leads to about a 70% increase over E+ in annual underground storage of CO2 by 2050 (Figure B8).

In the case of E+Land+, because the land sink makes a greater contribution to decarbonization than in E+, DAC is not needed at all, and less-costly negative emissions from biomass conversion with CCS are able to offset emissions from greater use of fossil fuels elsewhere in the economy, including as liquid fuels. With greater use of petroleum-derived liquid fuels, synthetic liquid fuels play a smaller role, as does electrolytic hydrogen needed for snyfuels (Figure B8). With no electricity demand from DAC and much-reduced demand from electrolysis, total electricity generation (Figure B4) and generating capacity are lower than for E+.

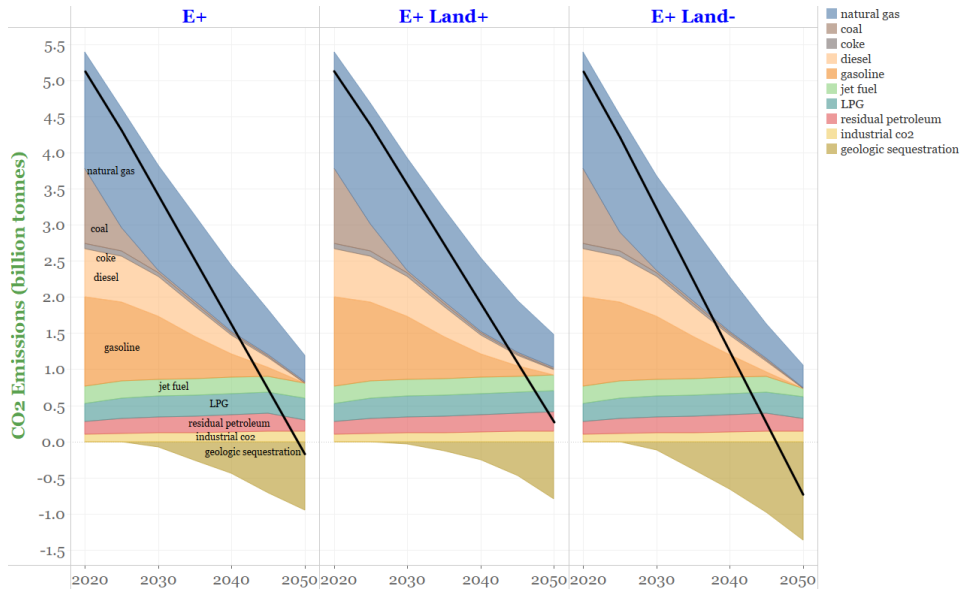

Figure B1. Energy and industrial CO2 emissions that contribute to achieving net-zero emissions economy wide in 2050.

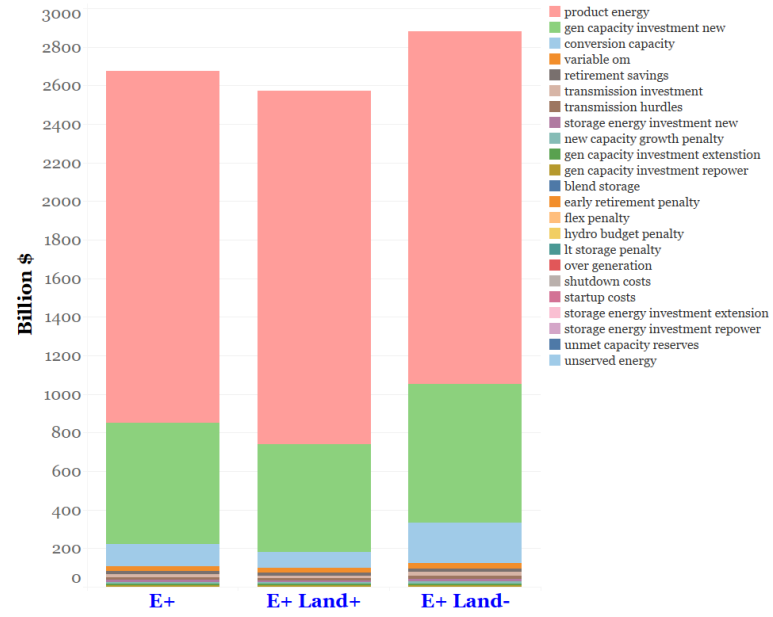

Figure B2. Optimized (minimum) net present value (NPV, 2% discount rate) of the sum of annualized energy-supply system costs from 2020 to 2050 for each scenario (2018$). Sunk costs as of 2020 are not included, and costs associated with energy delivery, such as electricity distribution, are also not included in this metric.

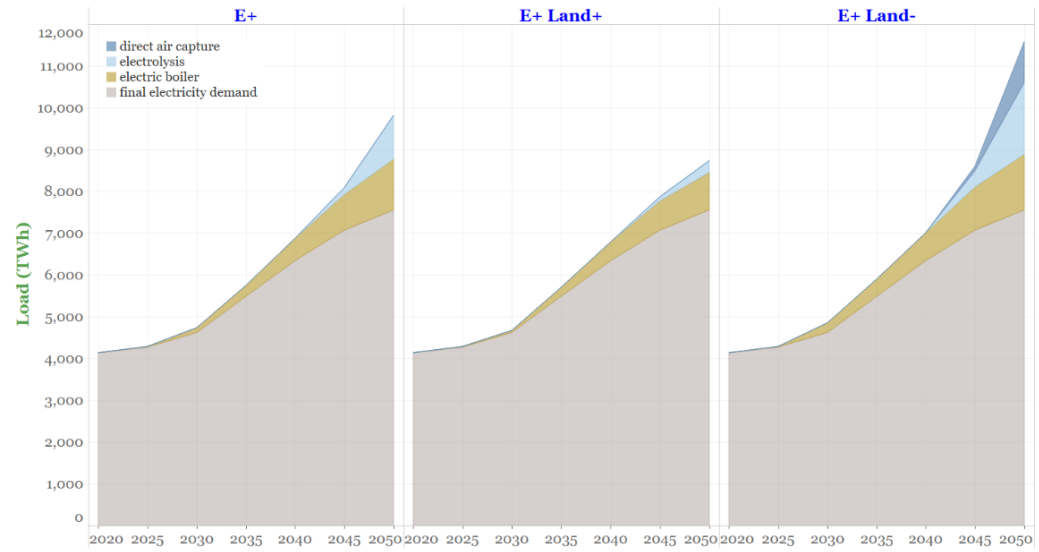

Figure B3. Total electricity load including intermediate, flexibly-operable loads.

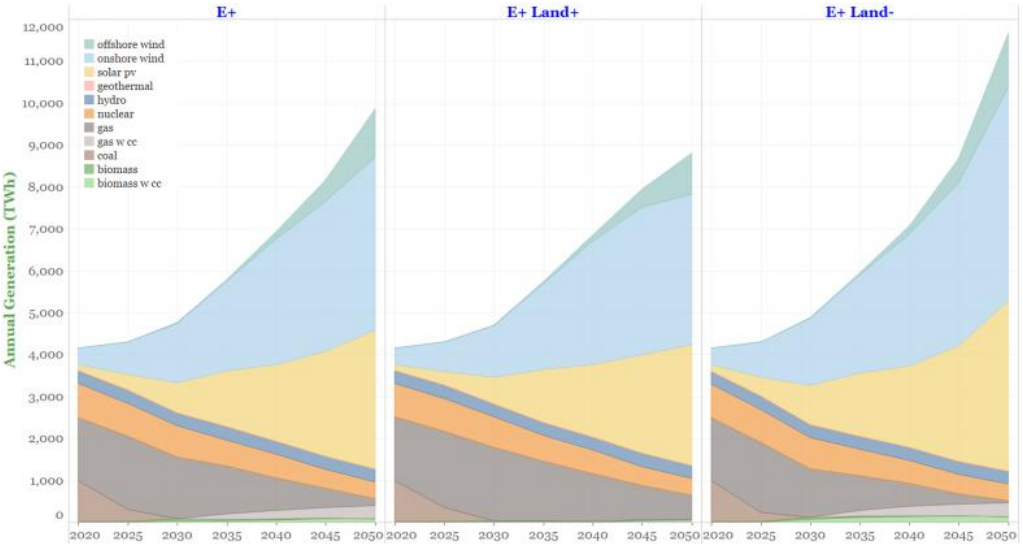

Figure B4. Yearly electricity generation by source.

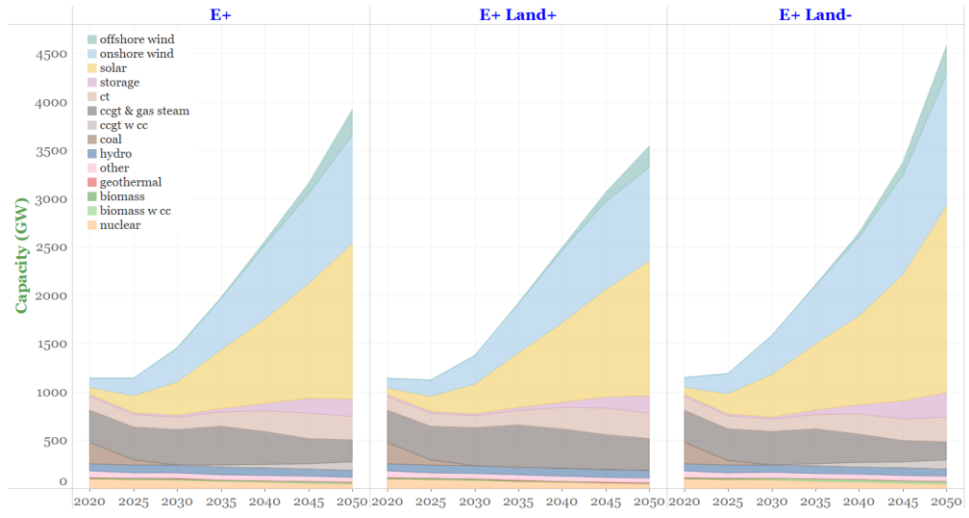

Figure B5. Electricity generating capacity by type of generator.

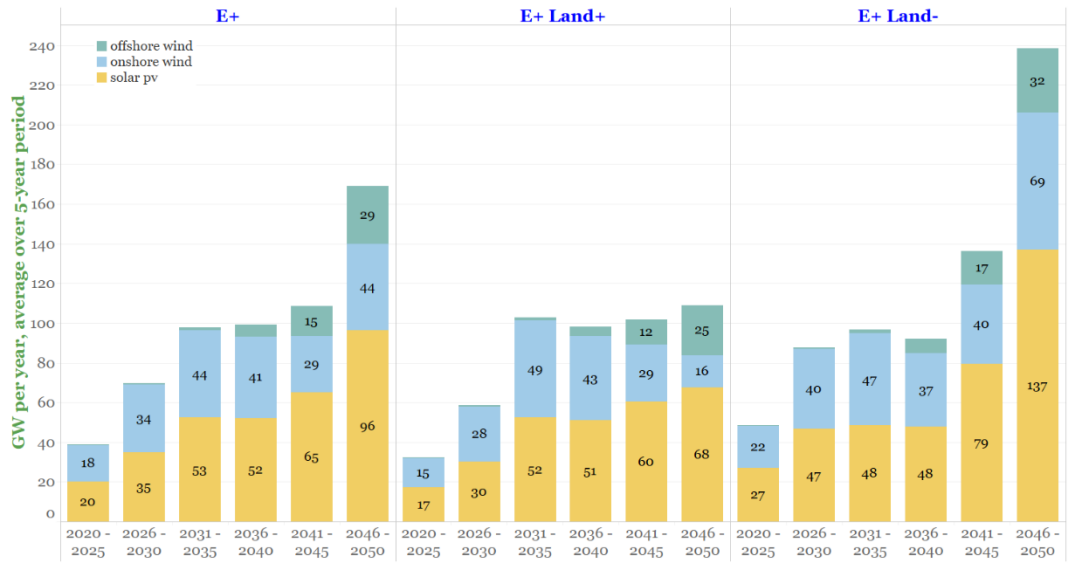

Figure B6. Average annual build rate of solar and wind generating capacity during each five-year period from 2020 through 2050.

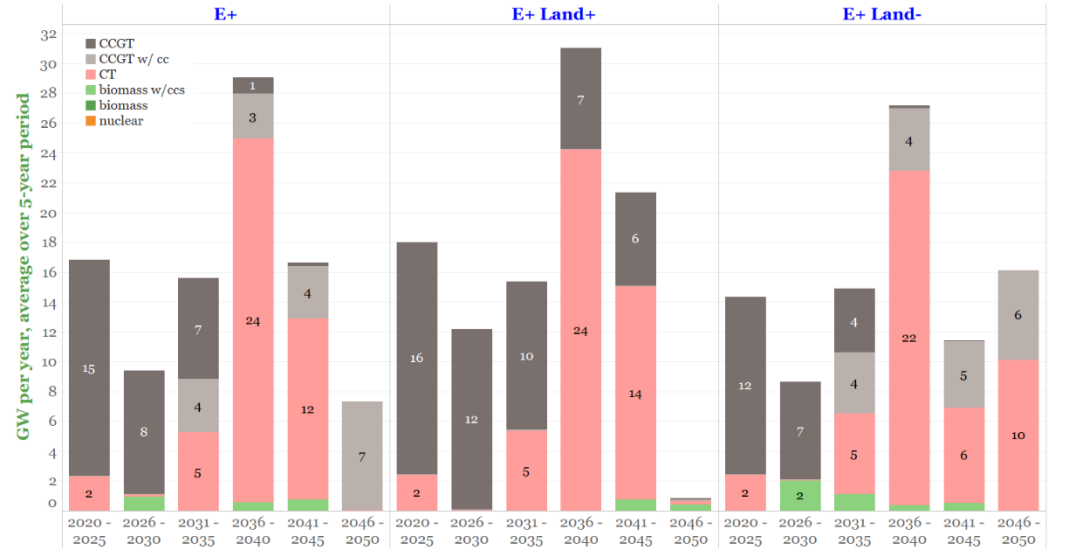

Figure B7. Average annual build rates for dispatchable thermal generating capacity during each five-year period from 2020 through 2050.

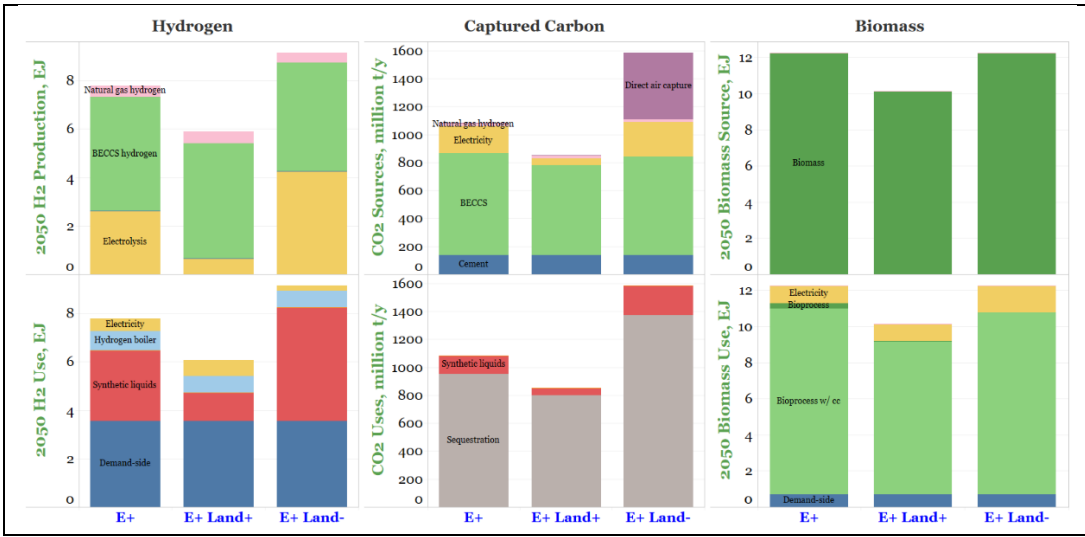

Figure B8. Production (top) and use (bottom) of hydrogen, captured carbon and biomass in 2050.

3.2 Natural gas prices

Future natural gas prices are uncertain. Because the demand for natural gas across all net-zero pathways decreases over time, all of the net-zero scenarios in our study assume natural gas prices follow the *Annual Energy Outlook 2019* [6] "High Oil and Gas Resource and Technology" scenario, i.e., the lowest gas price projections in that edition of the *AEO*. Higher assumed natural gas prices will negatively impact the competition between gas-fired technologies and alternatives, and lower prices potentially lead to increased use of gas. To quantify these impacts, two sensitivities were run on natural gas prices (Group B in Table B1).

In E+Gas+, the *AEO2020* [7] "Low Oil and Gas Supply" scenario was adopted as a proxy for a future where gas supply is short and thus prices are higher. Prices are 1.5 to 2.5 times those in the E+ scenario, across different regions of the U.S. Region-specific gas prices are input to RIO. Table B3 gives illustrative gas price values for the Texas region. For corresponding gas prices for other regions, the reader is referred to details in *AEO2020*.

In E+Gas-, the *AEO2020* "*High Oil and Gas Supply*" scenario is adopted as a proxy for a future where gas supply is high and thus prices are lower. In this scenario, prices range from 0.5 to 0.8 times those in E+. Table B3 shows gas price projections for the Texas region.

Table B3. Input assumptions that vary between cases in gas prices sensitivities

2016 $/GJHHV	E+	E+ Gas+	E+ Gas-
Source of price projection	AEO2019 High oil/gas tech & resource	AEO2020 Low oil&gas supply	AEO2020 Hi oil&gas supply
Prices in 2020, 25, 30, 35, 40, 45, 50	2.5, 2.8, 3.0, 3.1, 3.1, 3.1, 3.3	2.5, 3.5, 4.4, 4.9, 5.2, 5.6, 6.2	2.3, 2.3, 2.5, 2.5, 2.5, 2.4, 2.4

The gas price sensitivity run results in Figure B9 through Figure B15 offer the following insights:

(a) The sum of NPV of annual energy-supply system costs (Figure B9) from 2020-2050 increases by 2% in E+Gas+ and decreases by 2% in E+Gas- case. These changes can be mainly explained by two factors. First, the change in cumulative gas use over the 30-year period is relatively small across the sensitivities: 137 EJ for E+Gas+ and 158 EJ for E+Gas-, as compared with 148 EJ in E+. Thus, higher gas prices raise total costs and lower prices reduce it. Second, there is less natural gas power generation in E+Gas+ than in E+ and more in E+Gas- (Figure B11). These are compensated by more and less solar and wind generation, which further contributes to higher and lower system costs, respectively.

(b) Installed electricity generating capacity (Figure B12) and average annual capacity installation rates for solar and wind (Figure B13) and firm resources (Figure B14) are consistent with the above electricity generation results: solar and wind capacity and build rates are higher (lower) in E+Gas+ (E+Gas-) than in E+; in the case of firm resources, except for CCGT with CCS the installed capacity and capacity build rates are not very different across the 3 cases, because the firm resources operate with relatively low capacity factors in all cases. In the case of CCGT with CCS, additional capacity is built in E+Gas- to deliver the needed gas-fired generation. Additionally, modestly more grid storage capacity is added in E+Gas+ to help manage the larger variable generation from solar and wind.

(c) Electrolysis in E+Gas+ increases relative to E+ (Figure B10), because higher gas prices drive more wind and solar generation; electrolysis increases to help balance the increased variability in electricity supply mix while also providing a greater H_2 supply that is used in part to substitute the higher-priced natural gas. No symmetrical reduction in electrolysis is seen in E+Gas-, perhaps because the demand for electrolytic hydrogen has a more dominant role in determining the level of electrolysis than does the need for balancing solar and wind variability. In E+Gas- case, more H_2 from ATR is observed due to the lower gas prices.

(d) In E+Gas+, CO_2 capture from the power sector is reduced as a result of higher natural gas prices. On the other hand, more CO_2 capture is deployed in the power sector in E+Gas- to accompany greater use of gas-fired generation (Figure B15).

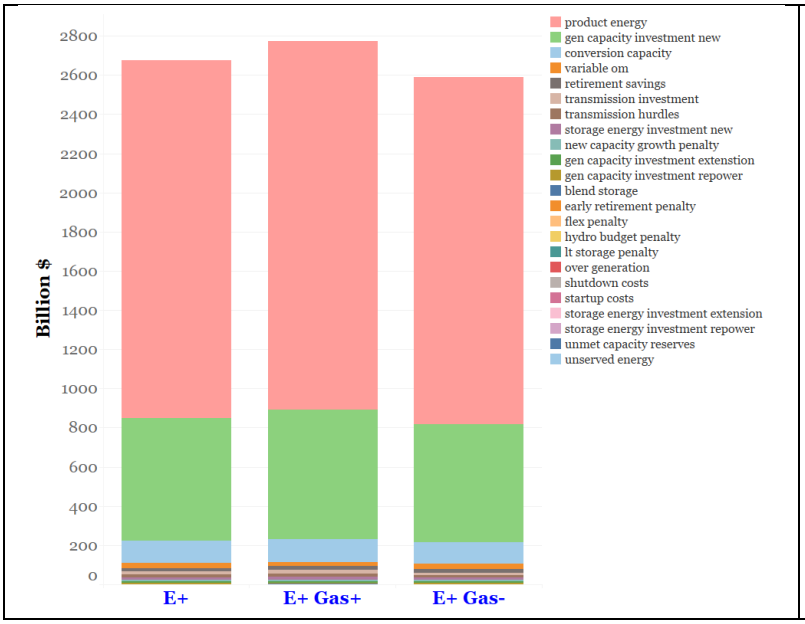

Figure B9. Optimized (minimum) net present value (NPV, 2% discount rate) of the sum of annualized energy-supply system costs from 2020 to 2050 for each scenario (2018$). Sunk costs as of 2020 are not included, and costs associated with energy delivery, such as electricity distribution, are also not included in this metric.

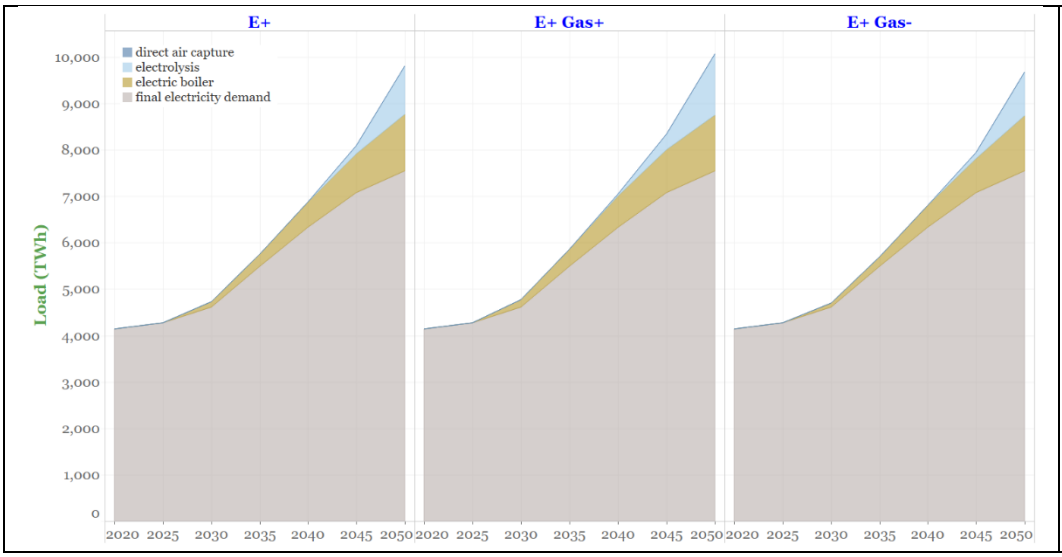

Figure B10. Total electricity load including intermediate, flexibly-operable loads.

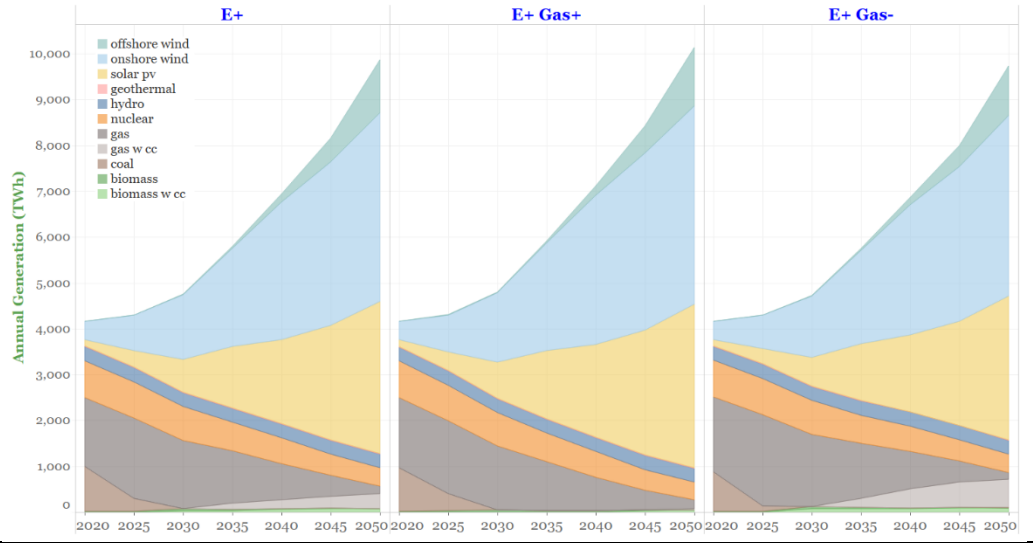

Figure B11. Yearly electricity generation by source.

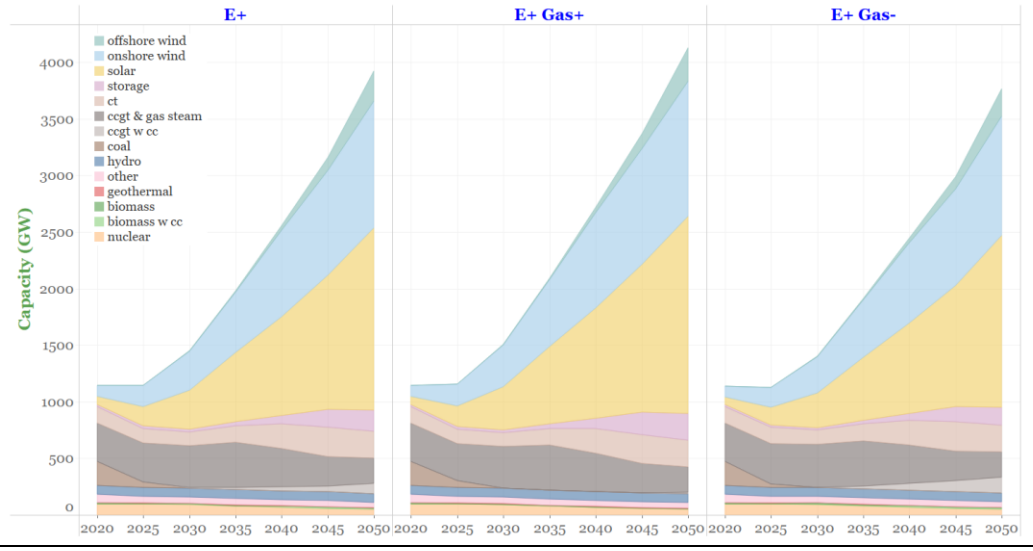

Figure B12. Electricity generating capacity by type of generator.

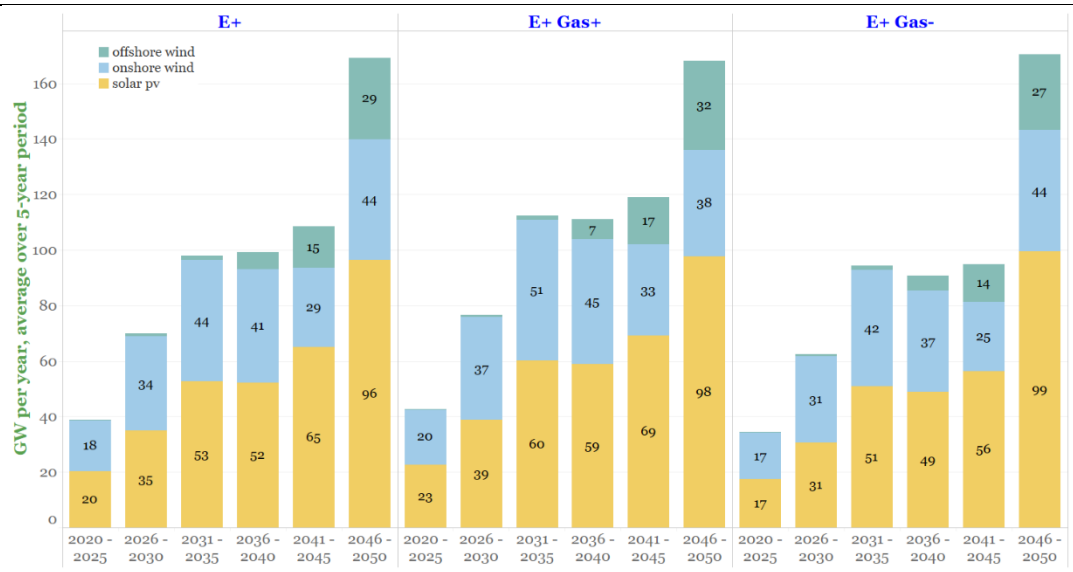

Figure B13. Average annual build rate of solar and wind generating capacity during each five-year period from 2020 through 2050.

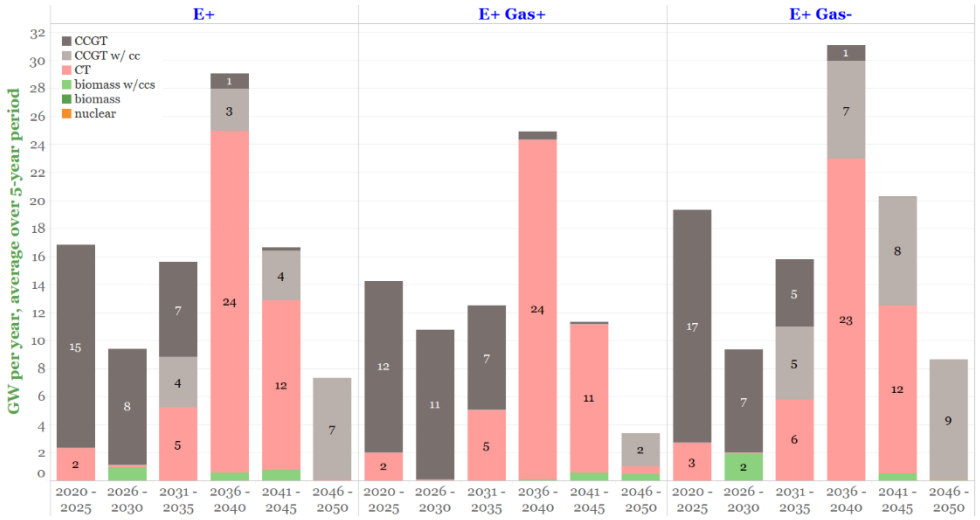

Figure B14. Average annual build rates for dispatchable thermal generating capacity during each five-year period from 2020 through 2050.

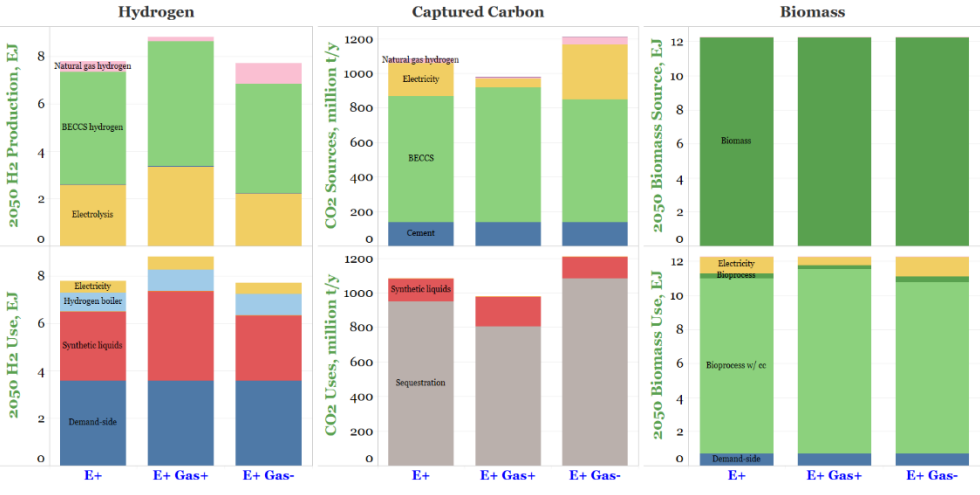

Figure B15. Production (top) and use (bottom) of hydrogen, captured carbon and biomass in 2050.

3.3 Power sector capital costs (non-nuclear)

The mix of electricity generating resources (e.g., solar/wind, gas, nuclear, etc.) in a net-zero scenario depends to a degree on the relative costs between resources, and there are intrinsic uncertainties in projections of future costs. With this in mind, we designed a number of sensitivity cases around the E+ scenario in which we varied capital costs. Here we discuss results for sensitivities on solar, wind, NGCC w/CC, and high-voltage transmission (Group C in Table B1). We examine sensitivities to nuclear generator costs (in both E+ and E+RE- scenarios) in Section 3.4.

For solar and wind capital costs, the E+ case uses NREL's ATB2019 mid-range projections [8]. For the high cost sensitivity (E+SW+) we use an average of the ATB 2019 mid-range and constant-value projections because, absent serious constraints on equipment supplies, the ATB 2019 constant-value projections are unrealistically high, given current trends with solar and wind costs. For the low-cost case (E+SW-) we use the ATB 2019 low-case cost projections. For the high and low NGCC w/CC cost cases (E+NGCC+ and E+NGCC-), we assume capital costs 50% higher and 20% lower than in the E+ case, respectively. The choice of +50%/-20% is consistent with accuracy guidelines for Class 4 to Class 5 cost estimates for projects (screening to

feasibility study level) published by AACE International [9]. For the high transmission (E+Trans+) case, we also assume capital costs 50% higher than in the E+ case. We did not run a sensitivity with lower transmission costs. Table B4 gives input changes for the sensitivity runs. In the case of solar, wind, and transmission representative subset of values are shown, since the values vary by resource quality and/or geographic region.

Table B4. Input assumptions that vary between cases in power sector technology cost sensitivities.

$/kW in 2050	E+	E+SW-/+	E+NGCC -/+	E+Trans+
NGCC w/CC	1,725	1,725	1,380 / 2,589	1725
Solar/wind (TRG1 NJ)*	PV: 869 Wind: 1,723	PV: 453; 1,144 Wind: 1,433; 2,280	PV: 869 Wind: 1,723	PV: 869 Wind: 1,723
Trans. (Mid-Atl/NY)*	2,821	2,821	2,821	5,642

* Capital costs for wind and solar generators in the model vary with resource quality and geographic location. Illustrative values are given here. For solar and wind, these are the values for the highest quality resource group for New Jersey locations.
** Modeled transmission costs vary with geography. Illustrative values are given here for interconnections between the New York state and Mid-Atlantic regions. Transmission costs would typically be expressed in units of $/MW-km or perhaps $/km, but the structure of the RIO model is such that units of $/kW are used. See Annex A [2] for additional discussion of transmission modeling.

Insights from results of these sensitivity runs shown in Figure B16 through Figure B23 include:

(a) With either higher or lower capital cost assumptions for NGCC w/CC, there are no discernable impacts on any of the results relative to E+. In the case of NGCC-, the cost reductions are not sufficient to lead to greater deployment of the technology. Greater deployment would entail removing additional CO_2 from the atmosphere to compensate for the small (but non-zero) emissions from NGCC w/CC systems, and the only option for achieving this would be costly direct air capture, since the option of bioconversion with CC is already fully utilized (Figure B23). With higher costs for NGCC w/CC, the increase in cost is not sufficient to deter building NGCC w/CC.

(b) In contrast, for the sensitivities around solar and wind capital costs,
    1. The NPV of annual energy-supply system costs from 2020-2050 (Figure B16) is about 1% higher for E+S/W+ and 1% lower for E+S/W-. In the latter case, the decrease is mainly due to higher cost NGCC w/CC generation being displaced by additional solar and wind generation (Figure B18). The reverse takes place with E+S/W+, with more NGCC w/CC generation displacing wind and solar.
    2. Neither bulk electricity nor electric boiler loads change much across the sensitivities (Figure B17), unlike the electrolysis load, which in E+S/W+ decreases due to higher solar/wind costs.
    3. Annual electricity generating capacity (Figure B19) and average annual installation rates for wind and solar electricity capacity (Figure B20) are consistent with the above observations. Additionally, in E+S/W-, modestly more grid storage capacity is added to help manage the larger variable generation from solar and wind (Figure B22).
    4. In E+S/W- more H_2 use is observed (Figure B23) due greater adoption of electrolysis that accommodates the greater contribution of variable solar and wind electricity. There is modestly less CO_2 capture due to less deployment of NGCC w/CC for power generation (Figure B23). On the other hand, in E+S/W+, there is more capture in the power sector due to greater use of NGCC w/CC (Figure B23).

(c) Inter-regional transmission plays an essential role in moving wind-generated electricity to demand centers in all cases. When capital costs for inter-regional transmission are increased (E+Trans+), onshore wind generation is reduced relative to E+ and compensated by a combination of more generation from solar and NGCC w/CC (Figure B18) and more electricity storage (Figure B19). However, the NPV of total system costs is essentially unchanged from that for E+ (Figure B16).

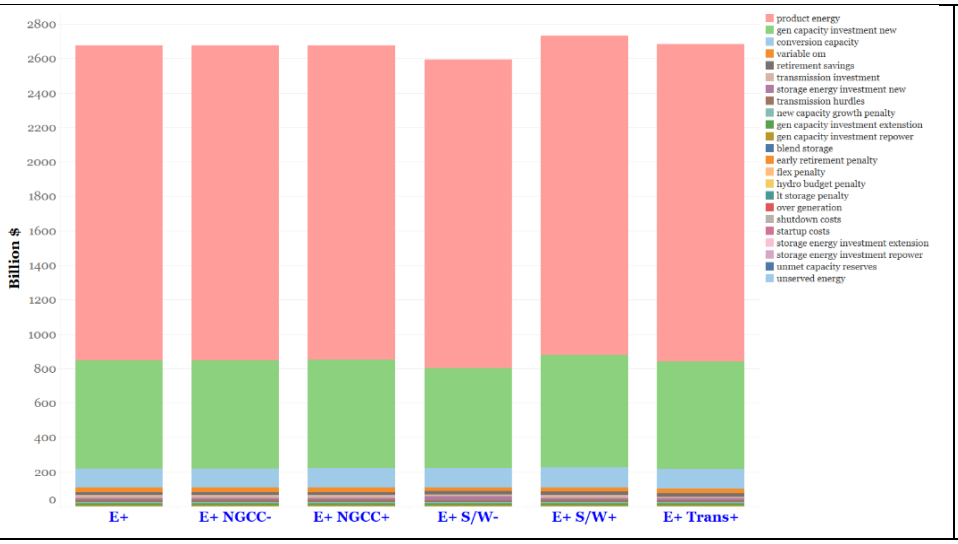

Figure B16. Optimized (minimum) net present value (NPV, 2% discount rate) of the sum of annualized energy-supply system costs from 2020 to 2050 for each scenario. Sunk costs as of 2020 are not included, and costs associated with energy delivery, such as electricity distribution, are also not included in this metric.

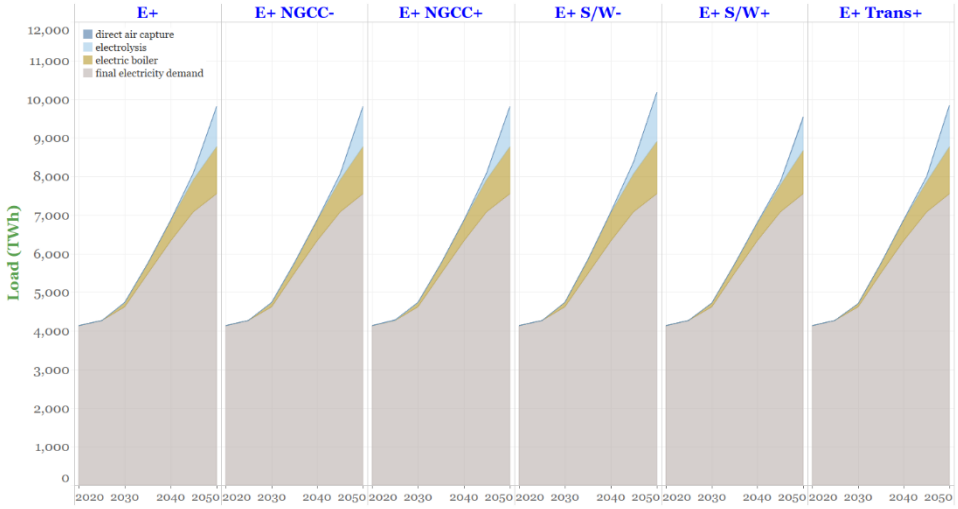

Figure B17. Total electricity load including intermediate, flexibly-operable loads.

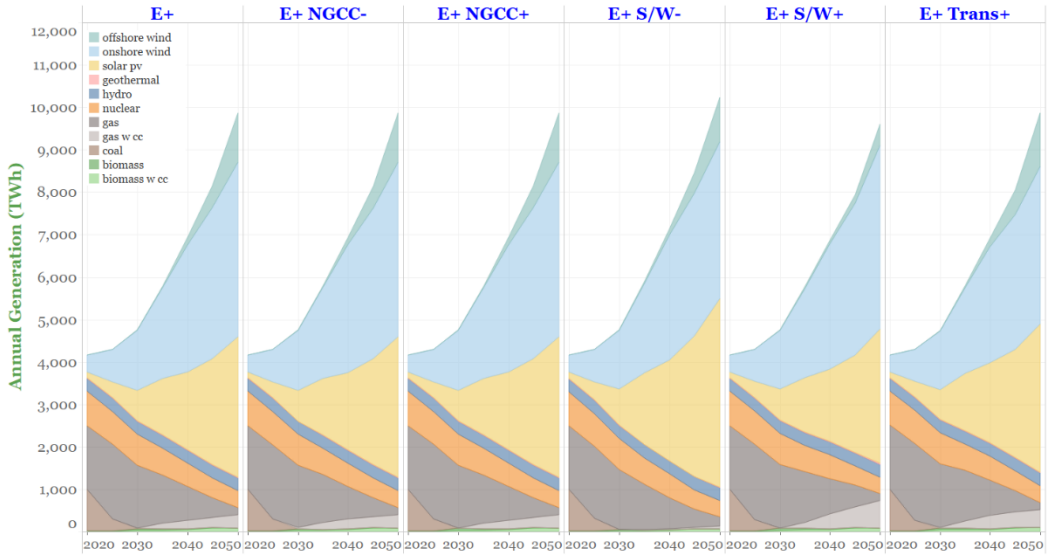

Figure B18. Yearly electricity generation by source.

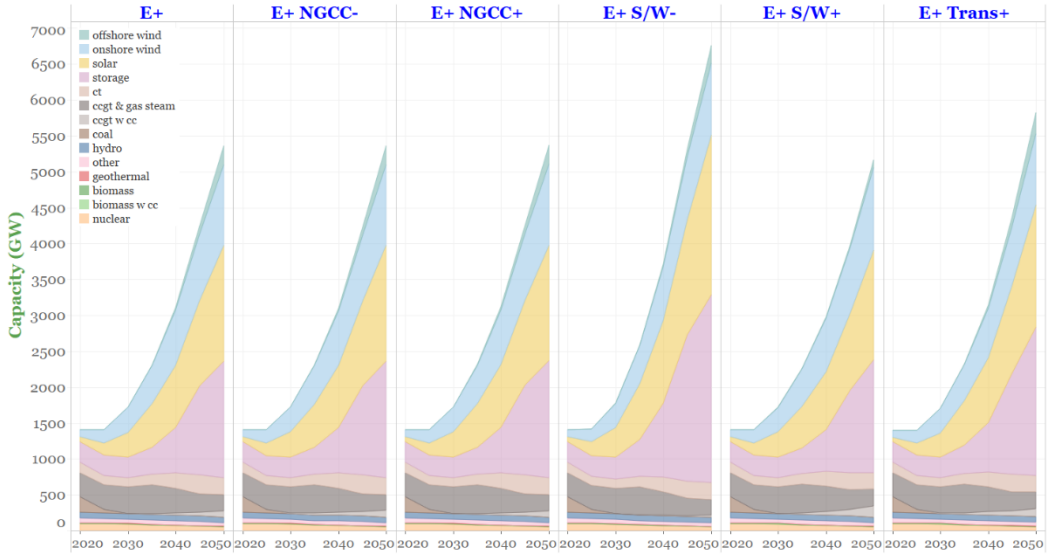

Figure B19. Electricity generating capacity by type of generator.

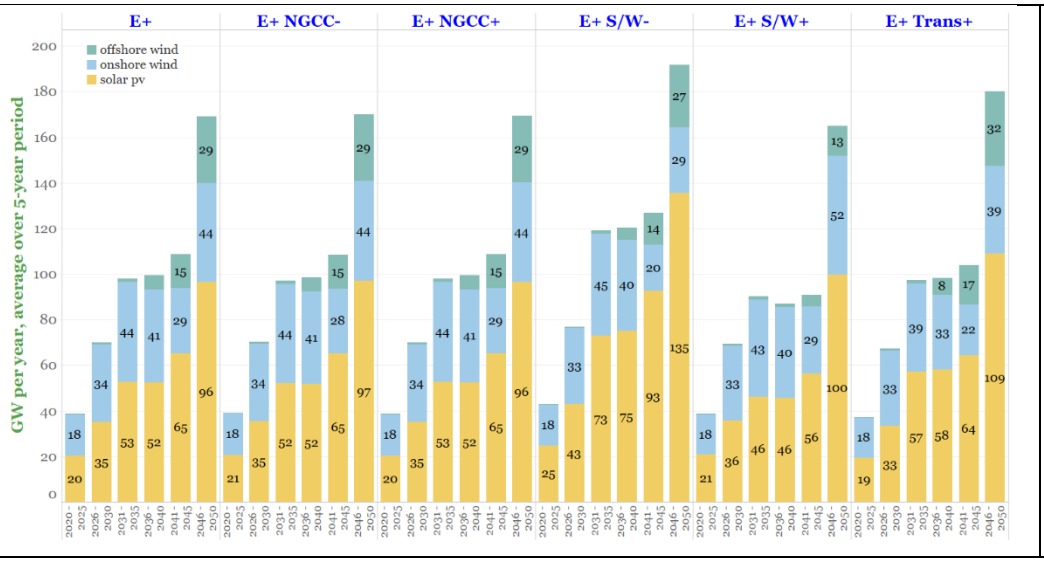

Figure B20. Average annual build rate of solar and wind generating capacity during each five-year period from 2020 through 2050.

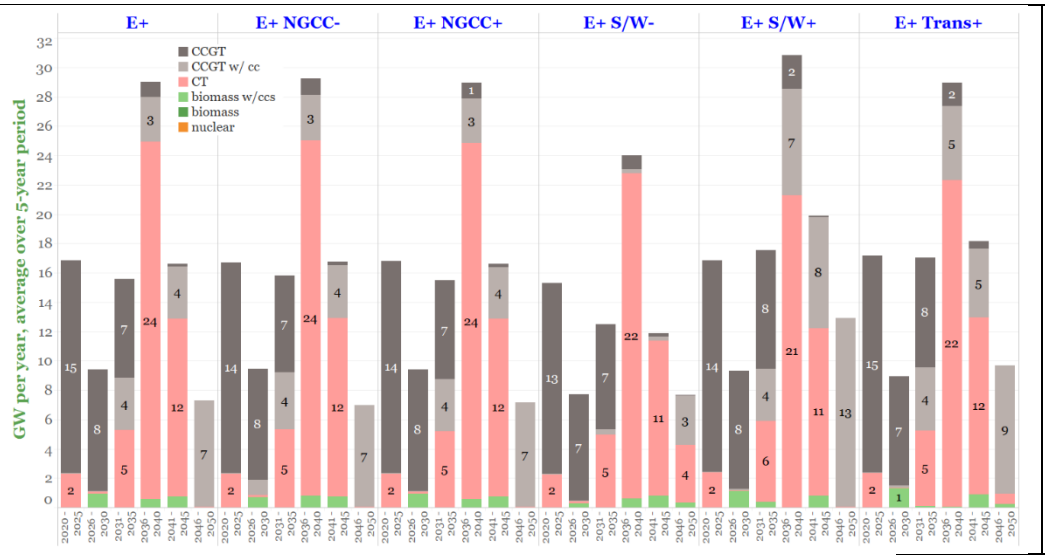

Figure B21. Average annual build rates for dispatchable thermal generating capacity during each five-year period from 2020 through 2050.

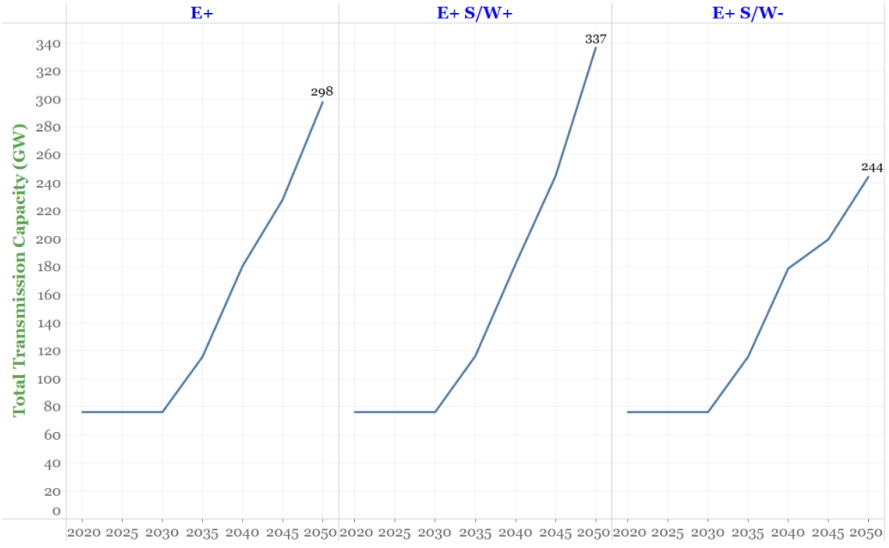

Figure B22. Increase in total high-voltage transmission capacity from 2020 through 2050.

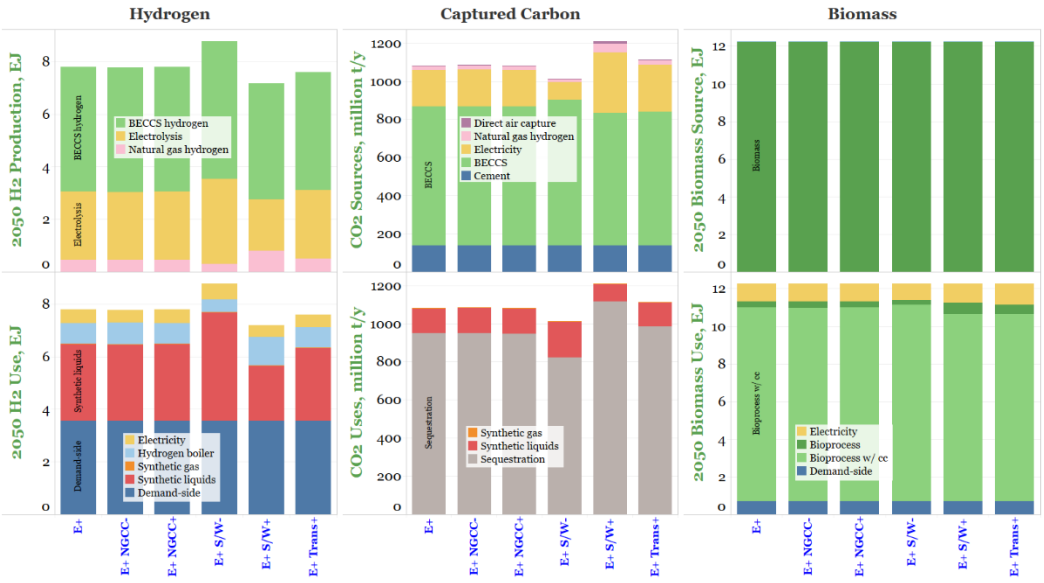

Figure B23. Production (top) and use (bottom) of hydrogen, captured carbon and biomass in 2050.

3.4 Nuclear power capital costs and build rates

Nuclear power is a potentially important low-carbon firm generating resource. Eight sensitivity cases were run to assess the impact of future costs and annual capacity build rates for nuclear (Table B1, Group D): 5 for the E+ scenario and 3 for the E+RE- scenario.

E+ sensitivities

The E+ sensitivities included ones for nuclear capital costs 50% higher (E+Nu+) and 20% lower (E+Nu-) than in the core E+ scenario (Table B5). The choice of +50%/-20% is consistent with accuracy guidelines for Class 4 to Class 5 cost estimates for projects (screening to feasibility study level) published by AACE International [9]. An additional case with very aggressive cost reductions was also run (E+Nu--) to explore the impact of the idea of quasi-mass production of small modular reactors, which some have proposed would dramatically reduce capital costs [10]. We also designed a constrained nuclear build-rate case (E+NuRate-), in which additions of nuclear capacity are limited to 10 GW per year starting in 2030, with no new capacity allowed in the 2020s. The 10 GW cap is close to the maximum amount of new capacity that has come on line in a single year in the U.S. (Nine GW were brought on line in each of 1973, 1974, 1985 and 1987 [11].) Finally, the E+Nu--Rate- case combines the very low capital cost and 10 GW/y build-rate cap.

Compared with the original E+ case, there are no discernable differences in total system cost (Figure B24) or electricity loads (Figure B25) among E+Nu+, E+Nu-, and E+NuRate-, and no new nuclear capacity is built in any of these cases (Figure B28): nuclear capacity is a more costly option for providing firm power to balance wind and solar variability than other means available in the model for accomplishing this. However, there is significant nuclear expansion in the E+Nu-- and E+Nu--Rate- cases, when capital costs are assumed to reach 1800 $/kW (Figure B26 and Figure B28). Nuclear primarily displaces wind and solar in these cases (Figure B27). These results underline the importance of aggressive nuclear cost reductions if the technology is to play an important role in the transition.

Table B5. Input assumptions relating to nuclear power generators in sensitivities around E+ scenarios.

	E+	E+Nu-	E+Nu+	E+NuRate-	E+Nu--	E+Nu--Rate-
Capex 2050, 2016$/kW	5,530	4,423	8,295	5,530	1,800	1,800
Build rate cap 2050, GW	None	None	None	10GW from 2030	None	10GW from 2030

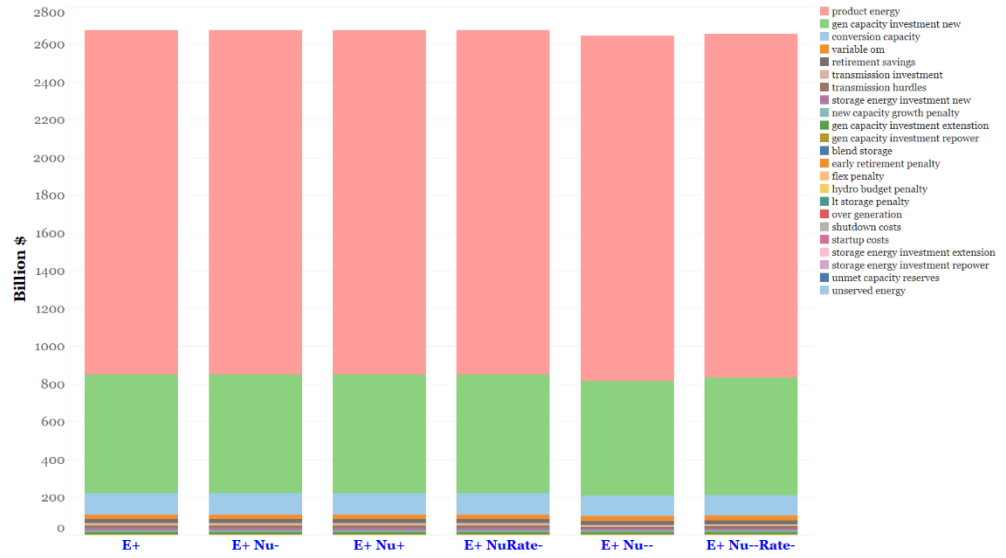

Figure B24. Optimized (minimum) net present value (NPV, 2% discount rate) of the sum of annualized energy-supply system costs from 2020 to 2050 for each scenario. Sunk costs as of 2020 are not included, and costs associated with energy delivery, such as electricity distribution, are also not included in this metric.

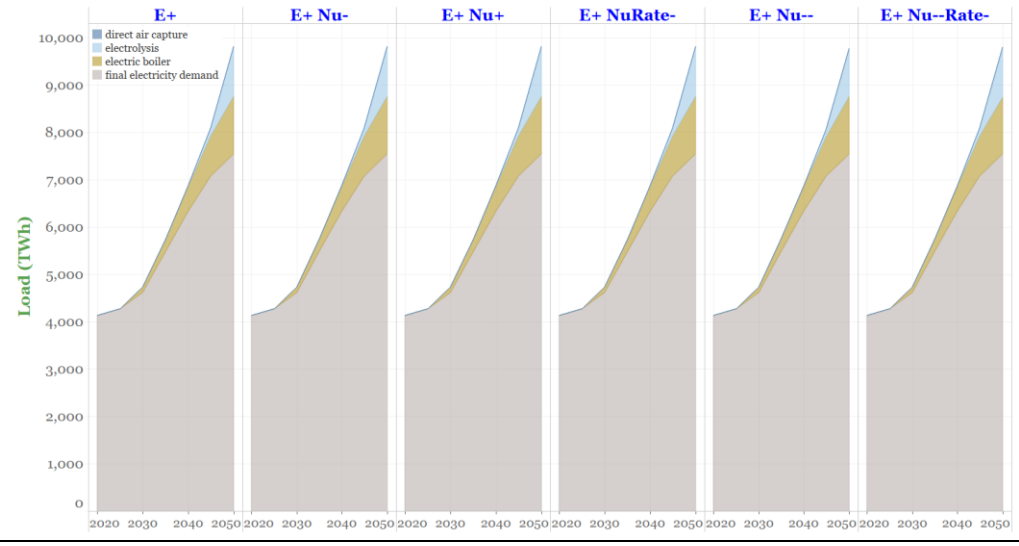

Figure B25. Total electricity load including intermediate, flexibly-operable loads.

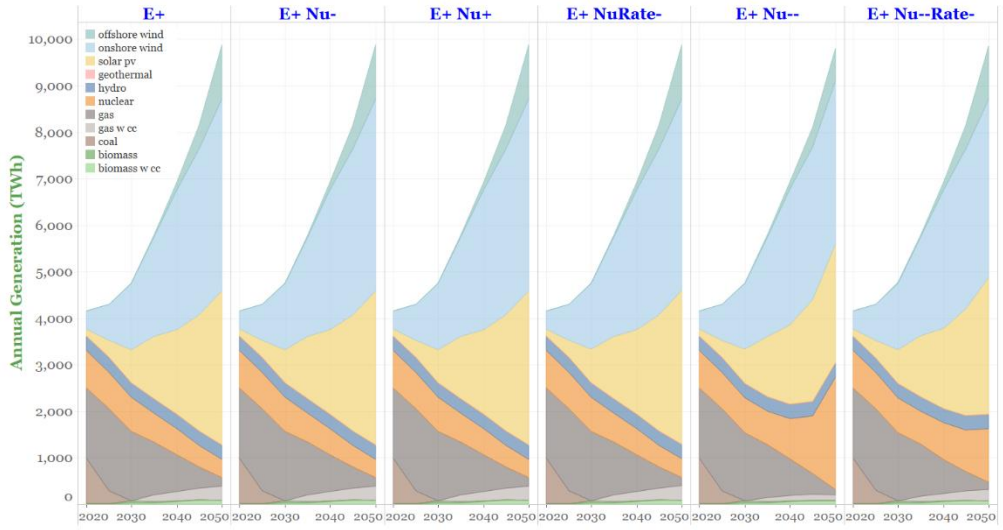

Figure B26. Yearly electricity generation by source.

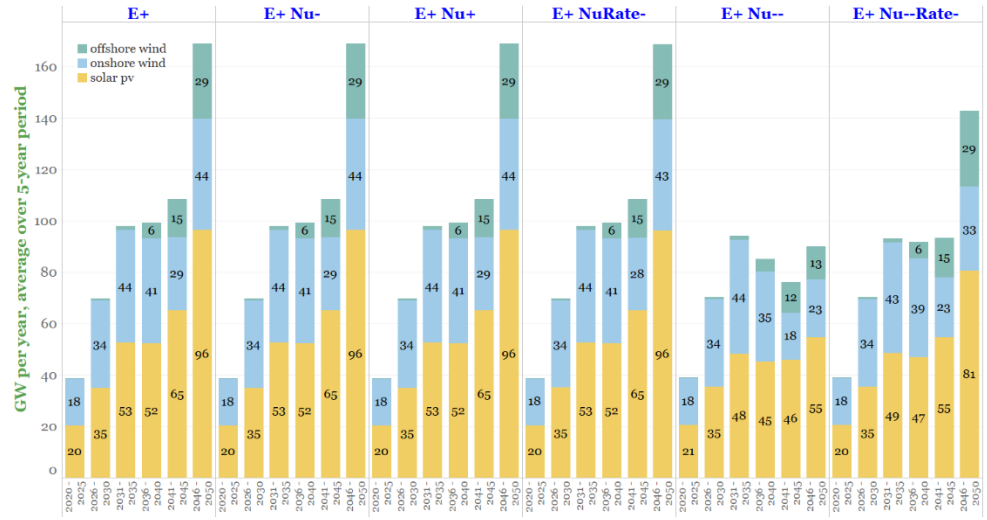

Figure B27. Average annual build rate of solar and wind generating capacity during each five-year period from 2020 through 2050.

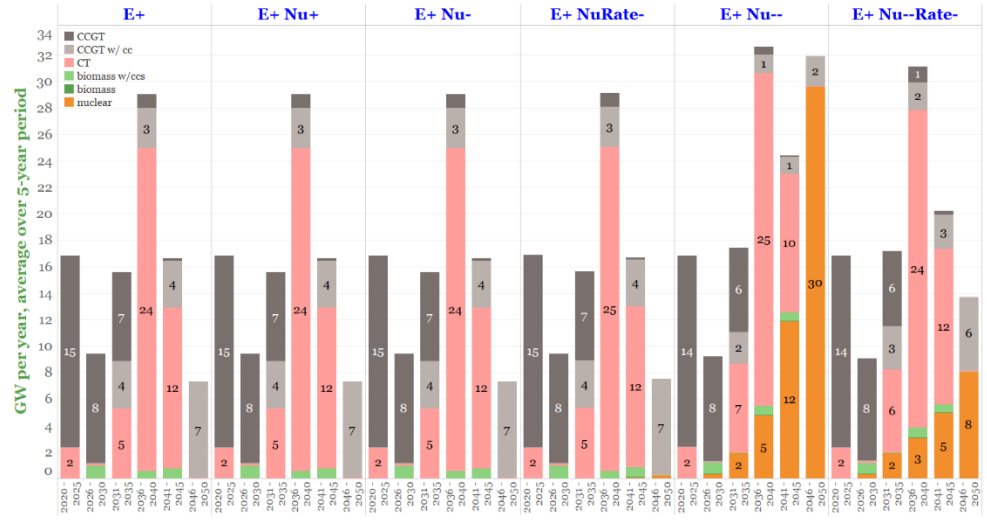

Figure B28. Average annual build rates for dispatchable thermal generating capacity during each five-year period from 2020 through 2050.

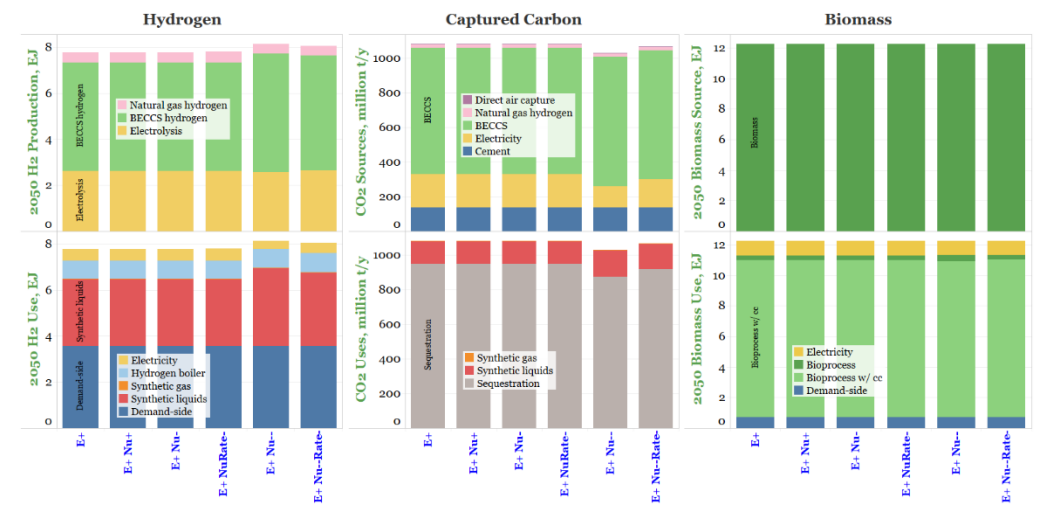

Figure B29. Production (top) and use (bottom) of hydrogen, captured carbon and biomass in 2050.

E+ RE- sensitivities

Three sensitivities were run for the E+RE- case (Table B6), the only one of the original five core scenarios where significant new nuclear capacity was deployed.

Table B6. Input assumptions relating to nuclear power generators in sensitivities around E+RE- scenarios.

	E+RE-	E+RE-NuRate-	E+RE-Nu--	E+RE-Nu--Rate--
Capex 2050, 2016$/kW	5,530	5,530	1,800	1,800
Build rate cap 2050, GW/y	None	10 from 2030	None	0.36 in 2025, up to 8 in 2050

In the original E+RE- case, the build rate for new nuclear capacity averages 25 GW/y as 2050 is approached (Figure B34), and a total of 285 GW of new nuclear capacity are built by 2050. In E+RE-NuRate-, where new nuclear capacity is constrained to grow no more than 10 GW/y, nuclear generation begins to grow earlier in the transition (Figure B34), and total nuclear capacity added through the transition is 204 GW, or roughly double today's U.S. nuclear capacity.

When nuclear capital costs are reduced by a factor of three and build rates are unconstrained (E+RE-Nu--), the build rate averages 30 GW/y as 2050 is approached, but lower build rates are observed earlier in the transition (Figure B34), resulting in a total of 245 GW of new capacity by 2050.

The third sensitivity, E+RE-Nu--Rate-- assumes the greatly reduced capital cost, but constrains the build rate to represent a possible programmatic roll out of small modular reactor technology. This roll out caps new build of nuclear at 0.36 GW/y in 2025 and at increasingly higher caps over time, reaching 8GW/y in 2050. In this case nuclear capacity is built out at the maximum rate allowed in each time step (Figure B34), resulting in a cumulative new build of 92 GW by 2050. Since wind and solar build rates are also constrained, the additional generation needed to meet electricity demand is provided primarily by more natural gas combined cycles, initially without CO_2 capture, but with increasing levels of CO_2 capture as the transition proceeds (Figure B32). To compensate for the added emissions from natural gas, the use of hydrogen in industrial

boilers and in power generation increases (Figure B35), displacing gas use. The additional hydrogen supply is produced by autothermal reforming of natural gas with CO_2 capture (Figure B35). There are residual CO_2 emissions from this process, and absolute emissions for the energy system as a whole are greater than in E+RE-. Some direct air capture is deployed near the end of the transition period (Figure B31), and contributes to the need for more sequestration of CO_2 (Figure B35).

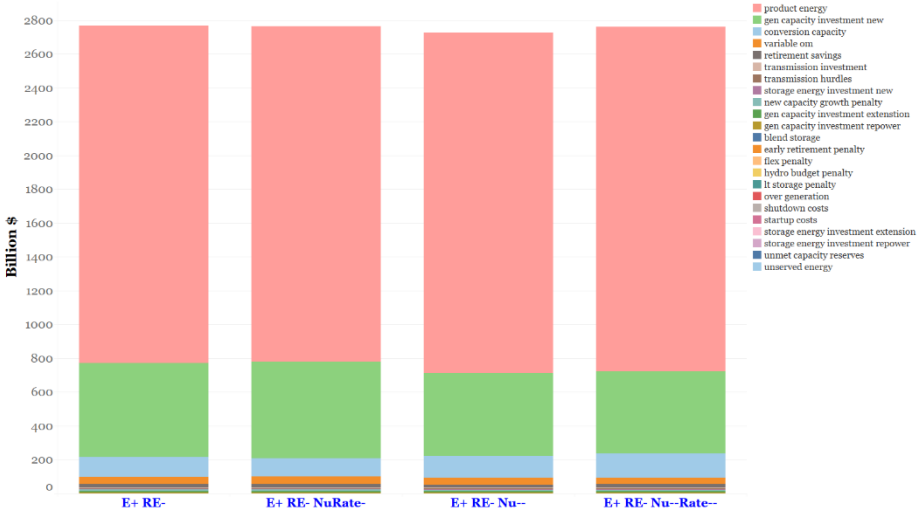

Figure B30. Optimized (minimum) net present value (NPV, 2% discount rate) of the sum of annualized energy-supply system costs from 2020 to 2050 for each scenario. Sunk costs as of 2020 are not included, and costs associated with energy delivery, such as electricity distribution, are also not included in this metric.

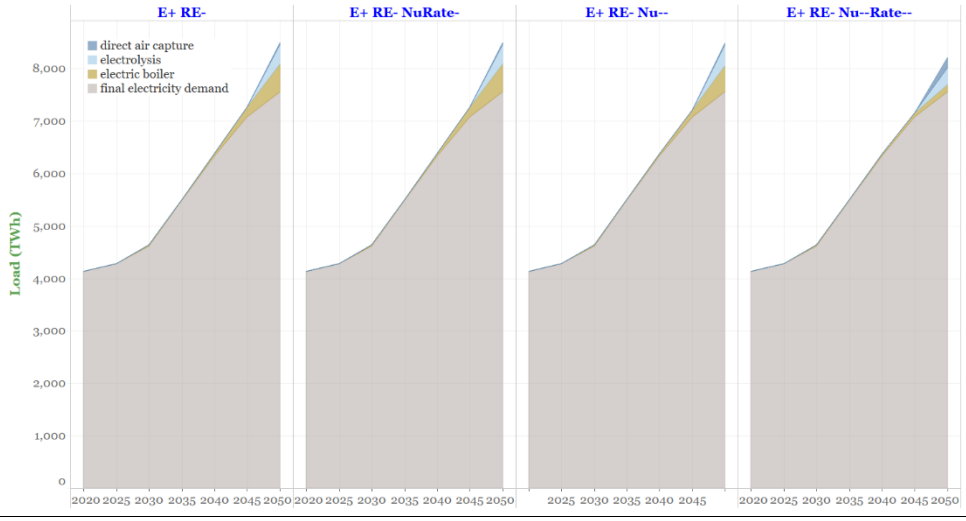

Figure B31. Total electricity load including intermediate, flexibly-operable loads.

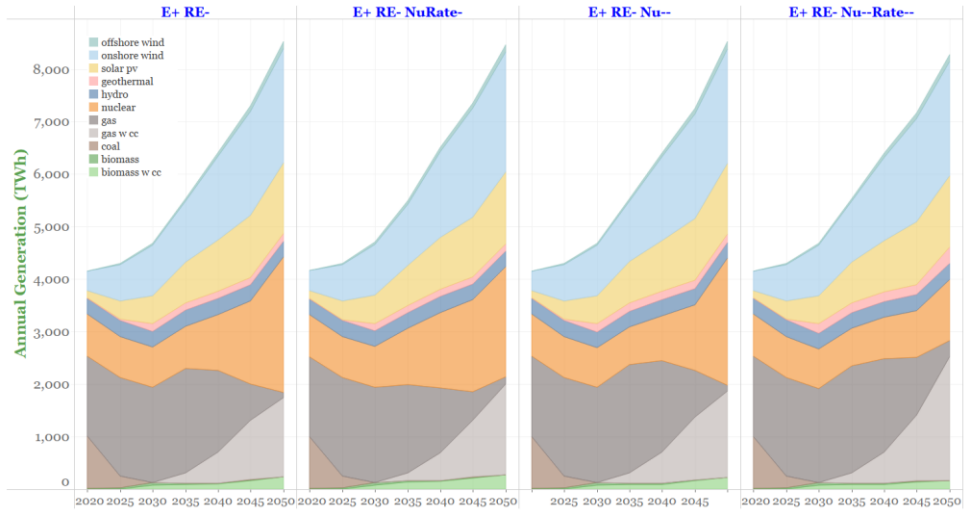

Figure B32. Yearly electricity generation by source.

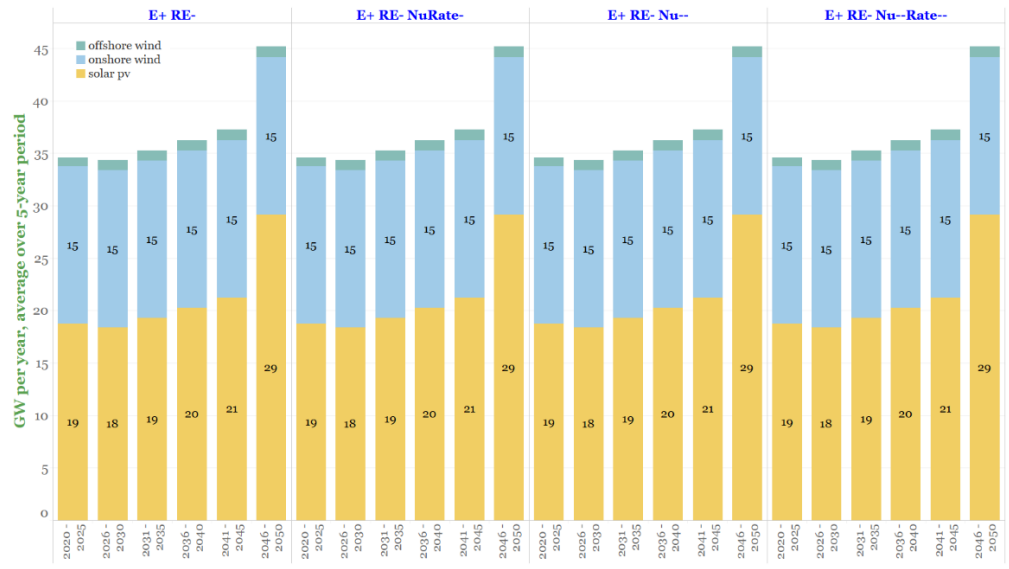

Figure B33. Average annual build rate of solar and wind generating capacity during each five-year period from 2020 through 2050.

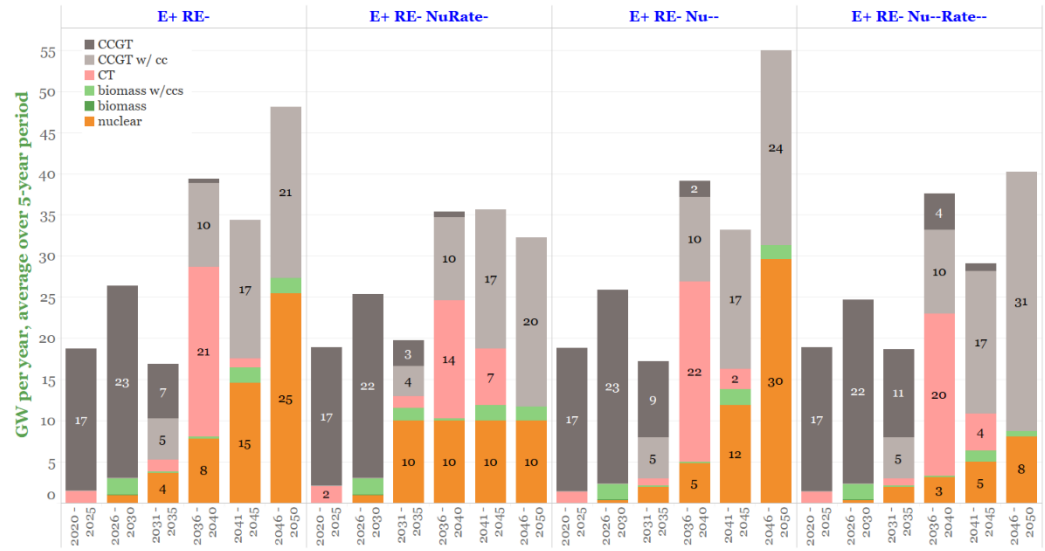

Figure B34. Average annual build rates for dispatchable thermal generating capacity during each five-year period from 2020 through 2050.

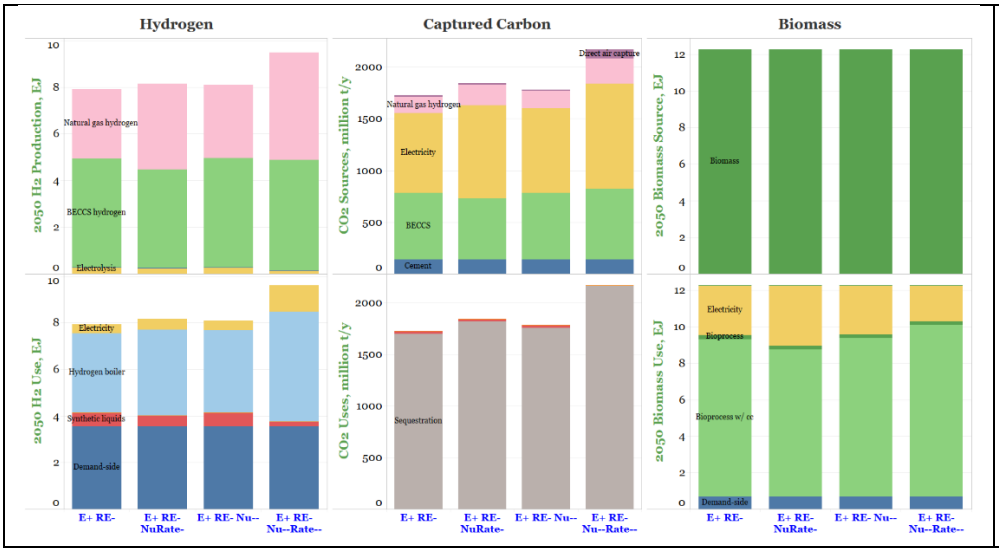

Figure B35. Production (top) and use (bottom) of hydrogen, captured carbon and biomass in 2050.

3.5 Wind and transmission capacity build-limit sensitivities

Siting/permitting, supply chain and/or other constraints may act in reality to slow the rate of plant and infrastructure deployment from the levels generated by RIO in the five core net-zero scenarios. To test constraints where some of the fastest build rates or most extensive build-outs are observed in the E+ scenario, sensitivity cases that capped the ultimate level of build-out of wind capacity and transmission capacity were run (Table B1, Group E).

The impacted input parameters for these sensitivities are shown Table B7. In the E+TrRate- case, inter-regional electricity transmission capacity was limited to a maximum of double today's capacity, down from a maximum of 10x allowed in the original E+ case. In E+ Wind-, the cumulative installed on and off-shore wind capacity in each of the 14 modelled regions was capped at half the level the model deployed wind in these regions in the E+ case. For example, the capacity of onshore wind deployed in the Mid-Atlantic/Great Lakes region is 150 GW in the original E+ case, for which the build cap was originally stipulated to be 270 GW. In E+Wind-, the build cap was therefore set to be 75 GW for the Mid-Atlantic/Great Lakes region. The E+ Tr&Wind- case combines the constraints of E+Wind- and E+TrRate-.

Table B7. Input assumptions that vary between cases in power sector technology build rate / build cap sensitivities

Cumulative build limits	E+	E+ Wind-	E+ TrRate-	E+ Tr&Wind-
Transmission	10x current	10x current	2x current	2x current
Wind (Mid-Atlantic/Great Lakes)	270GW	Half of E+ results	270GW	Half of E+ results

The following can be observed in Figure B36 through Figure B42:

(a) The NPV of all annual energy-supply system costs from 2020-2050 (Figure B36) does not change significantly across any of the sensitivities.

(b) Total electricity load is unchanged between E+ and E+TrRate-, but there is a reduction in load in both E+Wind- and E+ Tr&Wind- cases due to reduced electrolysis (Figure B37). The latter results from the reduced availability of low-cost wind generation.

(c) Figure B38 shows annual electricity generation by resource type. In E+Wind- and E+ Tr&Wind-, the reduced wind generation across the transition period is compensated by a combination of additional solar, new nuclear, and additional gas (without and with CCS). With transmission limits, wind generation decreases somewhat in E+TrRate- and is compensated by some additional solar and gas-fired generation. As shown in Figure B39, all three sensitivity cases include modestly more electric storage capacity than in E+.

(d) The electricity generating capacity mix (Figure B39), average annual installation rates for wind and solar capacity (Figure B40), and average annual installation rates for thermal generating capacity (Figure B41) reflect the trends seen in electricity generation.

(e) Because electrolysis deployment is reduced in E+Wind- and E+ Tr&Wind- cases, H_2 and liquid fuels synthesized using H_2 play smaller roles than in E+, while H_2 production and use is not significantly impacted in E+TrRate-, as shown in Figure B42 for 2050. Meanwhile, the increased use of gas w CC for power generation by 2050 in all three sensitivity cases, but especially in the two cases with lower wind capacity caps, leads to increased CO_2 capture and sequestration (Figure B42).

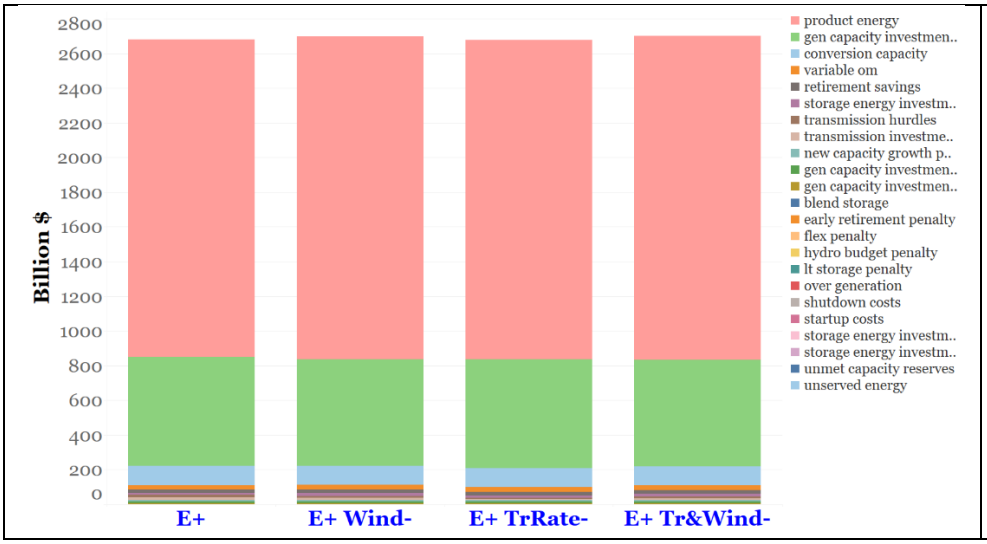

Figure B36. Optimized (minimum) net present value (NPV, 2% discount rate) of the sum of annualized energy-supply system costs from 2020 to 2050 for each scenario. Sunk costs as of 2020 are not included, and costs associated with energy delivery, such as electricity distribution, are also not included in this metric.

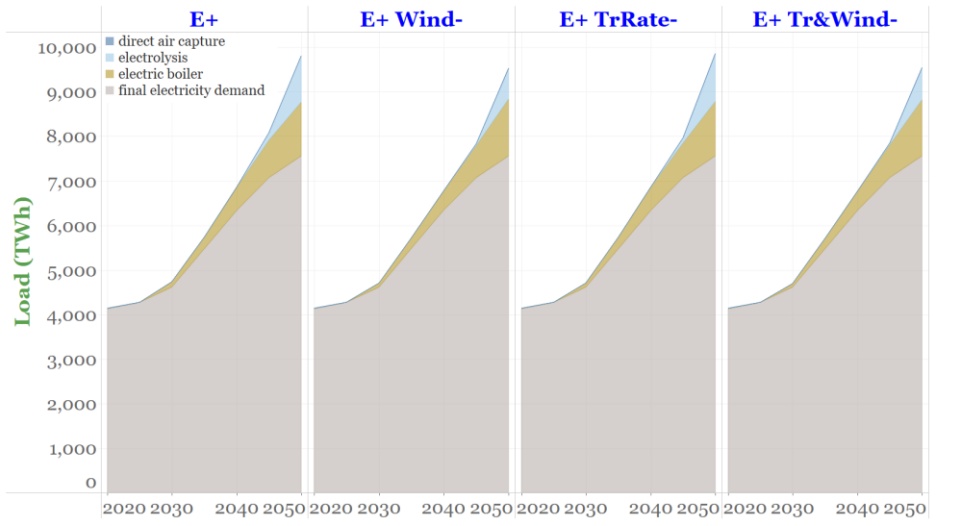

Figure B37. Total electricity load including intermediate, flexibly-operable loads.

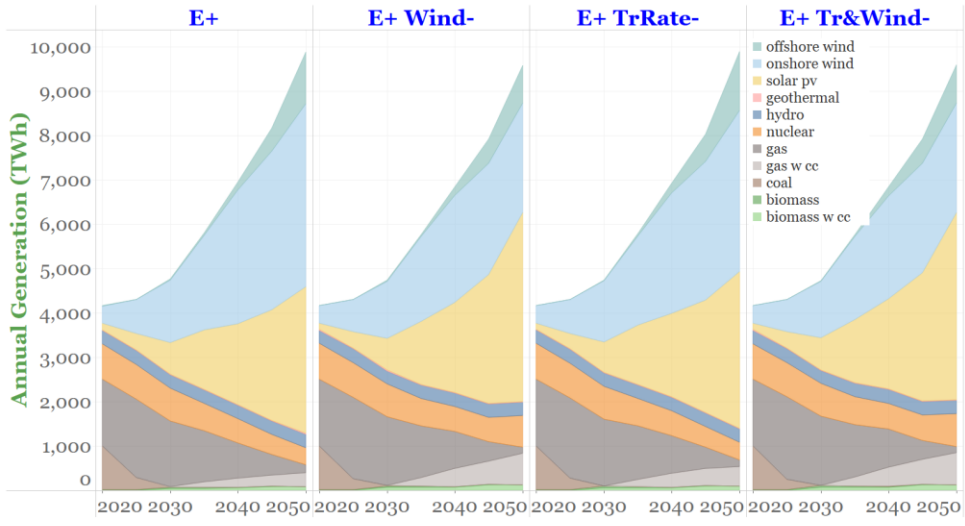

Figure B38. Yearly electricity generation by source.

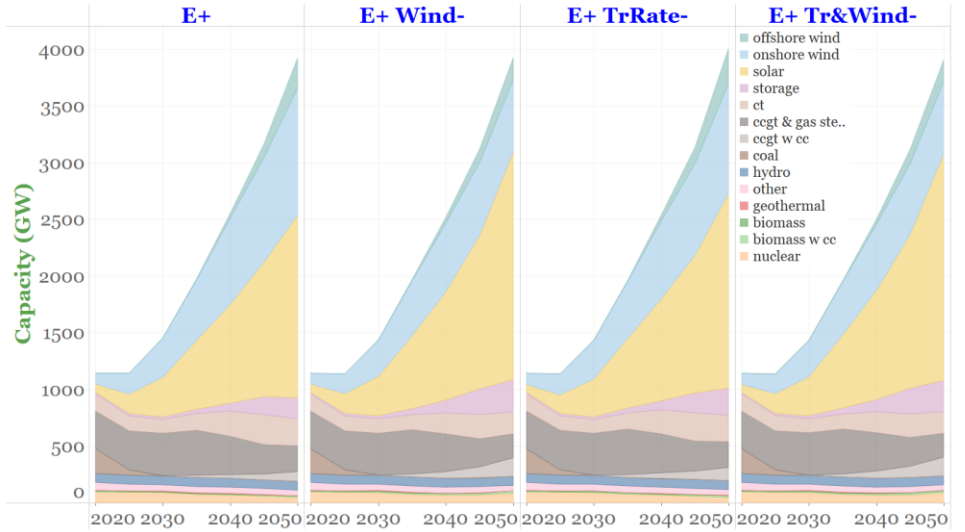

Figure B39. Electricity generating capacity by type of generator.

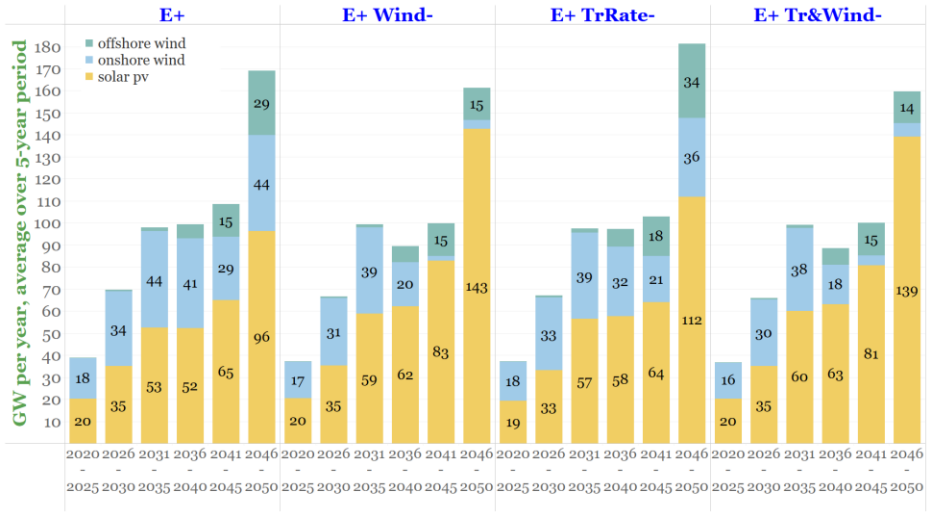

Figure B40. Average annual build rate of solar and wind generating capacity during each five-year period from 2020 through 2050.

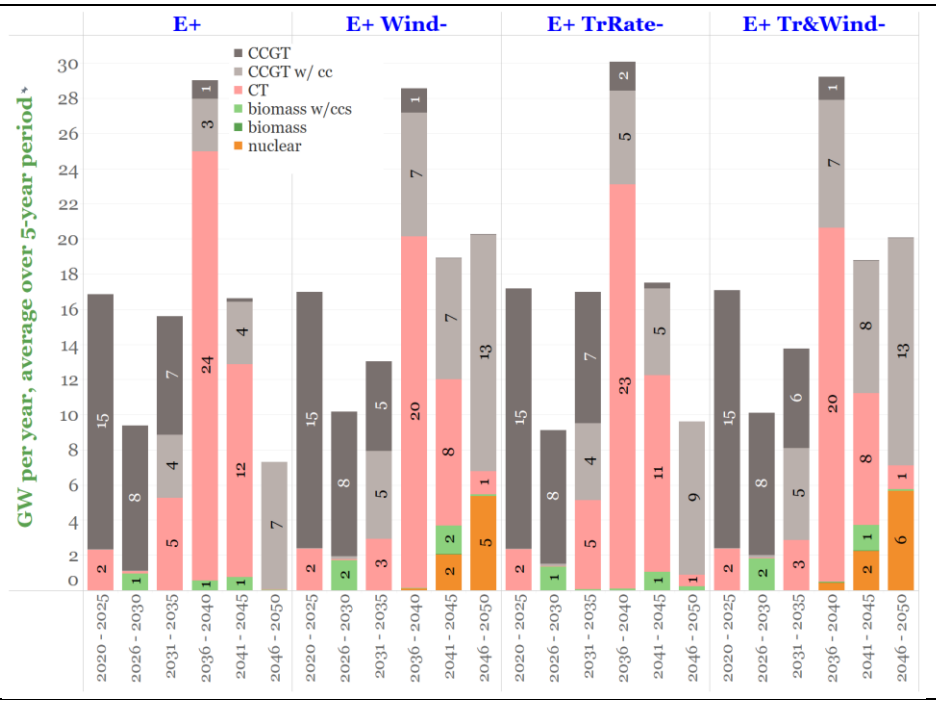

Figure B41. Average annual build rates for dispatchable thermal generating capacity during each five-year period from 2020 through 2050.

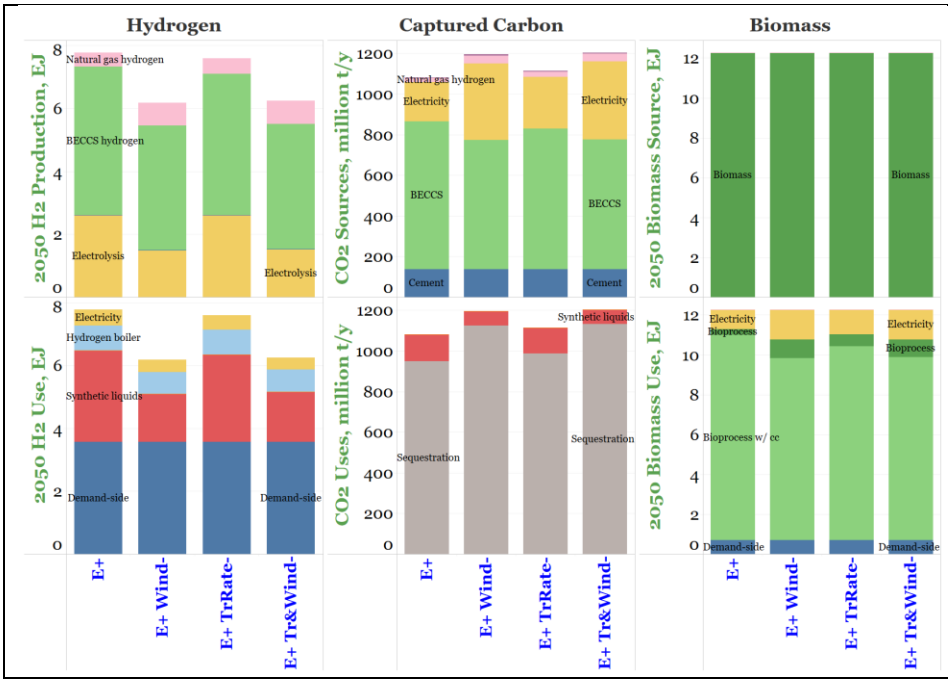

Figure B42. Production (top) and use (bottom) of hydrogen, captured carbon and biomass in 2050.

3.6 Hydrogen turbines

Using hydrogen as a gas turbine fuel in place of natural gas allows gas turbines to play continuing roles in net-zero emissions pathways. In the E+ scenario, hydrogen blending into methane for use in gas turbines is allowed starting in 2035, with caps placed on the fraction of the fuel (HHV basis) that can be H_2: 15% in 2035, increasing to 30%, 45% and 60% in 2040, 2045 and 2050, respectively. Higher hydrogen limits than these may become feasible, given that major turbine manufacturers today are pursuing development of high-hydrogen machines [12]. To test the impact of higher hydrogen blends, the E+H_2Turbine sensitivity lifts the blend caps on H_2 in gas turbine fuel to 33%, 66%, and 100% in 2035, 2040, 2045-2050, respectively (Table B8).

Table B8. Input assumptions that vary between cases in H2 turbine sensitivities

	E+	E+H_2Turbine
H2 fractional limit in fuel mix to gas turbines (2020,2025,2030,2035,2040,2045,2050)	0,0,0,0.15,0.3,0.45,0.6	0,0,0.33,0.66,1,1,1

There are no discernable differences in Figure B43 through Figure B47, which compare various features of the E+ and E+H_2Turbine cases. Figure B48 shows slightly higher H_2 production in E+H_2Turbine by 2050, with increased contributions from both biomass with CO_2 capture and autothermal reforming with CO_2 capture. The figure also shows H_2 use for electricity generation increases significantly in this case, indicating its attractiveness for this purpose.

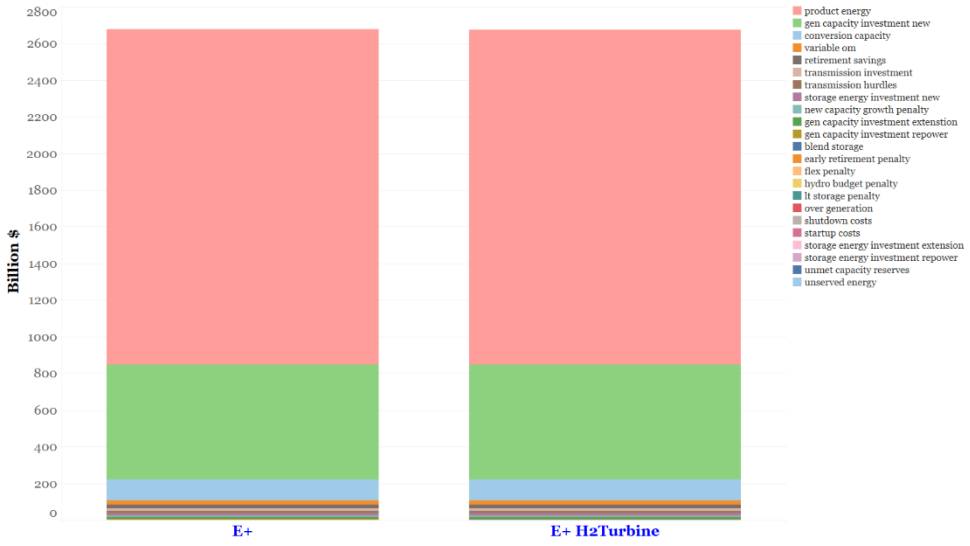

Figure B43. Optimized (minimum) net present value (NPV, 2% discount rate) of the sum of annualized energy-supply system costs from 2020 to 2050 for each scenario. Sunk costs as of 2020 are not included, and costs associated with energy delivery, such as electricity distribution, are also not included in this metric.

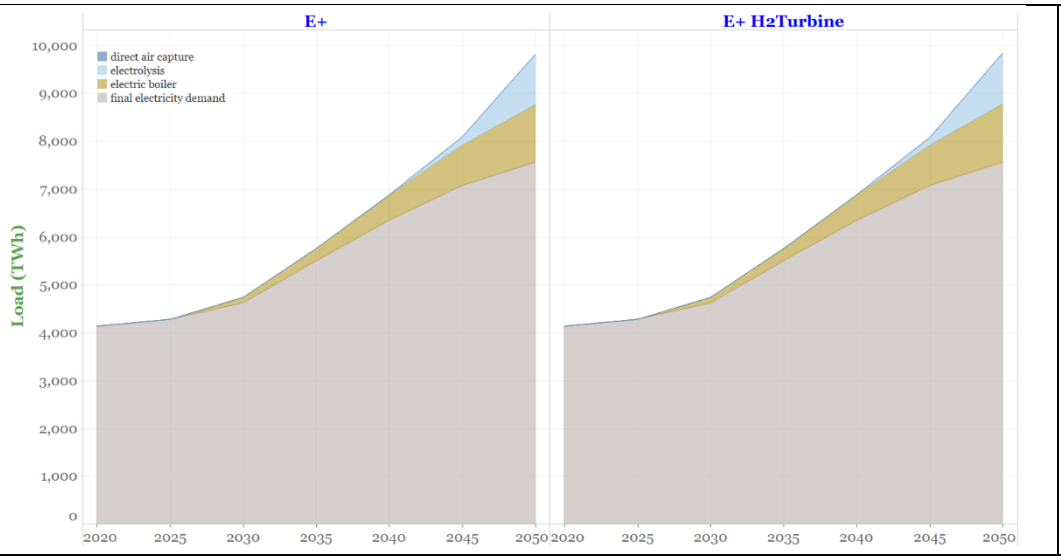

Figure B44. Total electricity load including intermediate, flexibly-operable loads.

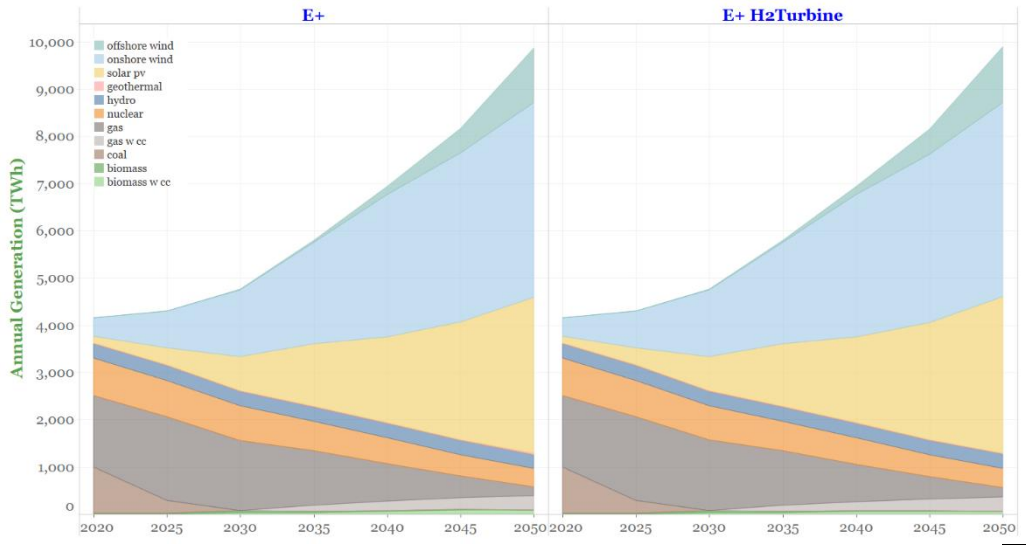

Figure B45. Yearly electricity generation by source.

Figure B46. Average annual build rate of solar and wind generating capacity during each five-year period from 2020 through 2050.

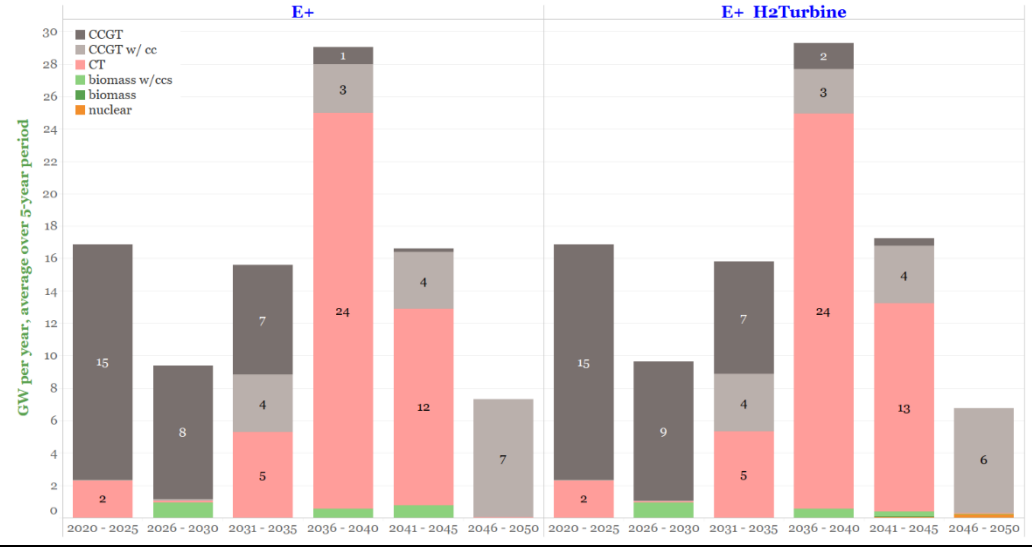

Figure B47. Average annual build rates for dispatchable thermal generating capacity during each five-year period from 2020 through 2050.

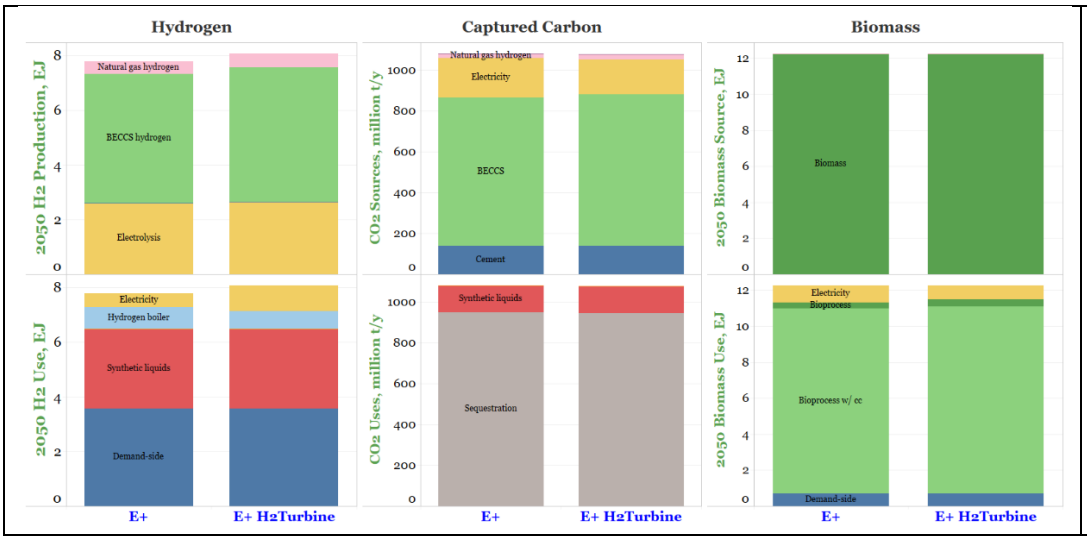

Figure B48. Production (top) and use (bottom) of hydrogen, captured carbon and biomass in 2050.

3.7 Flexible load options

Electricity-using technologies that operate flexibly are important features of the RIO model. These include Table B1 (Group G): intermediate-demand technologies that operate with hourly flexibility, namely electrolysis and electric boilers in industry, and end-use technologies that can time-shift when they draw power, namely electric vehicles when charging and residential and commercial water heating.

Flexible intermediate-demand technologies

RIO allows electrolysis and electric boilers in industry to be turned on or turned off for any given hour of the year so as to minimize total energy system costs over the full 30-year transition. In the case of electric boilers, these would be installed in parallel with gas-fired units; the least costly to run of the two options during each hour of the year is the option that RIO chooses to run. Because the application of these technologies in this manner is not practiced widely today, if at all, and future cost and performance under commercial conditions is far from certain, we designed two sensitivities to assess the impact of not having these options available in the mix of technologies that RIO can choose to deploy: "E+ No Electrolysis" and "E+ No Electrolysis No E-boiler" (Table B9).

Table B9. Input assumptions that vary between cases in flexible intermediate-load sensitivities

	E+	E+ No Electrolysis	E+ No Electrolysis No E-boiler
Electrolysis technology available?	Yes	No	No
E-Boiler technology available?	Yes	Yes	No

Results from the sensitivity runs are shown in Figure B49 through Figure B56:

(a) The NPV of total annual energy-supply system costs from 2020 to 2030 (Figure B49) is effectively unchanged in E+ No Electrolysis relative to E+, reflecting the small contribution that electrolysis makes to overall costs. It slightly increases in E+ No Electrolysis No E-boiler, which can be attributed to the greater expense on balance of additional boiler fuel replacing low-cost electricity used in E+.

(b) Bulk electricity load does not change across scenarios, but total electricity demand, including electrolysis and e-boiler loads decreases (Figure B50). The decrease is compensated to a small degree by additional demand for direct air capture (DAC), which RIO allows to operate with daily, but not hourly, flexibility and so is not able to exploit the use of low-cost electricity to the same extent as electrolysis or e-boilers. Additional factors driving DAC deployment are discussed in bullet (d) below.

(c) Annual solar and wind electricity generation decrease in both sensitivity cases (Figure B51) due to the reduction or complete elimination of hourly flexible demands that help balance solar and wind variability. Gas generation w CC takes on correspondingly greater balancing roles. Installed generating capacities (Figure B52) and annual average build rates for wind, solar electricity, and gas w CC (Figure B53 and Figure B54) reflect the changes in generation noted above.

(d) Variations from the E+ scenario are significant in the sensitivity cases in 1) how H_2 is produced and used and 2) what technologies are used to capture CO_2, as well as the total amount of CO_2 captured (Figure B55). In E+ No Electrolysis total hydrogen production is reduced by almost as much as the electrolytic production in E+; an increase in natural gas reforming with CO_2 capture compensates for some of the reduced electrolytic production. The corresponding reduction in H_2 uses is almost entirely in synthetic fuels production. Less zero-carbon synthetic fuel is generated and more fossil-derived diesel is used, in addition to the added pipeline gas used for hydrogen generation (Figure B56). The greater use of fossil fuels in turn drives the need for more DAC and CO_2 sequestration (Figure B55) to offset unavoidable emissions from the added fossil sources. Perhaps surprisingly, in E+ No Electrolysis No E-boiler, total hydrogen production is higher than in E+, with a large increase in natural gas reforming with CO_2 capture as the source. In this sensitivity, because E-boilers are not available, RIO chooses to burn a large fraction of the produced hydrogen to make industrial steam. The large hydrogen production from natural gas, during which about 5% of the byproduct CO_2 is not captured, drives the need for even more DAC and CO_2 sequestration than in E+ No Electrolysis (Figure B55).

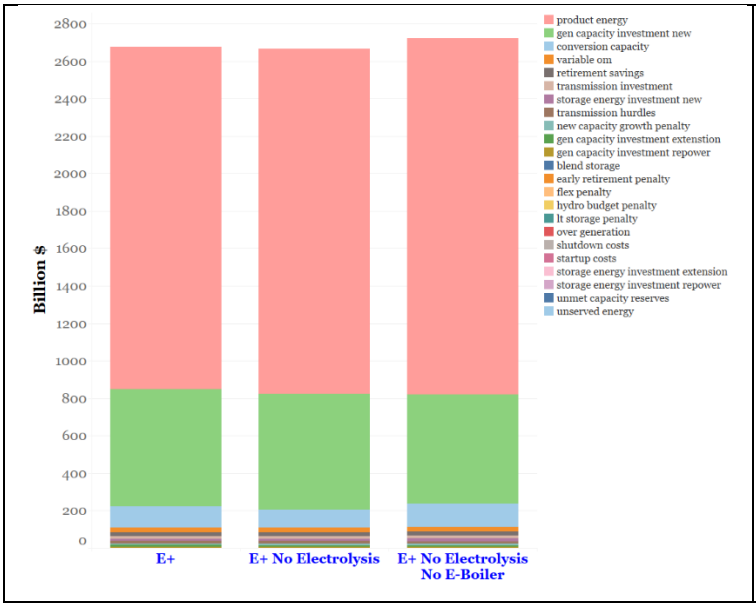

Figure B49. Optimized (minimum) net present value (NPV, 2% discount rate) of the sum of annualized energy-supply system costs from 2020 to 2050 for each scenario. Sunk costs as of 2020 are not included, and costs associated with energy delivery, such as electricity distribution, are also not included in this metric.

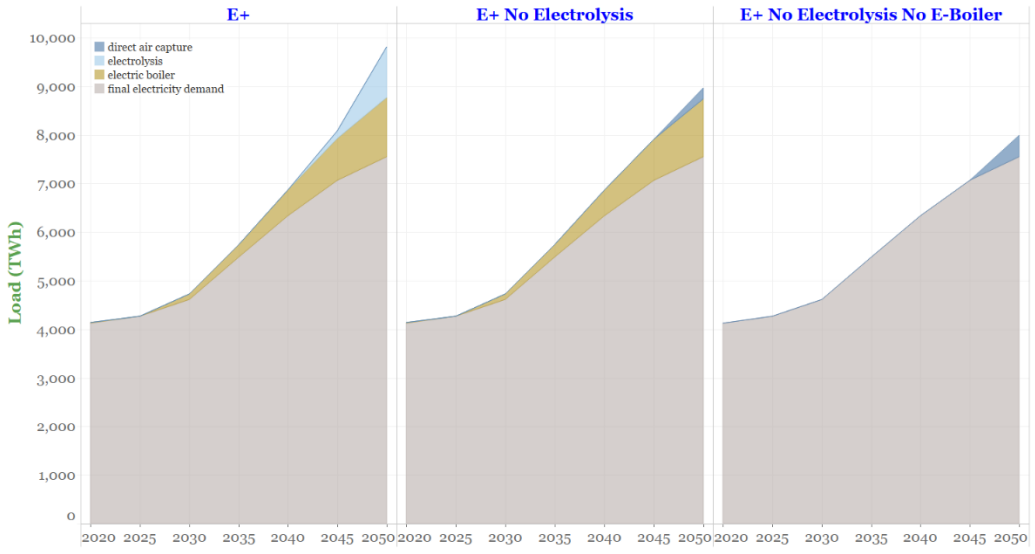

Figure B50. Total electricity load including intermediate, flexibly-operable loads.

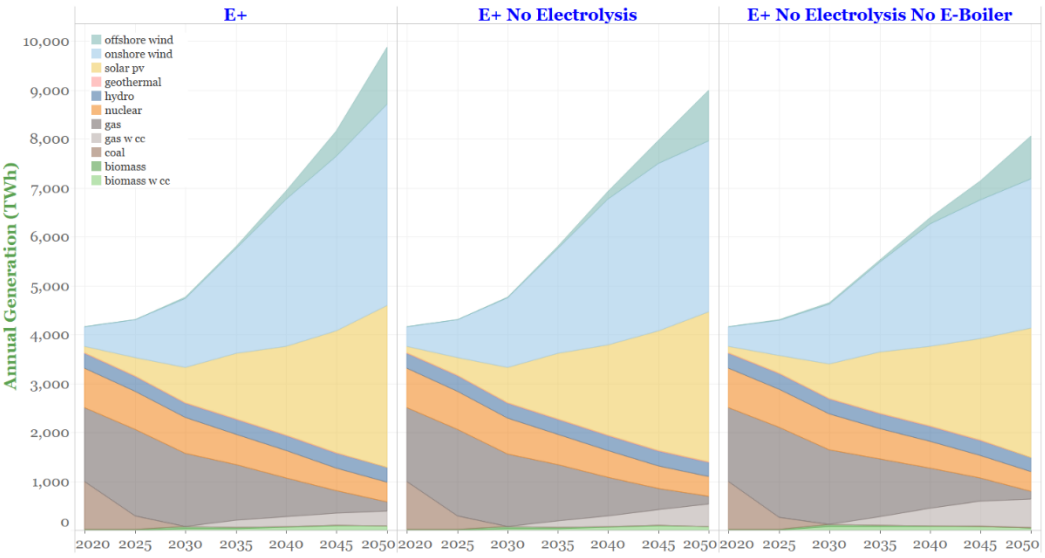

Figure B51. Yearly electricity generation by source.

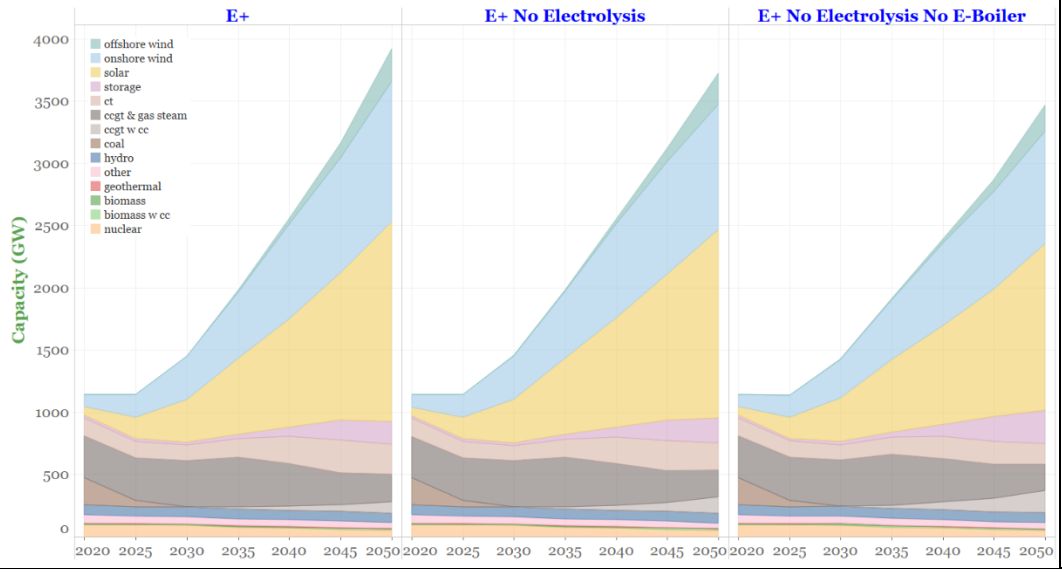

Figure B52. Electricity generating capacity by type of generator.

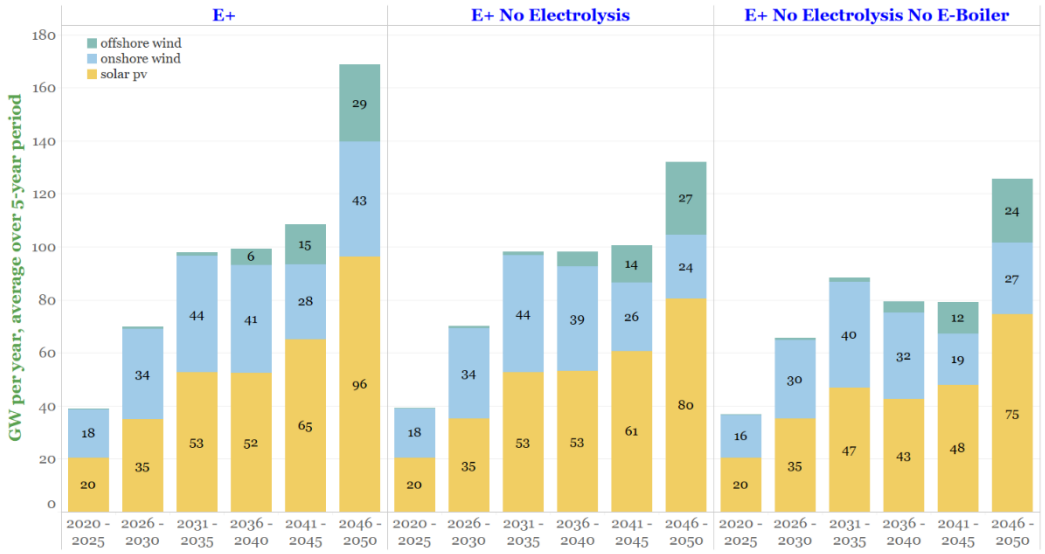

Figure B53. Average annual build rate of solar and wind generating capacity during each five-year period from 2020 through 2050.

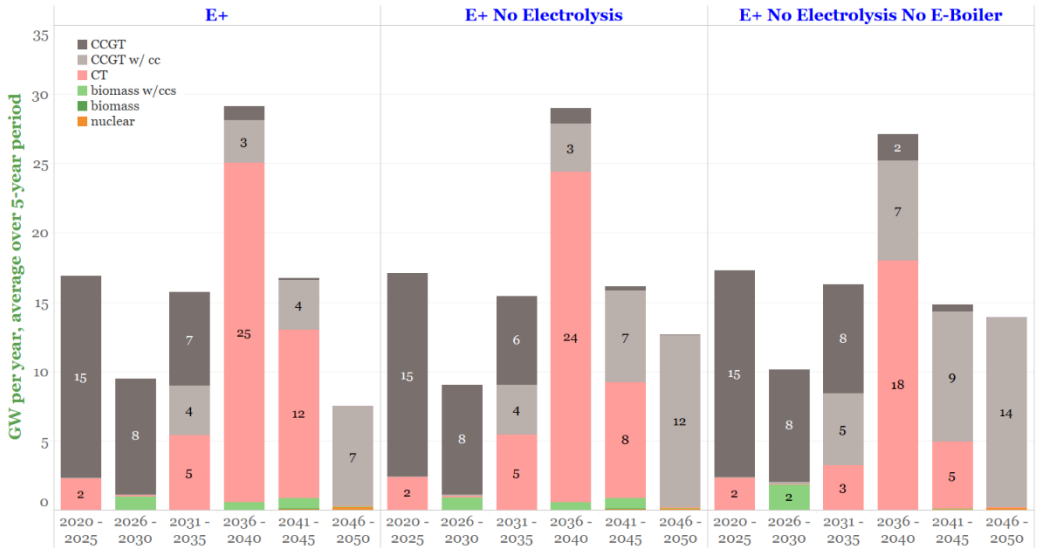

Figure B54. Average annual build rates for dispatchable thermal generating capacity during each five-year period from 2020 through 2050.

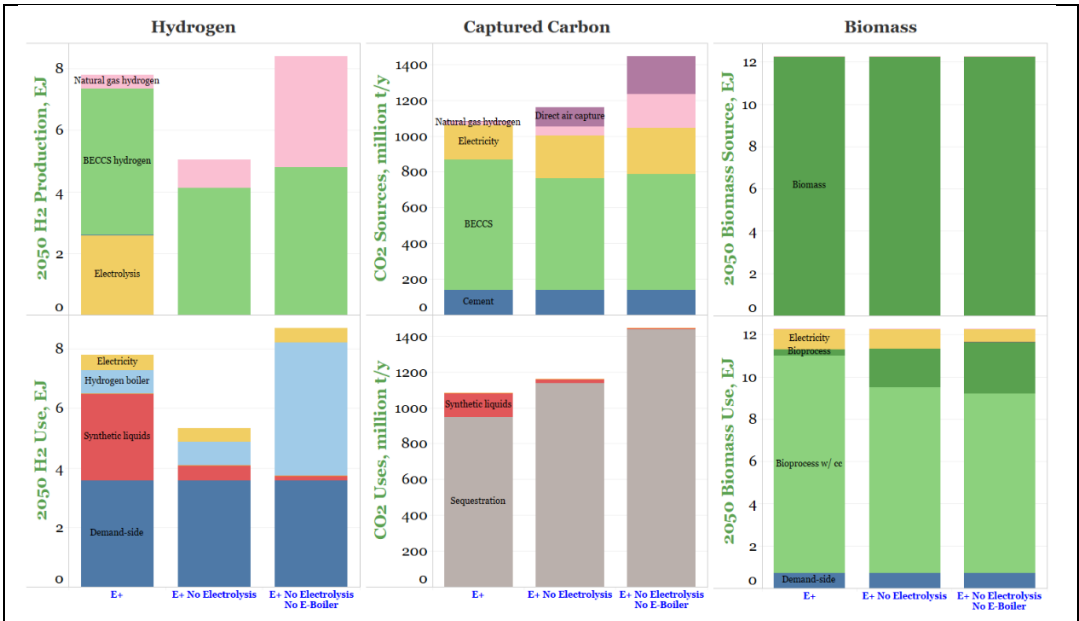

Figure B55. Production (top) and use (bottom) of hydrogen, captured carbon and biomass in 2050.

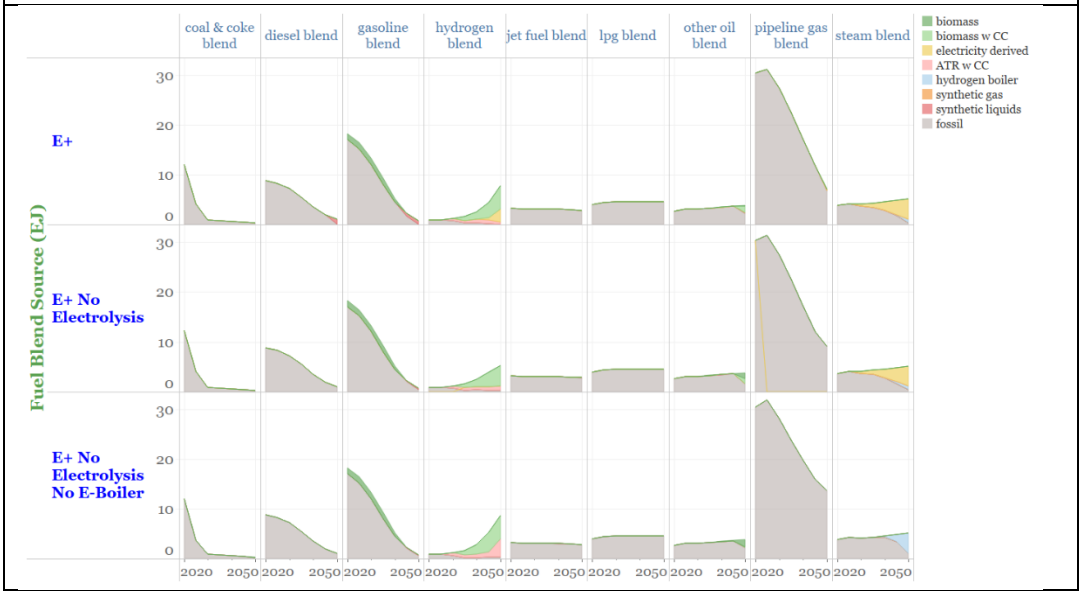

Figure B56. End-use fuels and steam consist of components that originate from different sources. The components of each fuel blend (and steam) are shown here by their source.

Flexible end-use technologies

With the high degree of vehicle and building electrification in our scenarios, the temporal patterns of electricity use in these sectors becomes an important factor in determining peak electricity loads, which in turn determine the electricity generating capacity needed. To allow for the possibility of reducing peak loads, RIO allows for up to 50% of electric vehicles to delay charging by up to five hours from a baseline charging profile that is considered "native" charging behavior. Native behavior assumes that vehicle charging begins in the early evening when people return home from work. In the case of electric water heaters in the residential and commercial sectors, taking advantage of the considerable heat capacity of water, RIO allows 20% of electric water heaters to delay or advance their electricity use by up to 2 hours from an assumed native use pattern.

To test the impact of these load-shifting measures on modeling results, two sensitivities of the E+ case were run. In one case, the option to time-shift loads for EVs and water heaters was disabled completely (E+EVflex0). In the second case, the fraction of the EV and water-heating fleets that were allowed to time shift was doubled – to 100% for EVs and to 40% for water heaters (E+EVflex+). See Table B10.

Table B10. Input assumptions that vary between cases in flexible end-use load sensitivities

Time-shifting from native profile for	E+	E+EVflex0	E+EVflex+
EV charging	50% of load may shift up to 5 hrs later	No shifting allowed	100% of load may shift up to 5 hours later
Electric water heating	20% of load may shift up to ± 2 hrs	No shifting allowed	40% of load may shift ± 2 hours

In terms of system cost (Figure B57), electricity loads (Figure B58), generation (Figure B59), and wind and solar capacity build rates (Figure B60), there are no significant differences between the original E+ case and either of the two variants.

The only features of the energy system where impacts are visible are in the technologies that provide the capability to balance variable wind and solar generation. The E+EVflex0 case builds combustion turbines at a greater rate in the middle of the transition period (Figure B61) and more battery storage throughout the transition (Figure B63). In contrast, E+EVflex+ shows modestly lower investments in combustion turbines and batteries.

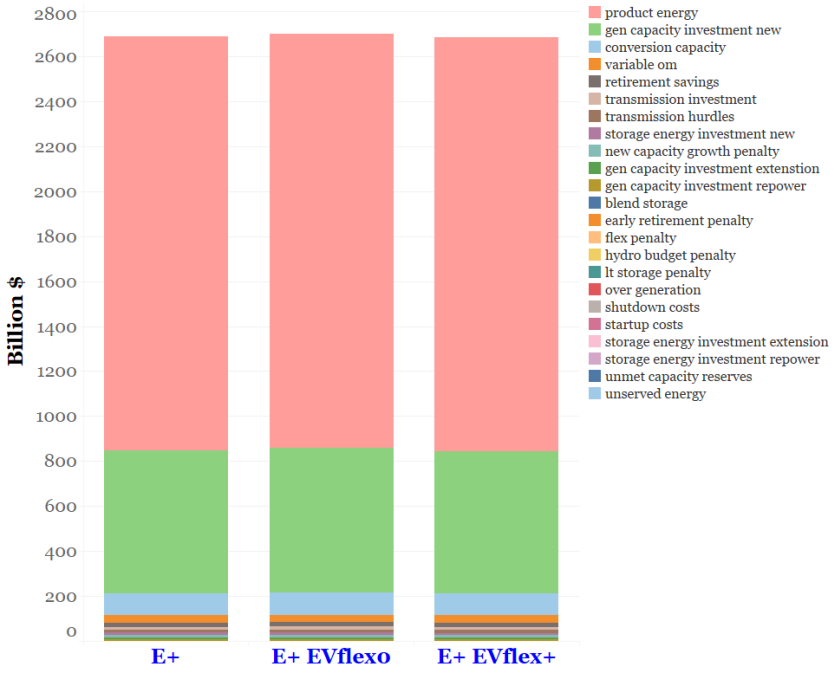

Figure B57. Optimized (minimum) net present value (NPV, 2% discount rate) of the sum of annualized energy-supply system costs from 2020 to 2050 for each scenario. Sunk costs as of 2020 are not included, and costs associated with energy delivery, such as electricity distribution, are also not included in this metric.

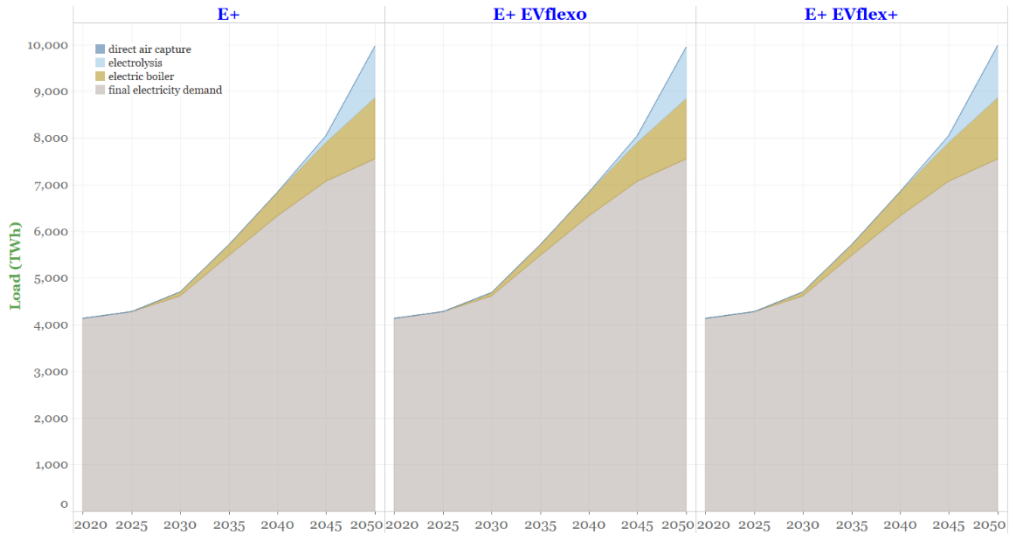

Figure B58. Total electricity load including intermediate, flexibly-operable loads.

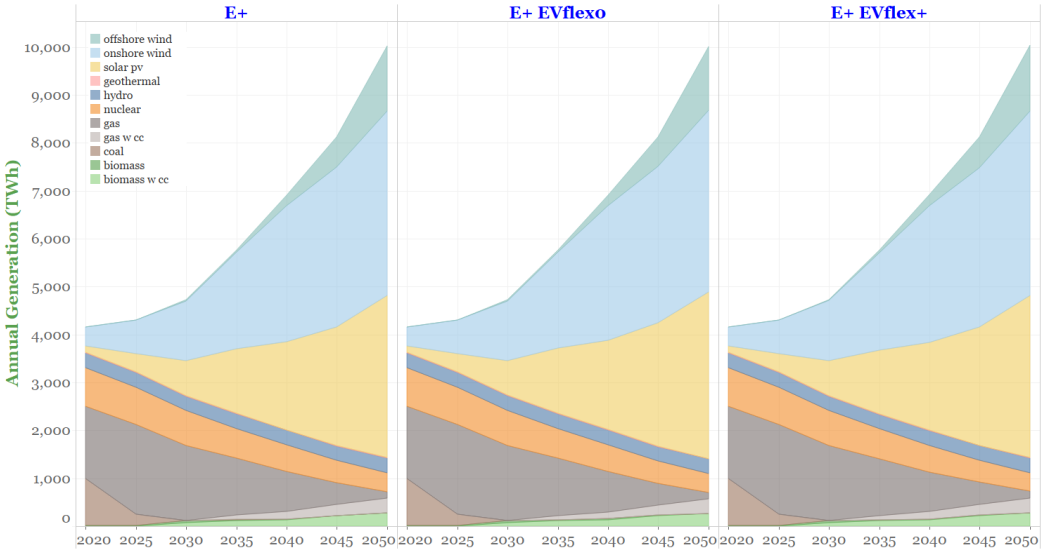

Figure B59. Yearly electricity generation by source.

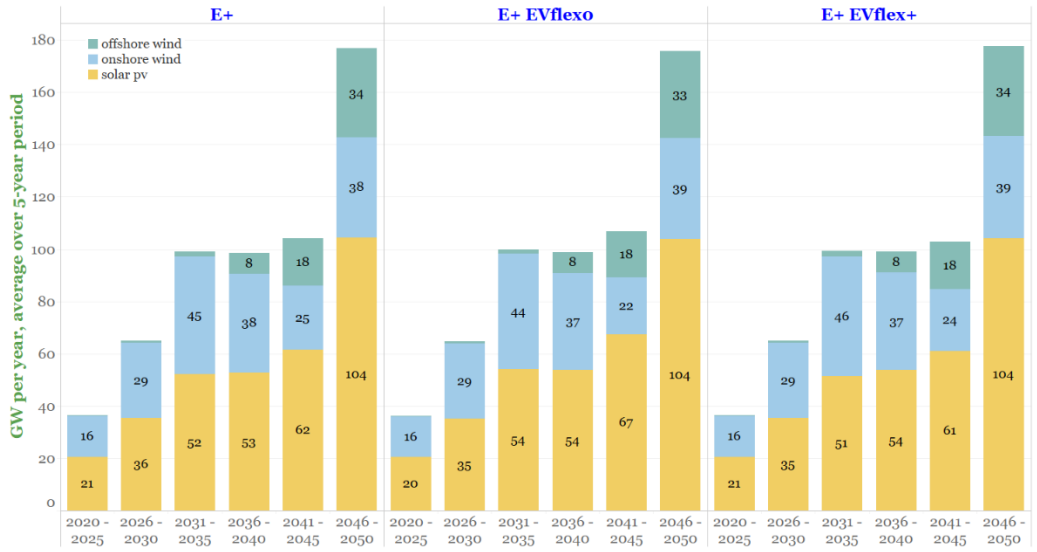

Figure B60. Average annual build rate of solar and wind generating capacity during each five-year period from 2020 through 2050.

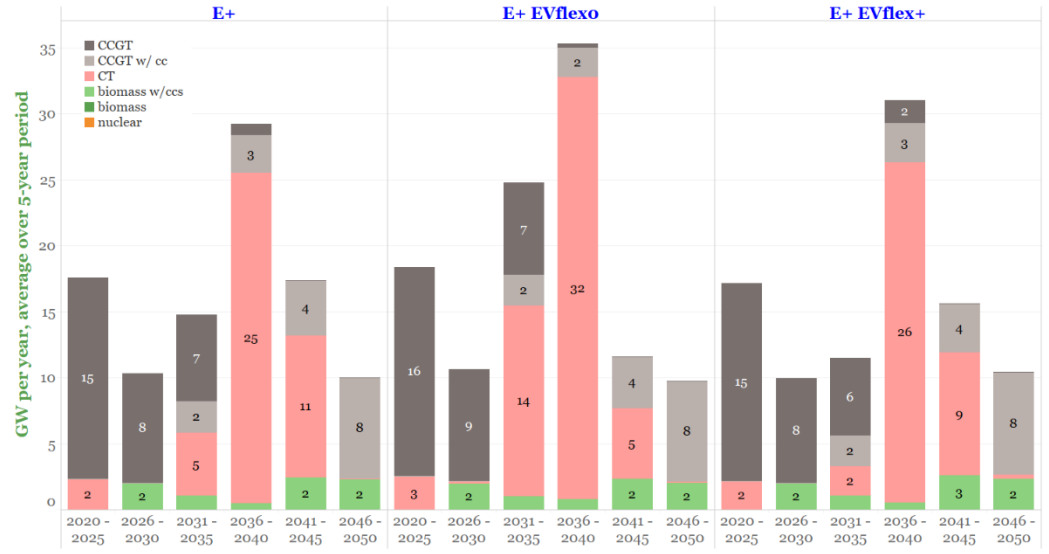

Figure B61. Average annual build rates for dispatchable thermal generating capacity during each five-year period from 2020 through 2050.

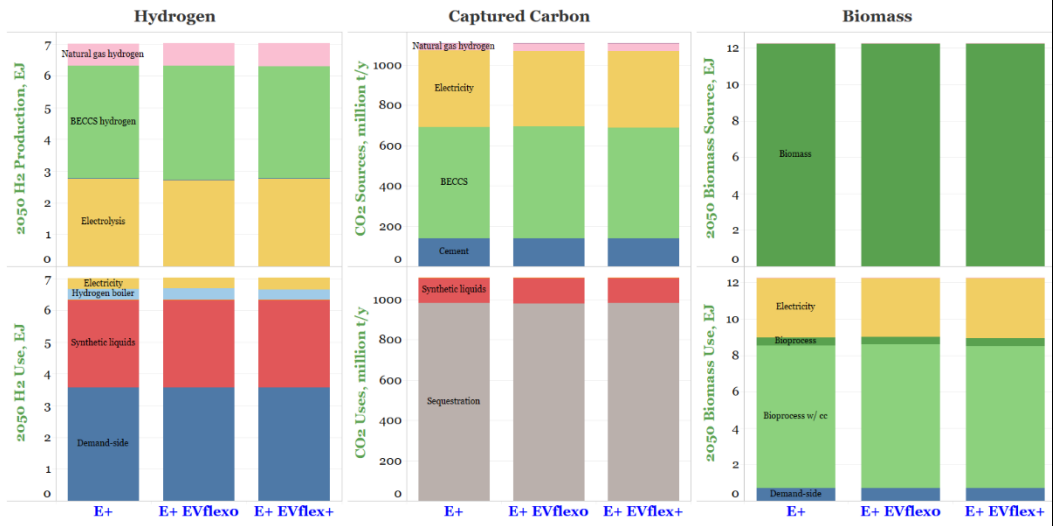

Figure B62. Production (top) and use (bottom) of hydrogen, captured carbon and biomass in 2050.

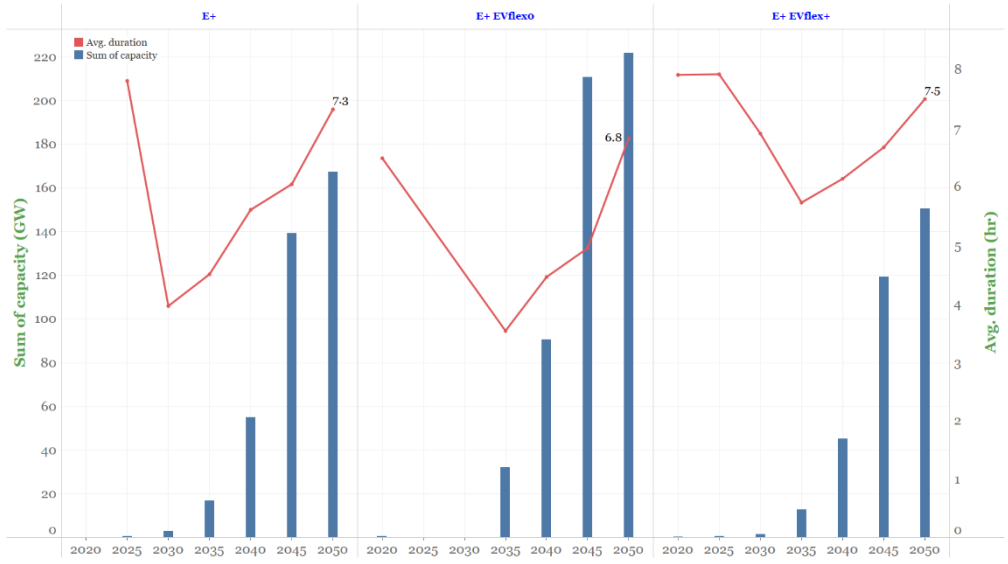

Figure B63. Installed battery capacity and average battery duration.

3.8 H_2 production capital costs

Given the key role of hydrogen in net-zero pathways and uncertainties as to future capital costs for hydrogen production technologies, we designed eight sensitivities to explore the impact of different H_2 production capital cost assumptions (Table B1, Group H). In RIO, there are three technology options for making low-, zero-, or negative-carbon H_2 [13]: autothermal reforming of natural gas with CO_2 capture (ATR), biomass gasification to H_2 with CO_2 capture ($BioH_2$), and water splitting using electricity (electrolysis). We ran sensitivities for capital costs of +50% and -30% for ATR and $BioH_2$, relative to costs assumed in the E+ scenario. We also designed two sensitivities for lower electrolysis cost projections, allowing for more aggressive capital cost reductions that have been suggested as possible [14,15] in part because of the modular nature of electrolysis. We additionally include here results for a case with no BECCS-H_2 technology option (E+NoBioH_2) and the E+NoElectrolysis case replicated here from Section 3.7. See Table B11.

Table B11. Input assumptions that vary between cases. Values here are the values in 2050 (in 2018US$). These capital costs are fixed across the full 30-year modeling period, except for electrolysis, which is assumed to see significant cost reductions over time. For example, the capital cost for electrolysis in the initial model year (2020) in the E+ scenario is 1862 $/kW$_{H2,HHV}$. Electrolysis costs in 2020 for the lower electrolysis-cost sensitivity cases shown in this table are correspondingly lower.

$/kW$_{H2,HHV}$	E+	E+BioH_2+	E+BioH_2-	E+NoBioH_2	E+ATR+	E+ATR-	E+ Electrolysis-	E+ Electrolysis--	E+NoElectrolysis
BECCS-H_2	2,700	4,050	2,160	--	2,700	2,700	2,700	2,700	2,700
ATR-CCS	813	813	813	813	1,221	651	813	813	813
Electrolysis	572	572	572	572	572	572	220	96	--

Results from all eight sensitivities are shown in Figure B64 through Figure B69.

One observes that the NPV of all annual energy-supply system costs (Figure B64) from 2020-2050 is not significantly different from that of E+ for any of the sensitivity cases, except E+NoBioH_2. The cost is higher in that case as a result of the deployment of more costly fuel conversion facilities to replace BECCS-H_2. In particular, there is greater deployment of electrolysis (Figure B65) and greater wind and solar generation drive electrolysis (Figure B66), as well as greater deployment of ATR-CCS to supply needed H_2 (Figure B69).

The cases with lower electrolysis costs deploy slightly more electrolysis than in E+, as might be expected (Figure B65), and correspondingly slightly more wind and solar generation (Figure B66). Slightly more hydrogen is produced and used in these cases (Figure B69).

None of the results are sensitive to the assumed ATR-CC costs. However, results are sensitive to the BECCS-H_2 cost assumptions. When these costs are lower (E+BioH_2-) nearly all biomass is used for H_2 production, and total H2 produced and used is higher than in E+ (Figure B69). When BECCS-H_2 costs are higher (E+BioH_2+), relatively little biomass is converted to H_2, and there is considerably less hydrogen produced and used in total. H_2 that is produced is primarily via increases in ATR and electrolytic H_2 (Figure B69). In E+BioH_2+ there is more significant amount of deployment of biopower with CO_2 capture (Figure B66), which enables biomass to continue to provide negative emissions comparable to those that can be produced by BECCS-H_2. Similar increases in biomass power with CO_2 capture can be seen in cases with lower electrolysis

costs because electrolytic H_2 is favored over BECCS-H_2 for minimizing system costs in those cases.

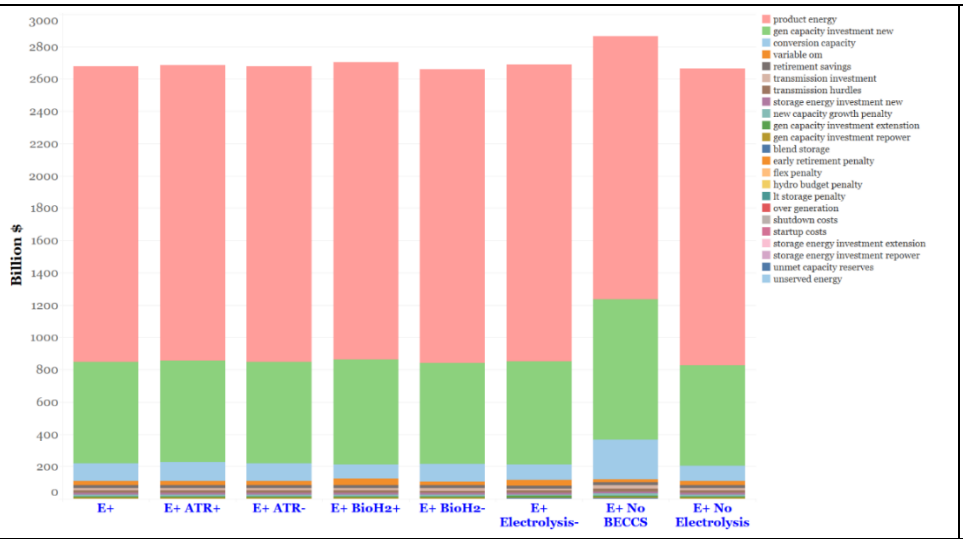

Figure B64. Optimized (minimum) net present value (NPV, 2% discount rate) of the sum of annualized energy-supply system costs from 2020 to 2050 for each scenario. Sunk costs as of 2020 are not included, and costs associated with energy delivery, such as electricity distribution, are also not included in this metric.

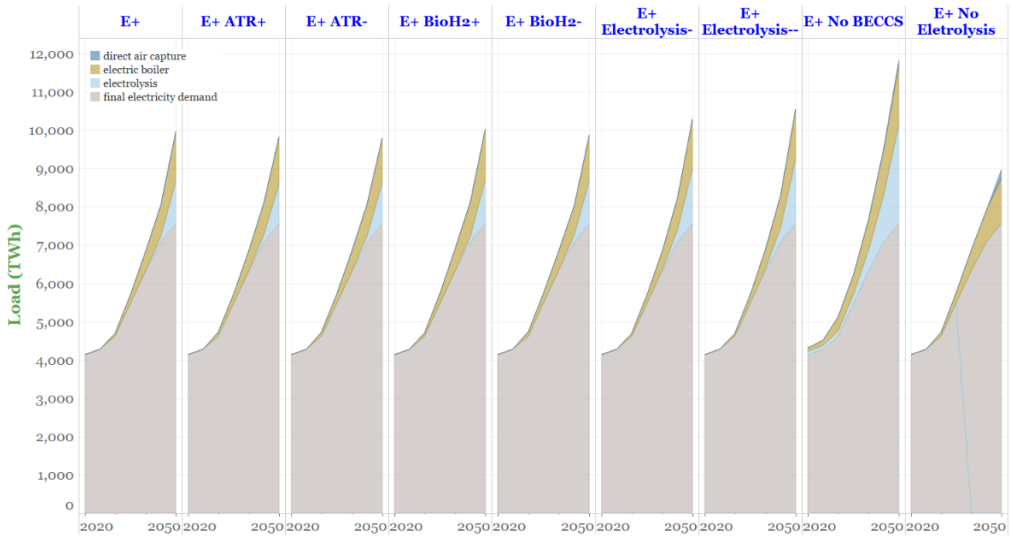

Figure B65. Total electricity load including intermediate, flexibly-operable loads.

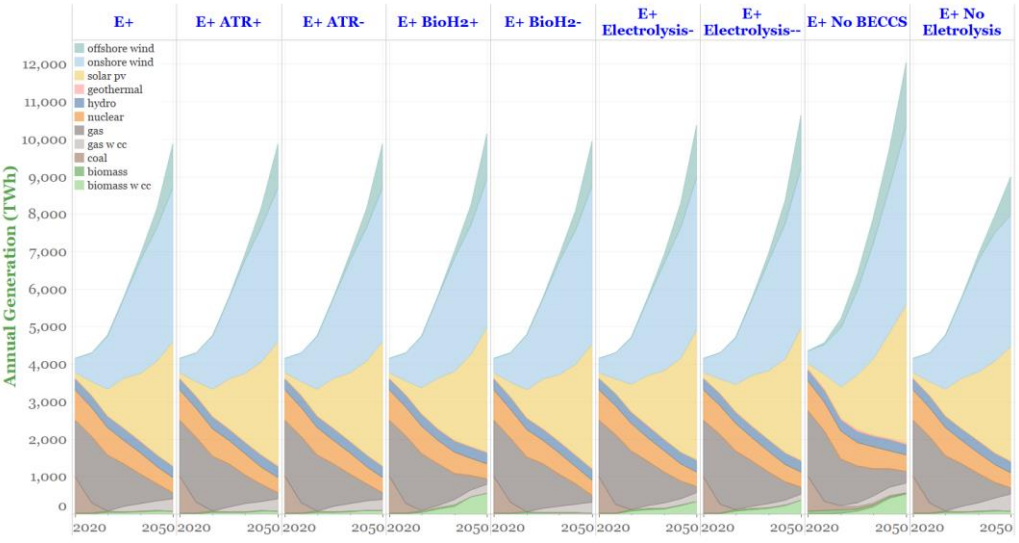

Figure B66. Yearly electricity generation by source.

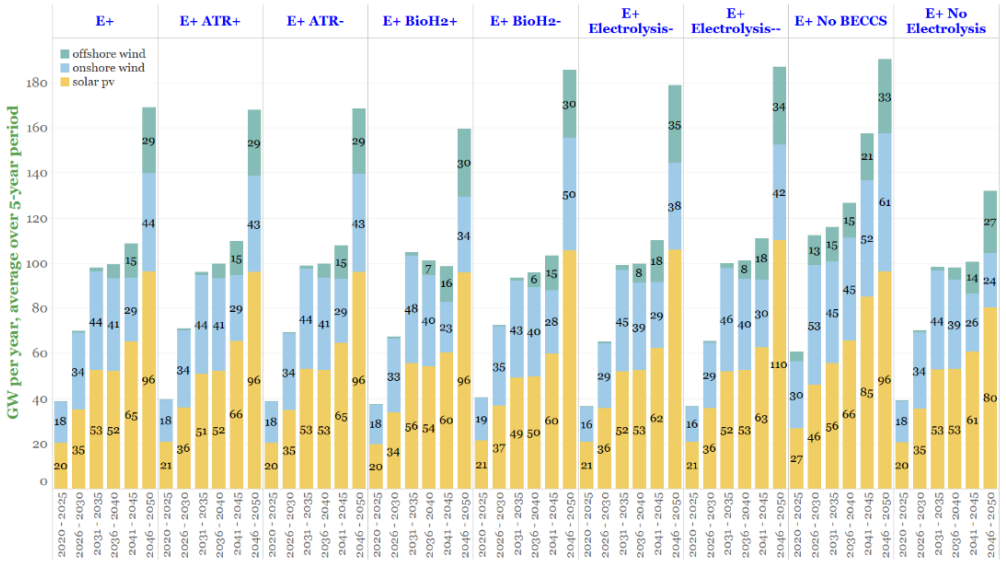

Figure B67. Average annual build rate of solar and wind generating capacity during each five-year period from 2020 through 2050.

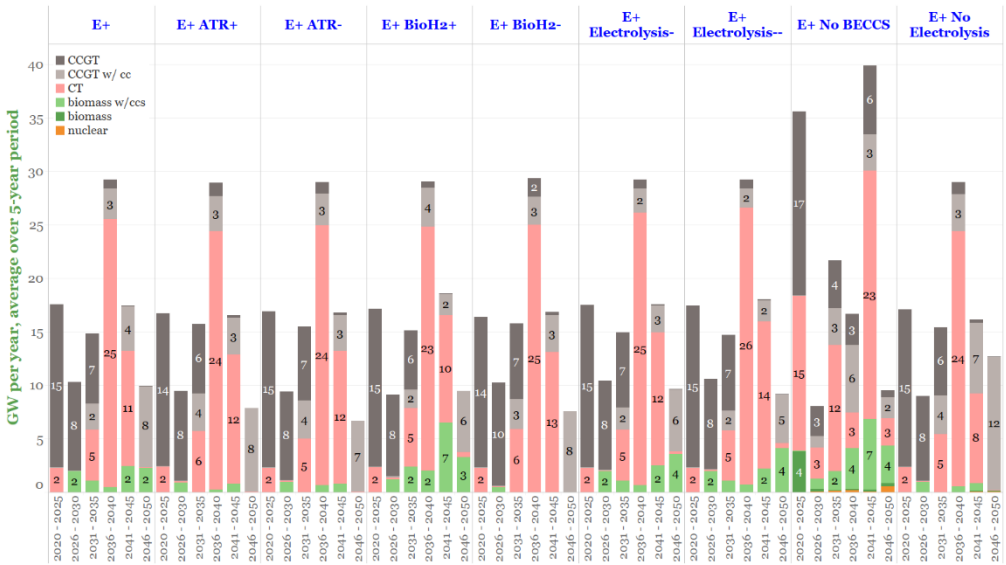

Figure B68. Average annual build rates for dispatchable thermal generating capacity during each five-year period from 2020 through 2050.

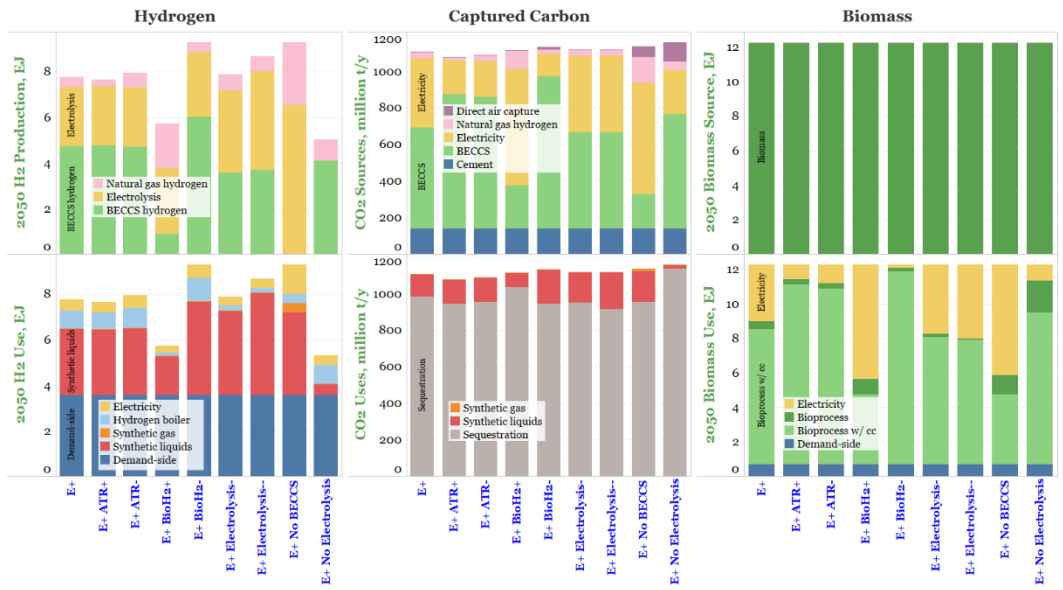

Figure B69. Production (top) and use (bottom) of hydrogen, captured carbon and biomass in 2050.

3.9 Liquid Fuels (Fischer-Tropsch) production capital costs

As with other technologies represented in the model results, future capital costs for technologies producing liquid fuels are uncertain. We ran four cases (Table B1, Group I) to test the sensitivity of results to these costs. The sensitivities considered capital costs that are +50% or -20% of those assumed for the E+ scenario for the two technology options in our model that can produce zero- or negative- carbon emissions Fischer-Tropsch fuels. The choice of +50%/-20% is consistent with accuracy guidelines for Class 4 to Class 5 cost estimates for projects (screening to feasibility study level) published by AACE International [9]. One technology gasifies biomass and converts the resulting syngas into liquids while capturing by-product CO_2. The other converts inputs of H_2 and CO_2 into liquid fuel. See [13] for discussion of these technologies. Table B12 gives the assumed input changes for the sensitivity cases.

Table B12. Input assumptions that vary between cases in liquid fuel production capital cost sensitivities

$/kWout,HHV in 2050	E+	E+ BioFT+	E+ BioFT-	E+FTS+	E+FTS-
Fischer-Tropsch synthesis	1,155	1,155	1,155	1,732	924
Biomass FT capital cost	3,962	5,984	3,172	3,962	3,962

As seen in Figure B70 through Figure B75, changing capital costs for the BioFT technology has no discernable impact compared with E+. With lower Fischer-Trospsh Synthesis (FTS) costs, the only observable differences from E+ are a slight increase in electricity demand for electrolysis (Figure B71), a corresponding slight increase in electricity generation from wind and solar (Figure B72), and a corresponding increase in synthetic liquid fuel production (Figure B75). With higher FTS costs, there are slight decreases in each of these three features of the transition relative to E+.

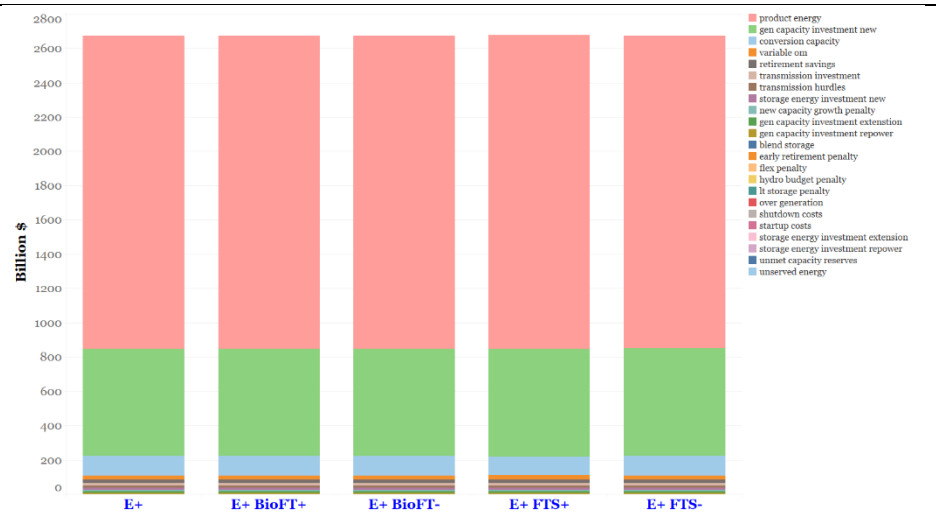

Figure B70. Optimized (minimum) net present value (NPV, 2% discount rate) of the sum of annualized energy-supply system costs from 2020 to 2050 for each scenario. Sunk costs as of 2020 are not included, and costs associated with energy delivery, such as electricity distribution, are also not included in this metric.

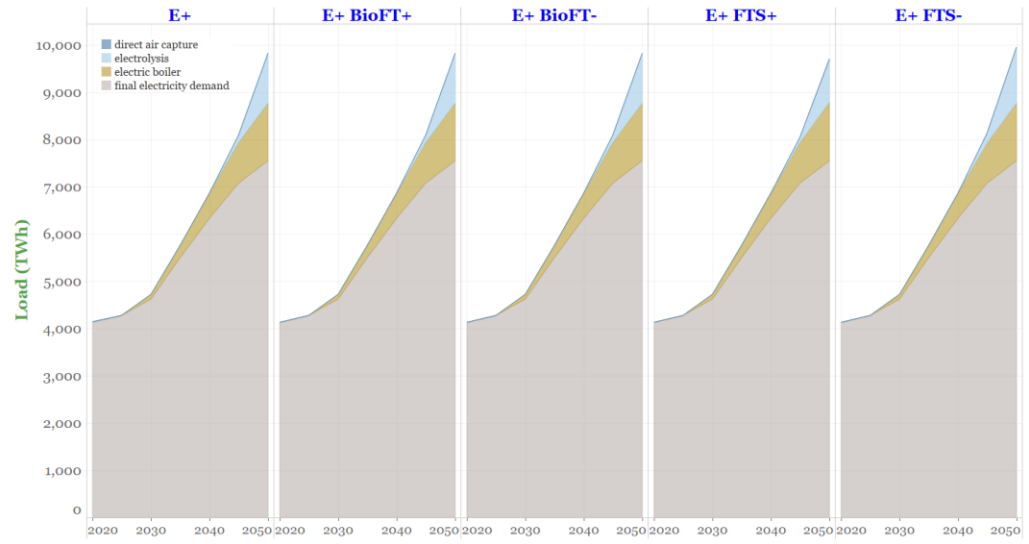

Figure B71. Total electricity load including intermediate, flexibly-operable loads.

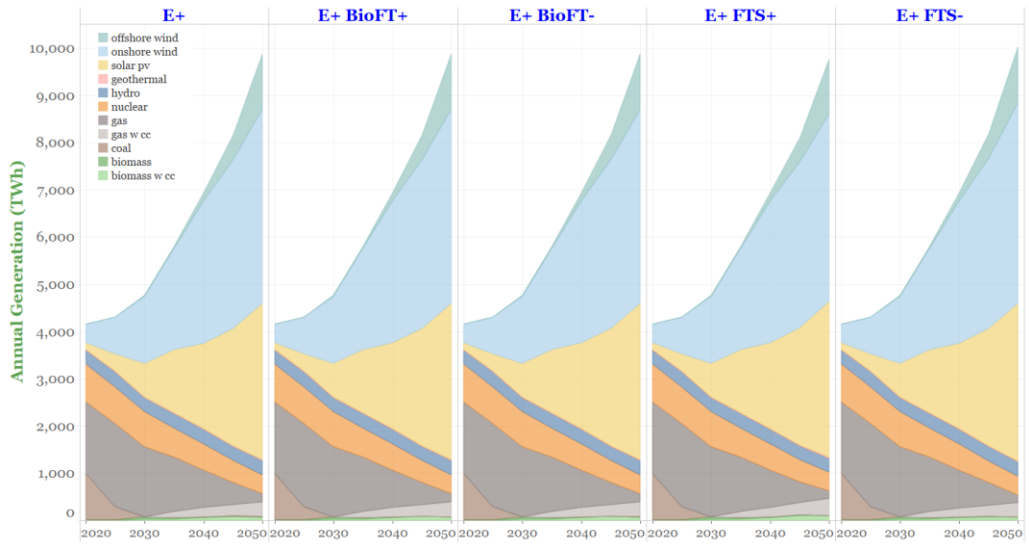

Figure B72. Yearly electricity generation by source.

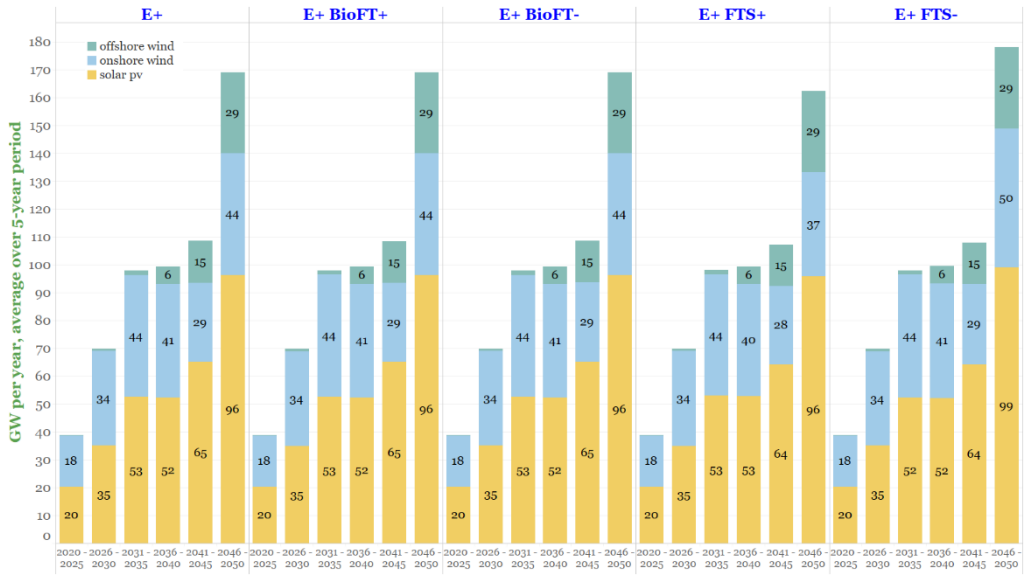

Figure B73. Average annual build rate of solar and wind generating capacity during each five-year period from 2020 through 2050.

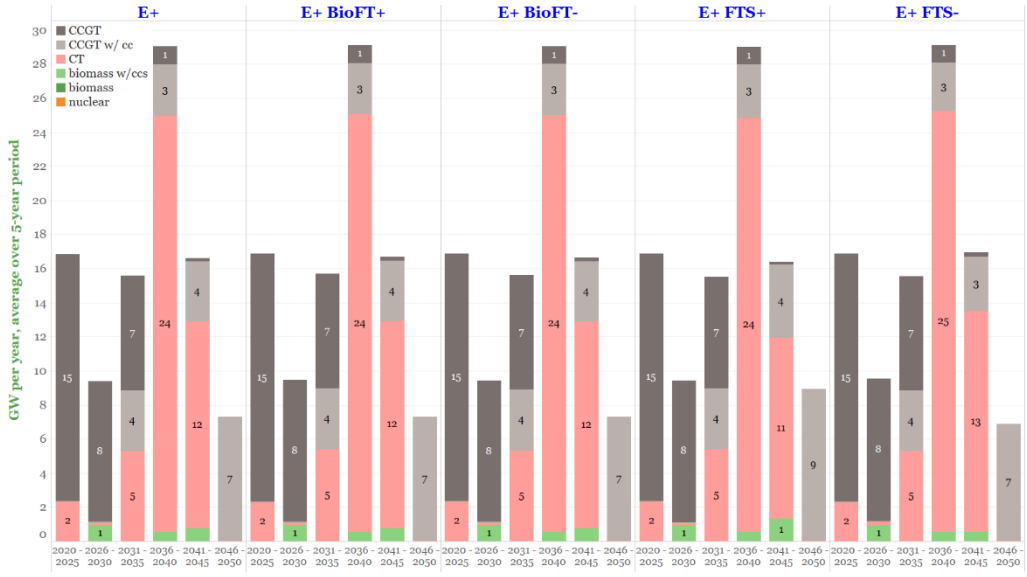

Figure B74. Average annual build rates for dispatchable thermal generating capacity during each five-year period from 2020 through 2050.

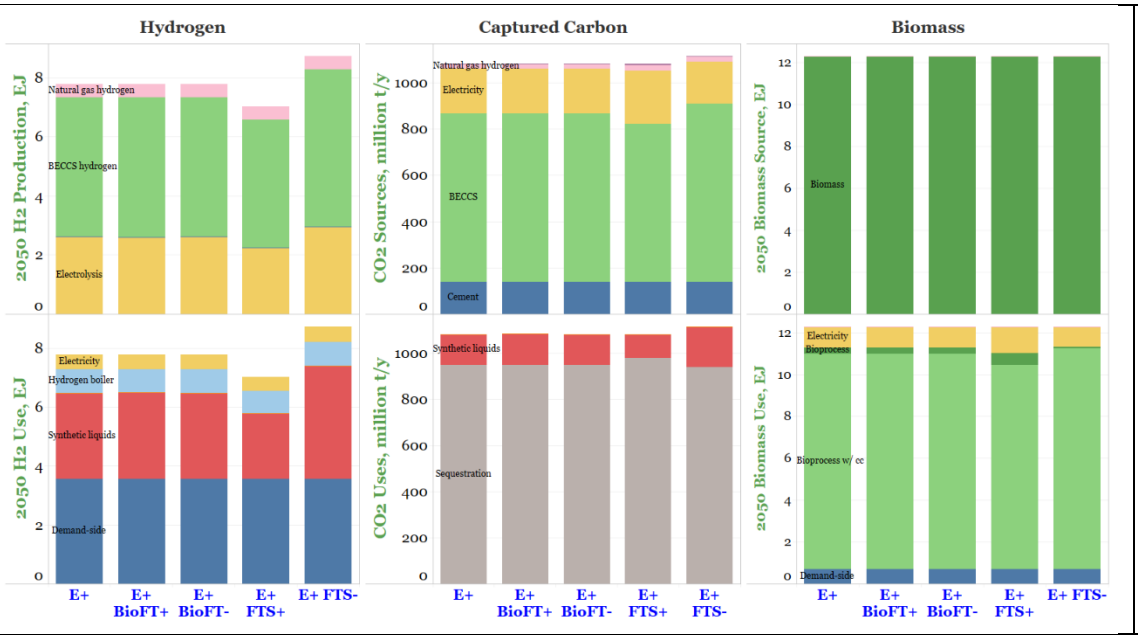

Figure B75. Production (top) and use (bottom) of hydrogen, captured carbon and biomass in 2050.

3.10 Direct air capture

Direct air capture (DAC) provides negative emissions to offset emissions from difficult-to-decarbonize sectors, such as aviation and agriculture. As noted in the main report, some DAC is deployed in E+RE+ and E- cases. It is not deployed in E+ or the other two net-zero cases. Given uncertainties in future performance and cost of DAC [16], sensitivity cases were run to explore whether DAC would play a bigger role in E+ if its capital cost were lower and/or its energy efficiency were higher (Table B1, Group J). In E+, the assumed capital cost and electricity input rate were based on the "optimistic variant" of the liquid-sorbent based system described in [17], but assuming that thermal energy input to the process would be supplied by electricity rather than fuel.

The lower-cost sensitivity case was based on costs estimates of Keith *et al.* [18]. For a sensitivity on energy efficiency, a somewhat arbitrary choice of halving the input energy requirements was adopted. Such a dramatic reduction may not be achievable with liquid sorbent (hydroxide-based) systems, and it is unclear whether a solid-sorbent based system might eventually be able to achieve such a reduction [19]. The third sensitivity adopted both the lower capital cost and lower energy input values. See Table B13.

Table B13. Input assumptions that vary between cases in direct air capture sensitivities

	E+	E+ DAC-	E+ DAC eff+	E+ DAC- eff+
Capital cost, $/(tCO2/y), 2016$	2,164	694	2,164	694
Electricity use, MWh/tCO2 captured	2	2	1	1

Results for the DAC sensitivity runs are summarized in Figure B76 through Figure B81. All results with lower cost and/or higher efficiency show hardly any discernable difference from the original E+ scenario, in which only a small amount of DAC capacity is deployed. Reducing capital cost by a factor three (E+DAC-) increases the amount of CO_2 captured via DAC only

slightly (Figure B81). Halving DAC electricity use per tonne of CO_2 captured (E+DAC eff+) also slightly increases the amount of CO_2 captured by DAC (Figure B81) and reduces total electricity use by DAC (Figure B77). In these two sensitivities, total electricity load also decreases due to a reduction in electrolysis. There are corresponding reductions in wind and solar generation that are partially offset by the increased use of gas for power generation, the emissions from which are offset by DAC. With both reduced capital cost and increased efficiency (E+DAC-eff+), CO_2 captured increases more than with the other two sensitivities and DAC electricity use falls, and DAC CO_2 capture increases.

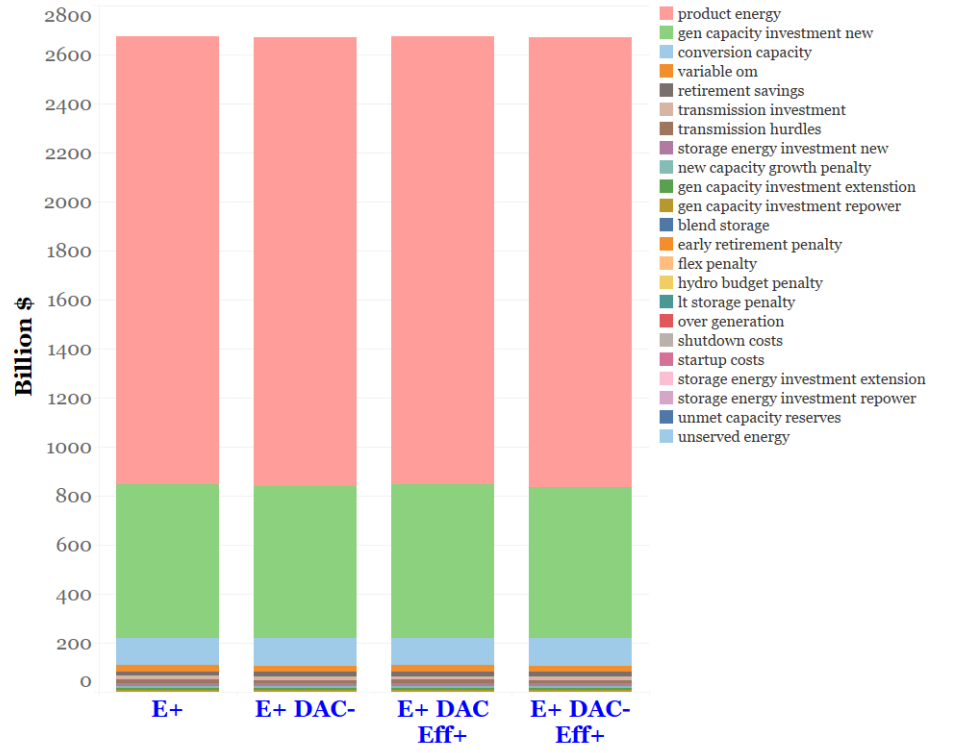

Figure B76. Optimized (minimum) net present value (NPV, 2% discount rate) of the sum of annualized energy-supply system costs from 2020 to 2050 for each scenario. Sunk costs as of 2020 are not included, and costs associated with energy delivery, such as electricity distribution, are also not included in this metric.

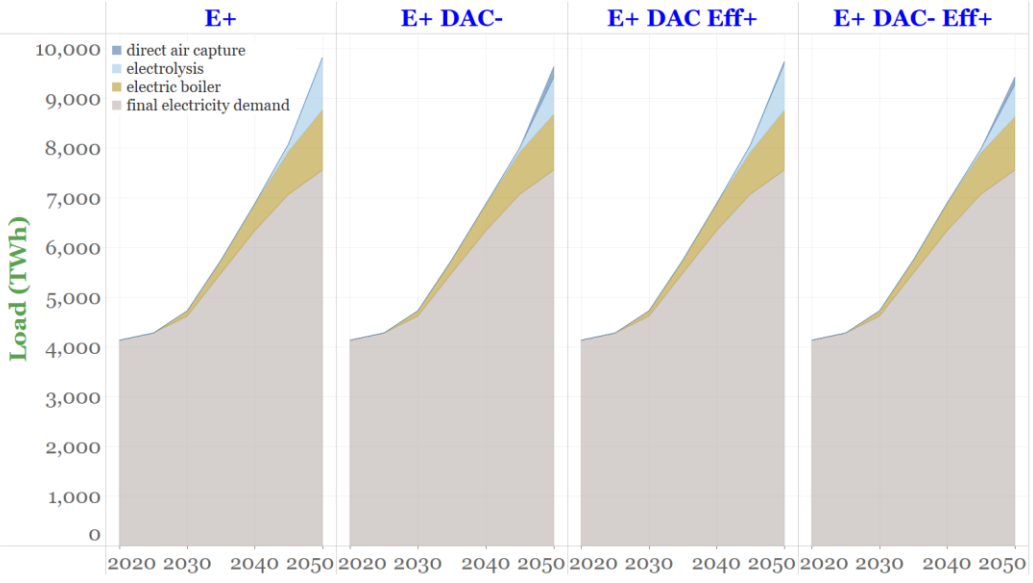

Figure B77. Total electricity load including intermediate, flexibly-operable loads.

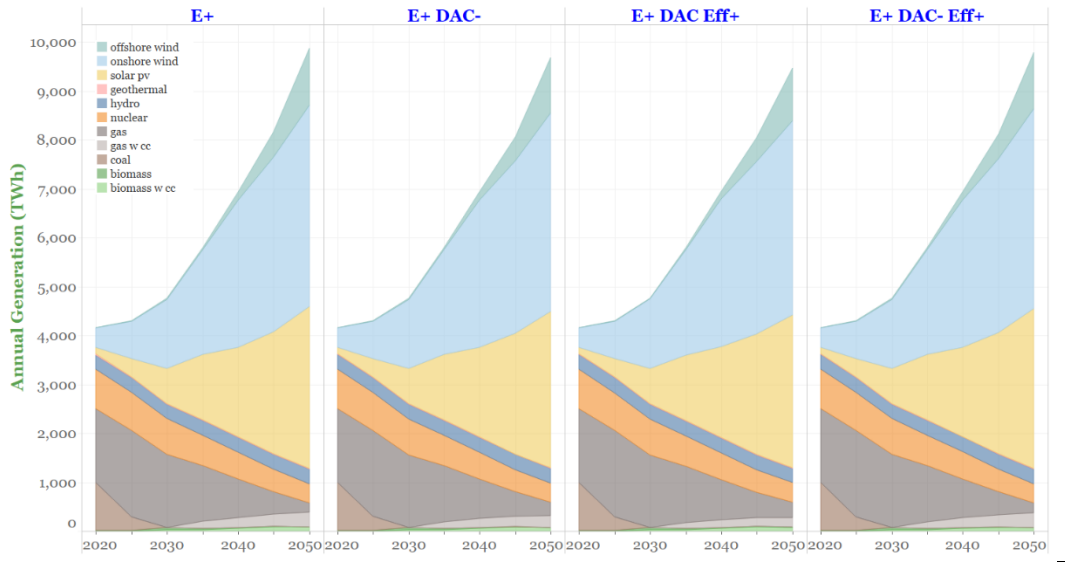

Figure B78. Yearly electricity generation by source.

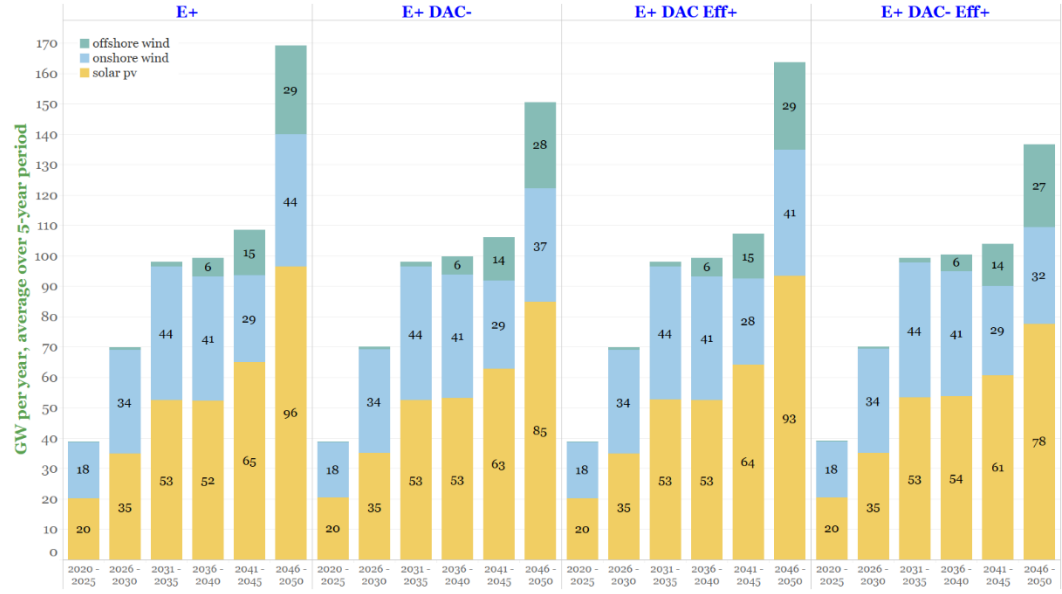

Figure B79. Average annual build rate of solar and wind generating capacity during each five-year period from 2020 through 2050.

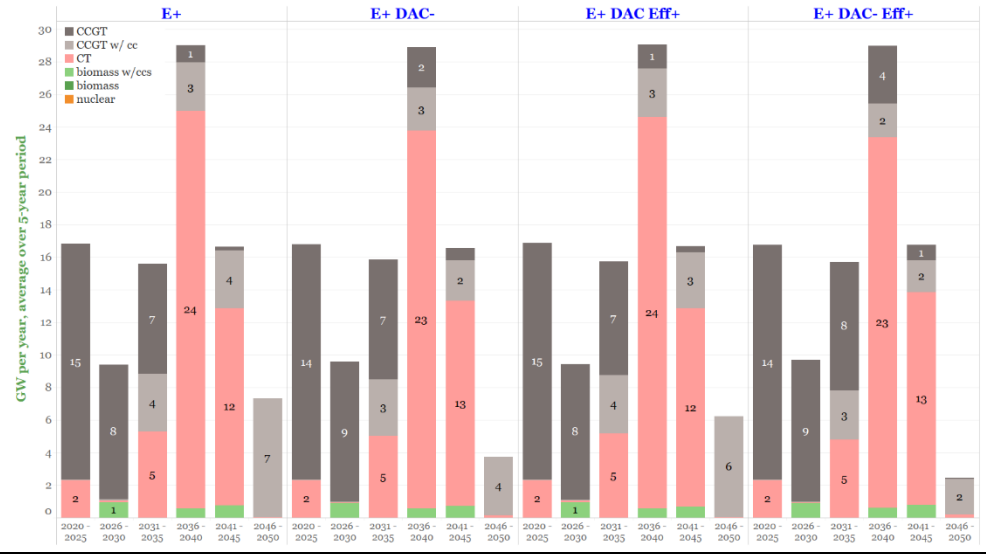

Figure B80. Average annual build rates for dispatchable thermal generating capacity during each five-year period from 2020 through 2050.

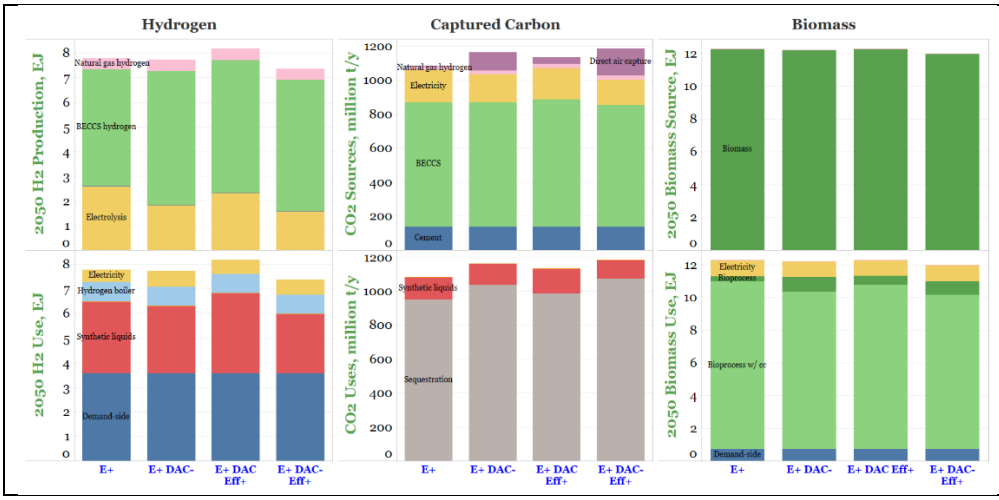

Figure B81. Production (top) and use (bottom) of hydrogen, captured carbon and biomass in 2050.

3.11 Higher energy efficiency

In addition to significant electrification of vehicles and buildings, which brings intrinsic final-energy efficiency improvements, the five core net-zero emission pathways assume relatively aggressive efficiency improvements in energy end-uses that do not fuel-switch to electricity.

In transportation and buildings in the core scenarios, EnergyPathways tracks equipment lifetimes and at the end of an equipment's life, selects a replacement technology that is the most efficient among the many technology options available in the model for that time period. In the industrial sector, due to the wide variety of energy-using processes, EnergyPathways handles efficiency gains differently. For the net-zero pathways, it assumes a rate of reduction of 1.9% per year in energy intensity (final-energy use per $ of industrial shipments). For comparison, the REF scenario (based on EIA's Reference case projection [20]), assumes 0.9% per year. The most rapid reduction in industrial energy intensity observed over any 30-year period historically was 3.1% per year (1979 – 2009), and the long-term average (1950 to 2019) is 1.9%/yr (Figure B82).

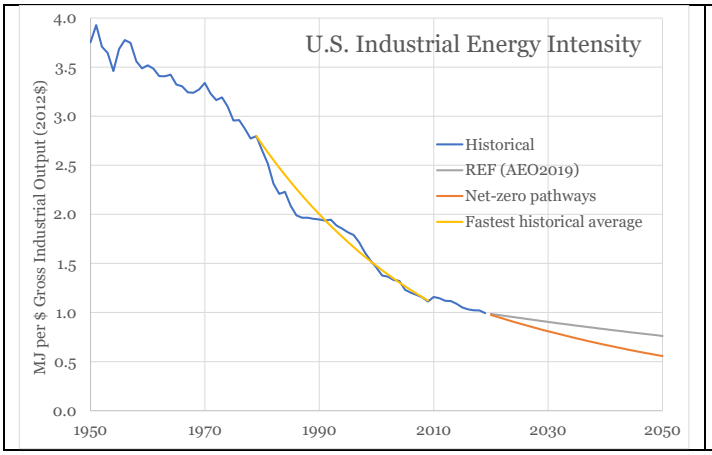

Figure B82. U.S industrial energy intensities. Historical values are calculated from industrial sector energy use [21] and gross output [22].

While efficiency gains over time are significant in our core scenarios (see [23] for examples in the transport and buildings sectors), we explored the impacts of still greater efficiency gains in transport, buildings, and/or industry through four sensitivity cases (Table B1, Group K)

For the transportation sensitivity case (E+VMT-), we stipulated that light-duty vehicle-miles travel by 2050 should be 15% less than in E+. (This could equivalently be viewed as 15% less energy use per vehicle mile traveled by 2050.)

For a buildings sector sensitivity (E+Beff+), we stipulated a more aggressive reduction in final-energy intensity (e.g., MJ/m^2 floor area) for residential and commercial space heating and cooling than in the core E+ scenario. Because final-energy is, effectively, an input to the RIO model, but not final-energy intensity, we modified the final energy inputs to RIO for building space conditioning to represent the more rapid energy intensity reductions. In E+, final energy for building space conditioning declines 1.9% per year from 2020 to 2050. We modified this to be 2.9% per year. For the residential sector, where energy service demands increase by about 4%/y in E+, the implied reduction in final-energy intensity in space conditioning is nearly 7% per year (or an 87% decline over 30 years). For commercial buildings, energy service demands increase 1%/y from 2020 to 2050, which implies a 4%/y decrease in final-energy intensity (or a 40% decline over 30 years).

In the industrial sector sensitivity (E+Ieff+), the pace of reduction in industrial energy-intensity was increased from 1.9% per year in the core scenarios to 3% per year. The fourth sensitivity (E+Eff+) combined all three of the above changes.

Table B14 summarizes the four sensitivity cases.

Table B14. Input assumptions that vary between cases in higher energy efficiency sensitivities

	E+	E+ VMT-	E+ Beff+	E+ Ieff+	E+ EFF+
Light duty vehicle-miles traveled in 2050, thousand VMT per vehicle	12.9	12.9 * 0.85	12.9	12.9	12.9 * 0.85
Buildings' heating/cooling final-energy demand reduction rate, %/yr	1.9	1.9	2.9	1.9	2.9
Industrial energy productivity ($ shipments/MJ) increase rate (vs. REF), %/y	1.9	1.9	1.9	3.0	3.0

Results of these sensitivity cases are shown in Figure B83 through Figure B89.

Perhaps surprisingly, none of the results for E+VMT- and E+Beff- are discernably different from the E+ results. Because the E+ case already assumes relatively aggressive efficiency gains and electrification rates in the transportation and buildings sectors, final energy demand in these sectors falls significantly through the transition period and additional efficiency improvements have vanishingly small impacts.

In contrast, with the energy-intensity reductions assumed in the industrial sector, final energy demand stays relatively constant through the transition period, and this sector accounts for nearly 50% of all final-energy use by 2050. With the more aggressive energy intensity reduction assumed in E+Ieff+, there is a considerable reduction in total electricity demand (Figure B84) and a corresponding reduced need for generation that manifests itself in less solar, wind, and gas-fired generation by 2050 (Figure B85). There is a modest reduction in hydrogen production and use (Figure B89). With less energy supply required, the NPV of all annual energy-supply system costs from 2020 to 2050 is about 2% lower (Figure B83).

Given the much larger impact of industrial energy intensity over the transportation and buildings sector efficiency improvements assumed in the sensitivity cases, the results for the sensitivity

case when efficiency improvements in all three sectors are included (E+Eff+) closely resemble those of the E+Ieff+ sensitivity.

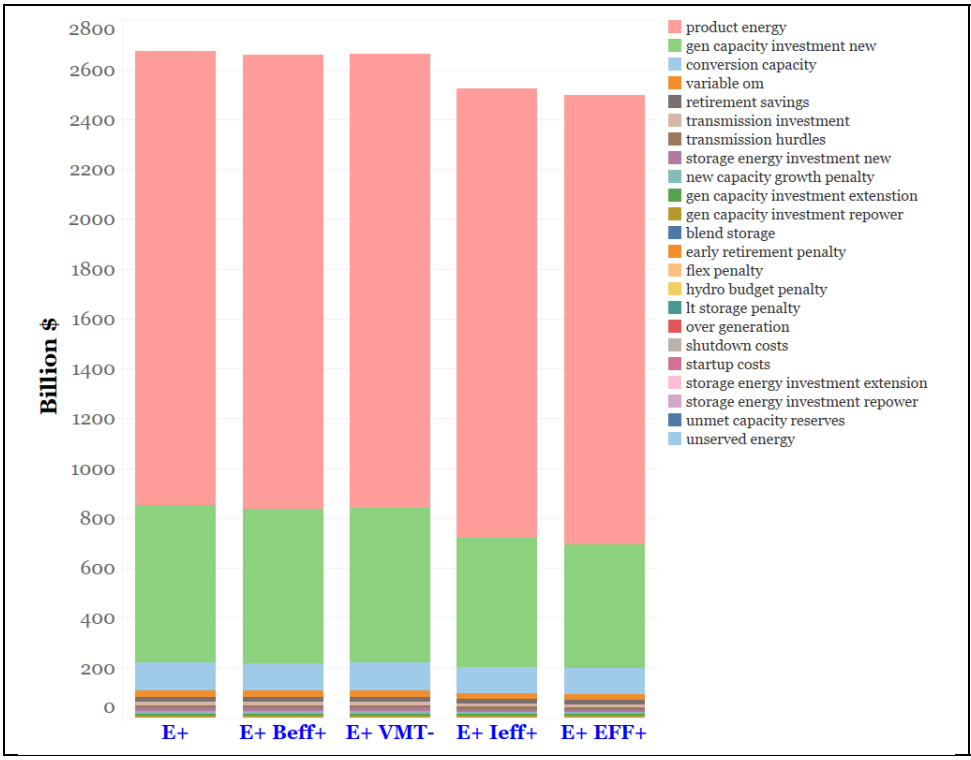

Figure B83. Optimized (minimum) net present value (NPV, 2% discount rate) of the sum of annualized energy-supply system costs from 2020 to 2050 for each scenario. Sunk costs as of 2020 are not included, and costs associated with energy delivery, such as electricity distribution, are also not included in this metric.

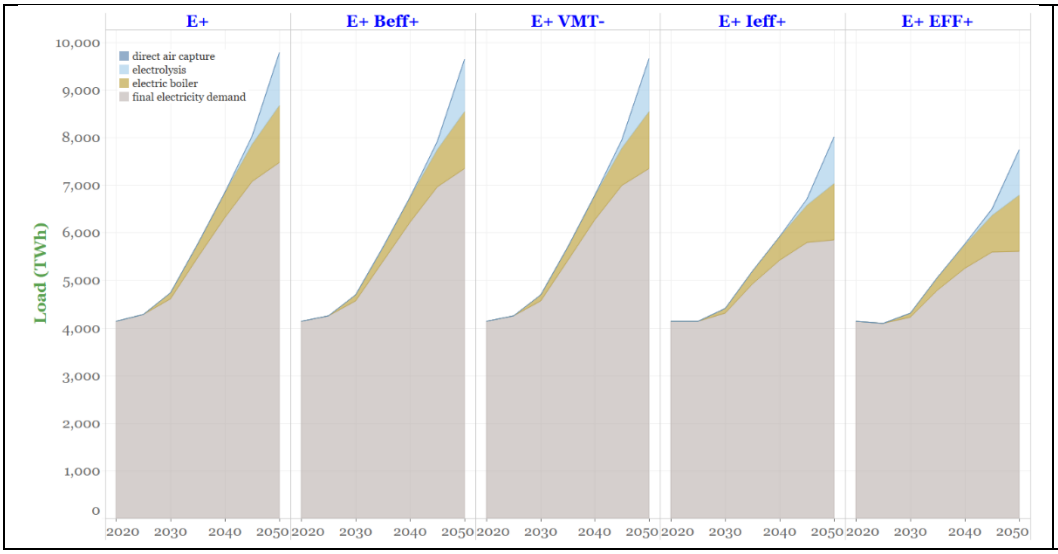

Figure B84. Total electricity load including intermediate, flexibly-operable loads.

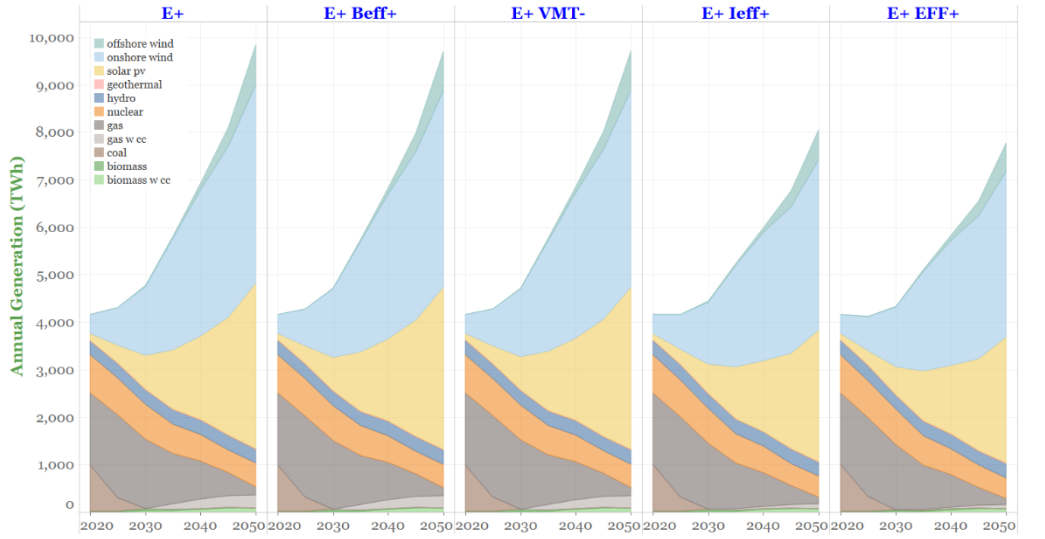

Figure B85. Yearly electricity generation by source.

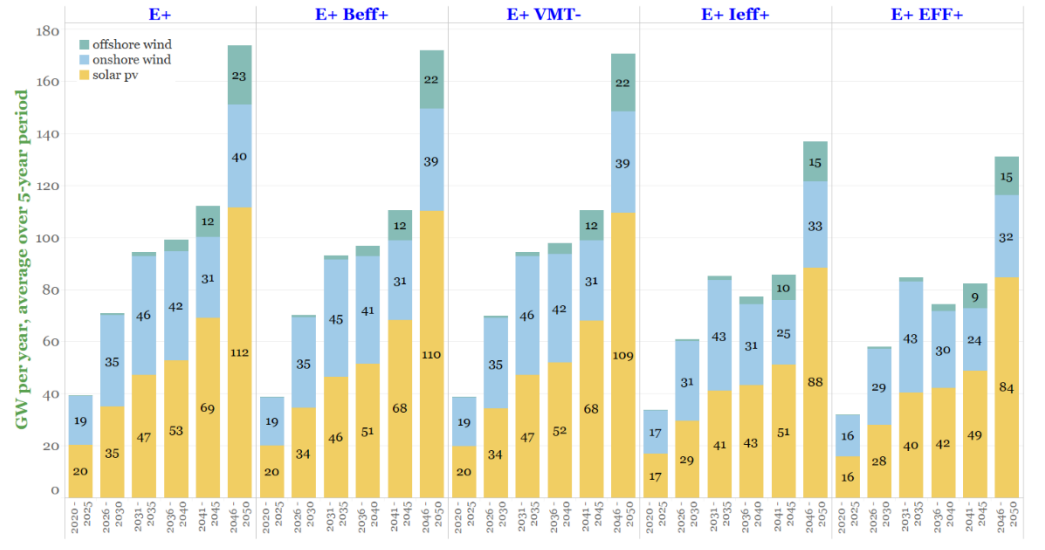

Figure B86. Average annual build rate of solar and wind generating capacity during each five-year period from 2020 through 2050.

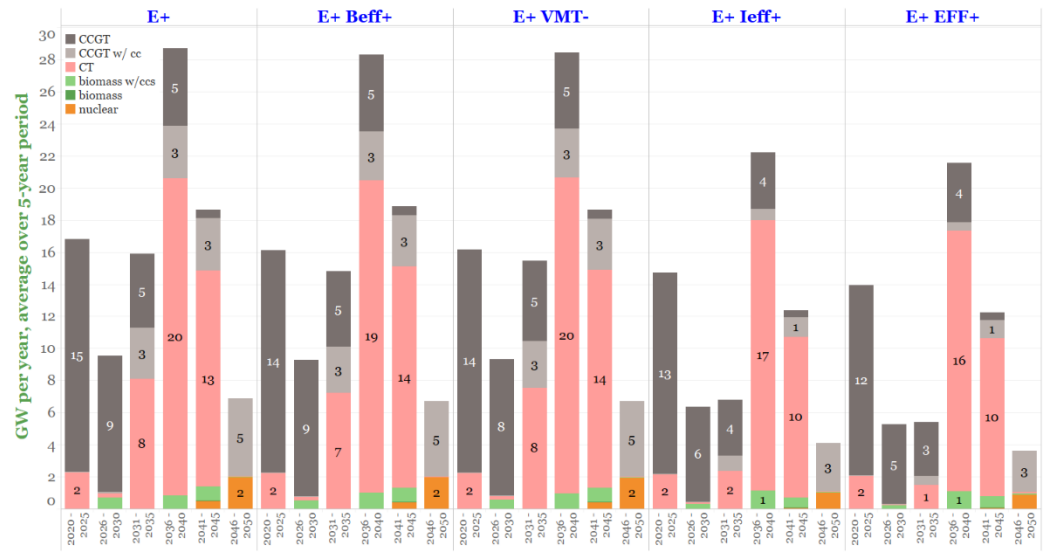

Figure B87. Average annual build rates for dispatchable thermal generating capacity during each five-year period from 2020 through 2050.

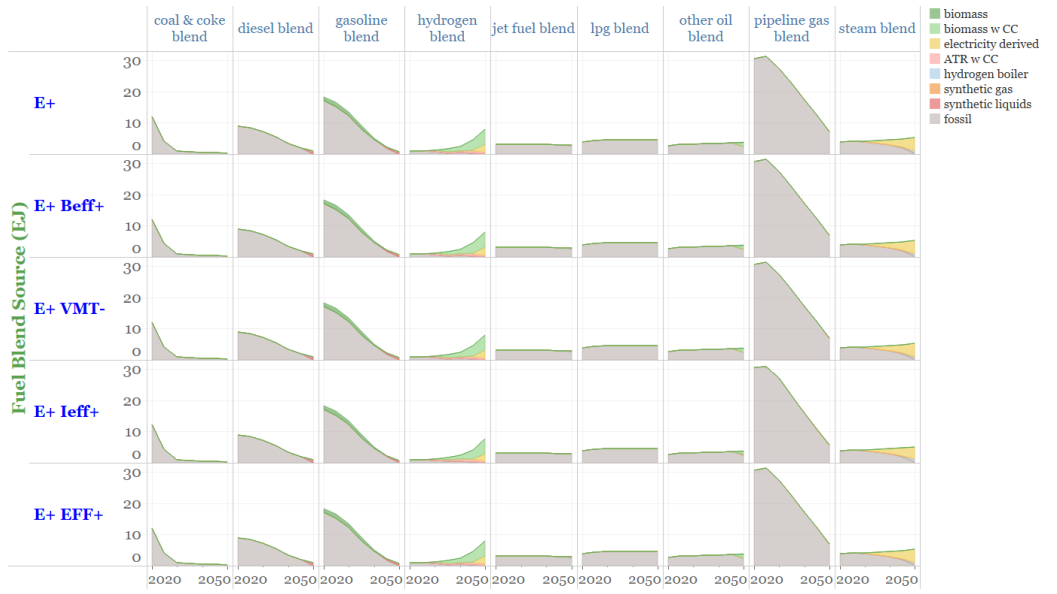

Figure B88. End-use fuels and steam consist of components that originate from different sources. The components of each fuel blend (and steam) are shown here by their source.

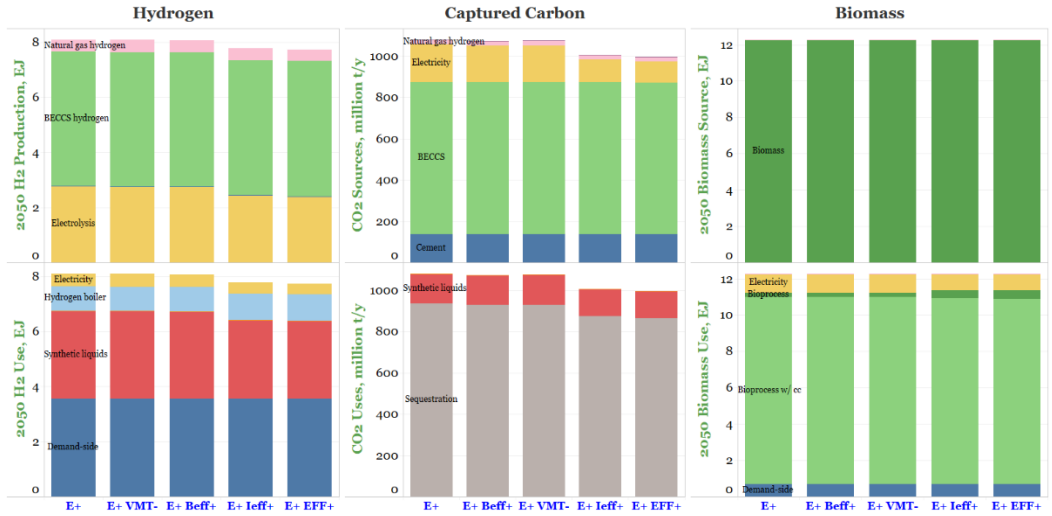

Figure B89. Production (top) and use (bottom) of hydrogen, captured carbon and biomass in 2050.

3.12 No new biomass

Biomass is a critical resource in all five core net-zero scenarios: essentially all biomass resources available in the model for energy uses are completely used by 2050 in every scenario, and much of the biomass is used in processes with CO_2 capture, thereby providing negative emissions when the CO_2 is sequestered. It is plausible that a bioenergy industry on the scale of that envisioned in the core scenarios might not develop. What would be the path to a net-zero emissions economy in that case? To help answer this question, two sensitivity cases were run in which any use of additional biomass (beyond today's use) was not allowed (Table B1, Group L). The E+ and E+RE- cases were selected for these sensitivity runs (Table B15).

Table B15. Input assumptions that vary between cases in no new biomass sensitivities

	E+	E+B-	E+RE-	E+RE-B-
Maximum new biomass use allowed by 2050 (Gt/y)	0.7	0	0.7	0

Results from the sensitivity cases and their counterpart core net-zero cases are shown in Figure B90 through Figure B97. The NPV of energy-supply system costs from 2020-2050 (Figure B90) increases by 3% in E+B- compared to E+ and by 15% in E+RE-B- compared to E+RE-. These significant increases are attributed primarily to direct air capture (DAC) being deployed in the B- cases to provide negative emissions that were provided by biomass use in the core scenarios. DAC is a much more costly option for negative emissions than biomass in the model, and this cost difference is compounded by higher total electricity demands to supply DAC units with power (Figure B91). The higher demands are met via larger electricity supply from solar, wind, and gas (without and with CO_2 capture) in E+B- and by added generation from gas (without and with CO_2 capture) in E+RE-B- (Figure B92, Figure B93, and Figure B94). In E+B-, the costs are further compounded by greater deployment of electrolysis to substitute for H_2 from biomass with CO2 capture than in E+ (Figure B97). Costs are further compounded in E+RE-B- by significant expansion in natural gas reforming with CO_2 capture to make H_2, the demand for which is higher due increased use in power generation and industrial boilers displacing natural gas in both of these applications (Figure B97). Finally, the carbon sequestration level in each sensitivity case is higher than in its counterpart core scenario. Sequestration in the E+RE-B- case is especially large – nearly double in 2050 the sequestration in E+RE- (Figure B97). This reflects the significantly larger use of natural gas in E+RE-B- (Figure B96) resulting from fossil fuel substitutes being unavailable (biomass-derived fuels) or more costly (fuels synthesized from H_2 and capture CO_2).

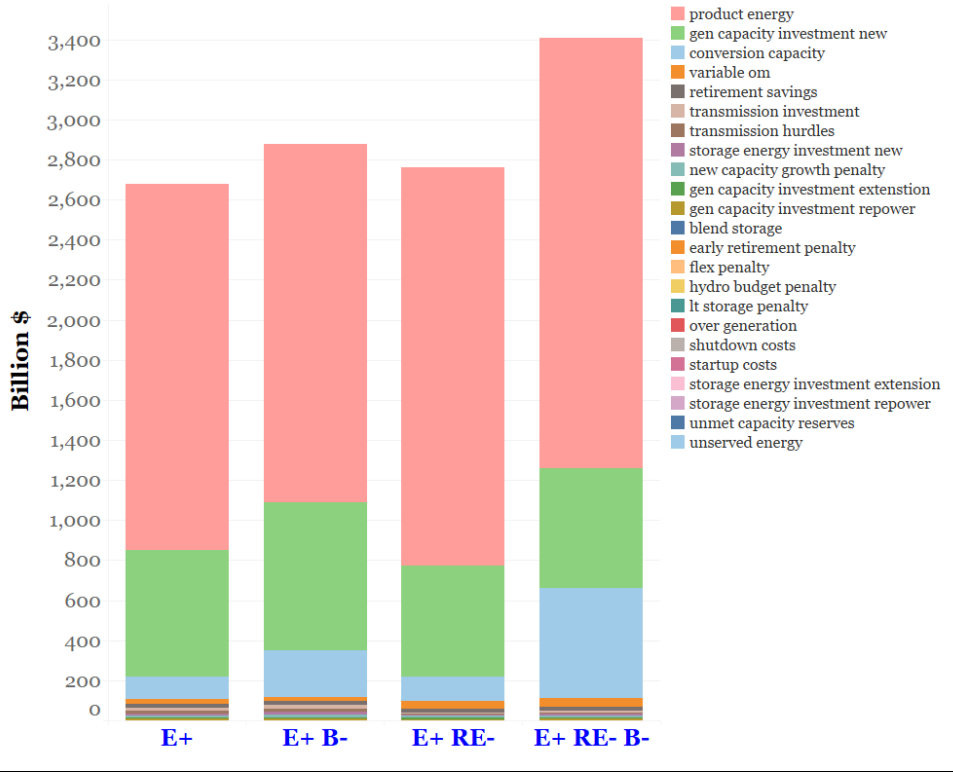

Figure B90. Optimized (minimum) net present value (NPV, 2% discount rate) of the sum of annualized energy-supply system costs from 2020 to 2050 for each scenario. Sunk costs as of 2020 are not included, and costs associated with energy delivery, such as electricity distribution, are also not included in this metric.

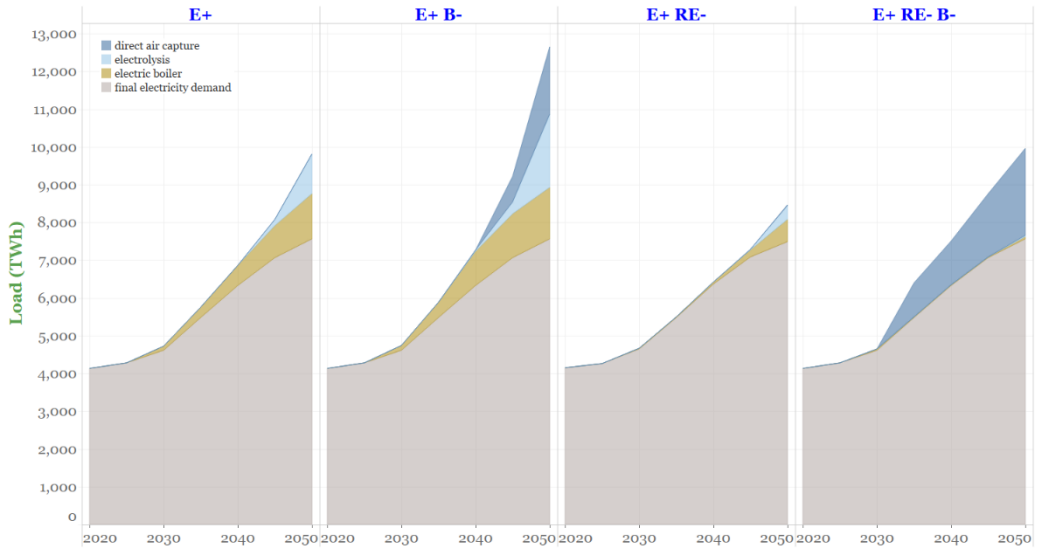

Figure B91. Total electricity load including intermediate, flexibly-operable loads.

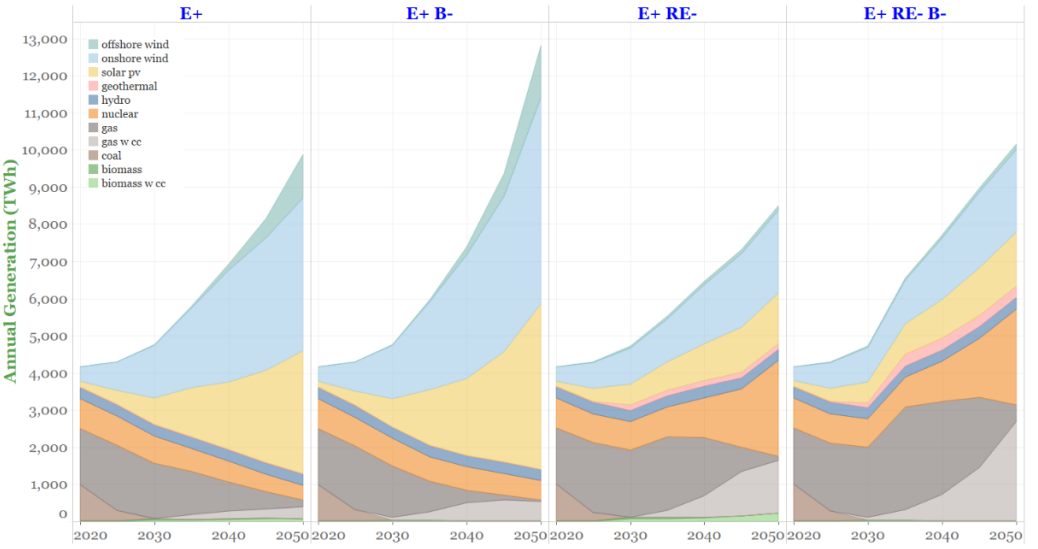

Figure B92. Yearly electricity generation by source.

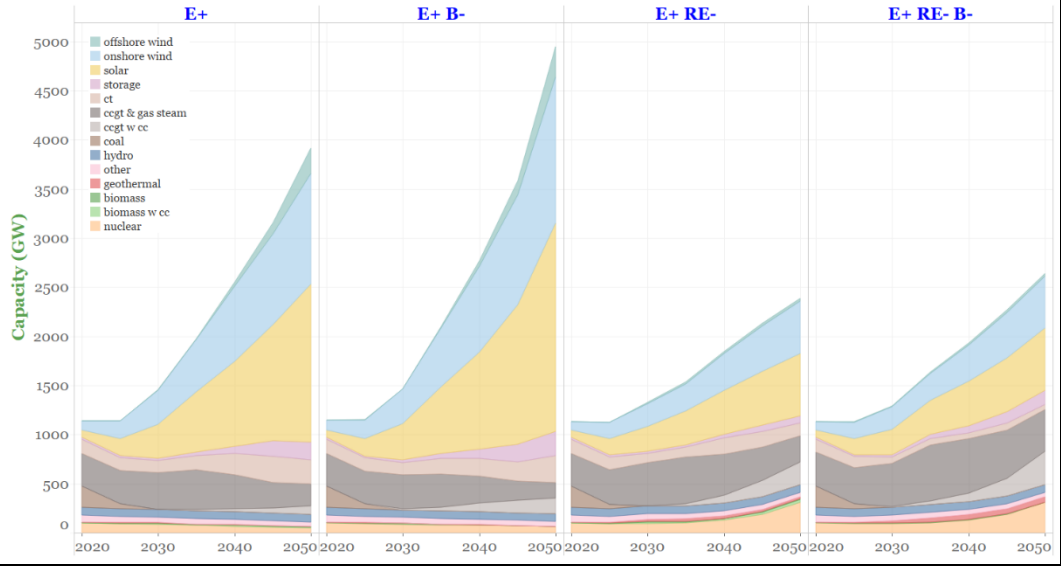

Figure B93. Electricity generating capacity by type of generator.

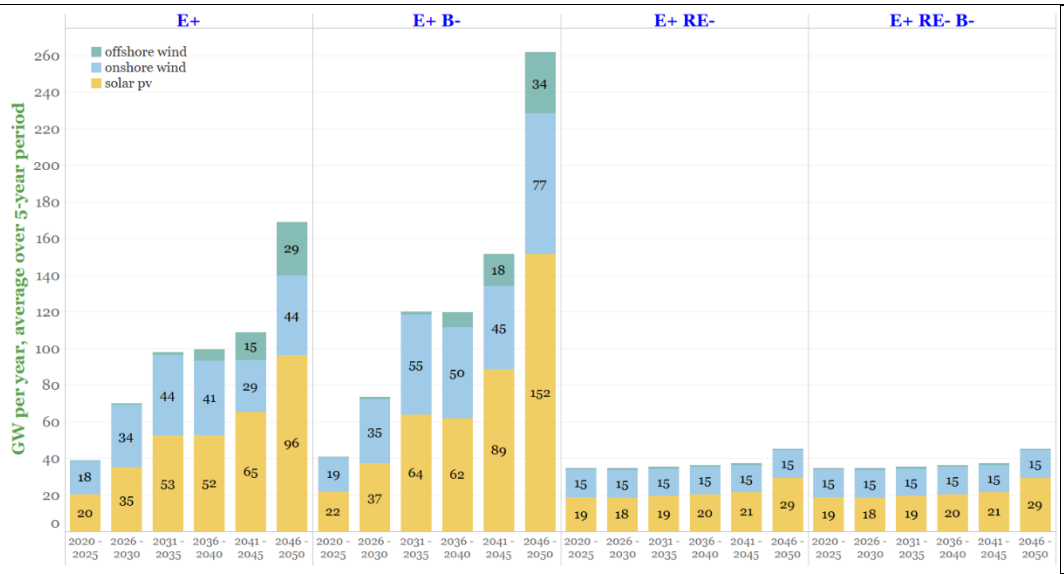

Figure B94. Average annual build rate of solar and wind generating capacity during each five-year period from 2020 through 2050.

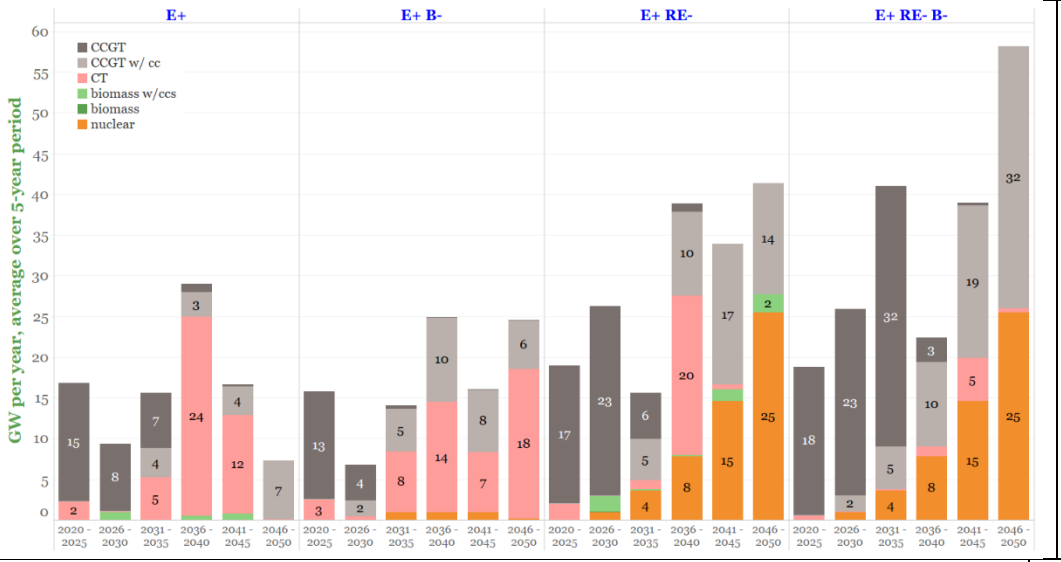

Figure B95. Average annual build rates for dispatchable thermal generating capacity during each five-year period from 2020 through 2050.

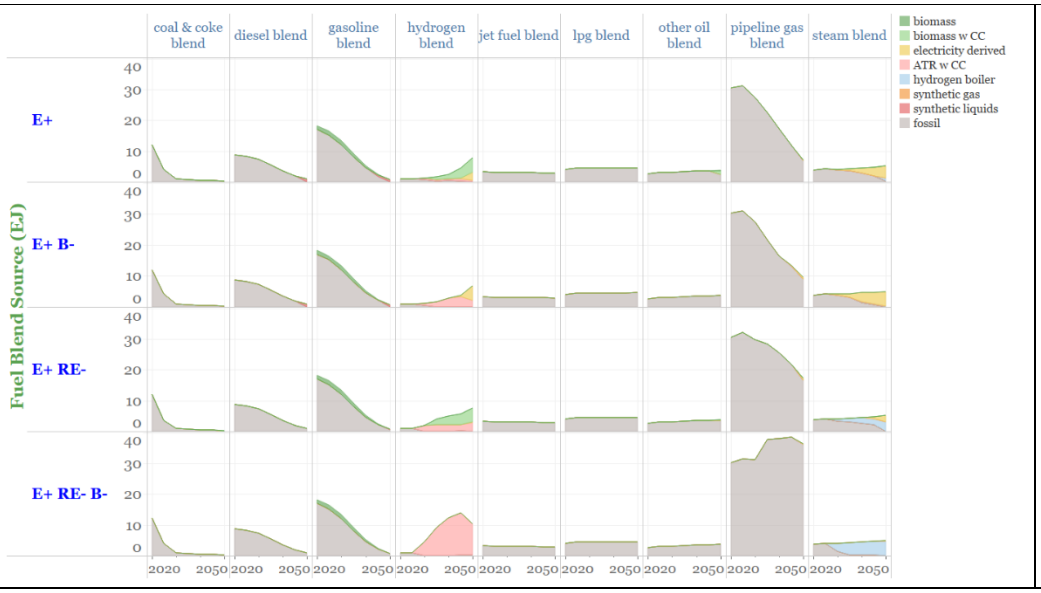

Figure B96. End-use fuels and steam consist of components that originate from different sources. The components of each fuel blend (and steam) are shown here by their source.

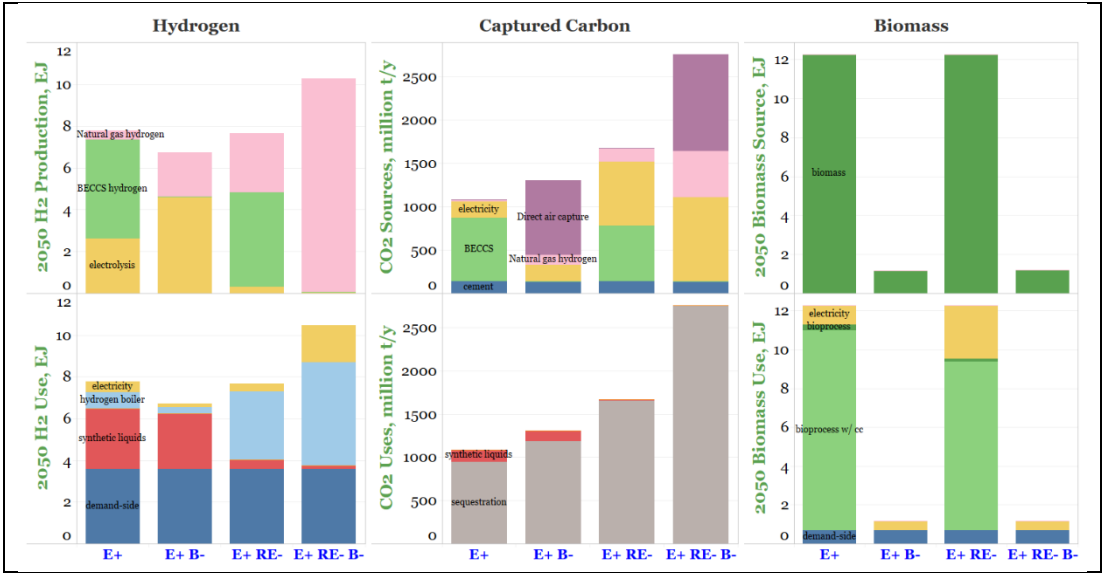

Figure B97. Production (top) and use (bottom) of hydrogen, captured carbon and biomass in 2050.

3.13 Higher biomass supply

As discussed in [24], two biomass supply scenarios are represented in the core set of scenarios. In the E+, E-, E+RE-, and E+RE+ cases, the potentially available biomass supply is limited to the amount that can be provided with no change in land use from current (2020) use of land. In addition to the use of agricultural and forestry-industry residues, this allows for the use of land growing corn for ethanol production today to be transitioned to growing a perennial bioenergy crop such as switchgrass or miscanthus. In the high-biomass scenario (E-B+), the full future biomass supply potential estimated in [25] is allowed. This would involve some conversion of cropland or pasture to energy crops.

In addition to the four core scenarios that use the lower biomass potential (E+, E-, E+RE-, E+RE+) we modelled, a fifth scenario also with the lower biomass availability: E-RE- combines less-aggressive electrification on the demand side with constrained wind and solar build rates on the supply side. We ran all five scenarios also with the high biomass availability (Table B1, Group M and Table B16).

Table B16. Input assumptions that vary between cases in higher biomass supply sensitivities

	E+, E-, E+RE-, E+RE+, E-RE-	E+B+, E-B+, E+RE-B+, E+RE+B+, E-RE-B+
Biomass potential (by 2050)	0.7 Gt/y (13 EJ)	1.3 Gt/y (24 EJ)

Results from all ten cases are shown in Figure B98 through Figure B103, for which the following are notable observations.

For each pair of cases, e.g., E+ and E+B+ or E-RE- and E-RE-B+, the NPV of total energy-supply system costs is always lower for the case with greater biomass availability (Figure B98). The differences in NPV between two cases in a given pair is very small for pairs that involve high electrification on the demand side, e.g., the E+ and E+B+ pair. The differences are quite significant for cases involving less-aggressive demand side electrification: E- and E-B+ differ by about 5%; E-RE- and E-RE-B+ differ by about 7%.

For each pair of cases, total electricity load is lower when biomass availability is higher (Figure B99). In the E+ and E+RE+ pairs, electricity demand for electrolysis is reduced because less hydrogen is needed, but also because hydrogen from biomass is less costly and so hydrogen is produced instead using additional biomass (Figure B103). In the E+RE- pair, when there is higher biomass availability, electrolysis is essentially eliminated because there is less hydrogen demand (Figure B103). Electricity from biomass with CO2 capture increases: the associated negative emissions provide value sufficient for the biopower to displace more costly nuclear and higher-emitting gas-fired generation (Figure B100). In the E- and E-RE- pairs of cases, electricity load falls when biomass availability is higher due to the elimination of direct air capture (DAC) and large reductions in electrolysis and electric boiler demands (Figure B99). The carbon removal provided by DAC in the core scenarios is provided at lower cost instead by using some additional biomass for hydrogen production and for power generation with CO_2 capture (Figure B100 and Figure B103).

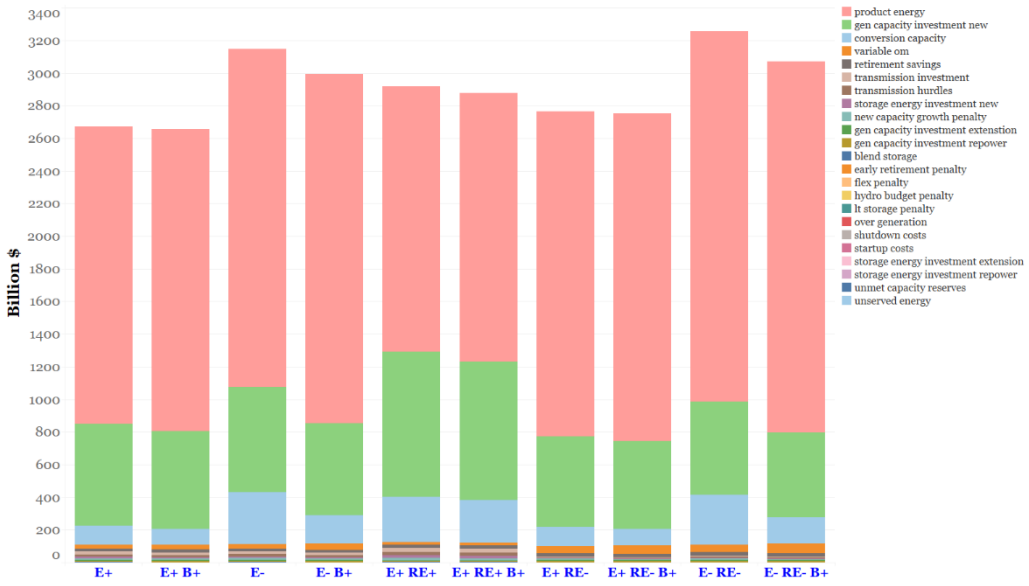

Figure B98. Optimized (minimum) net present value (NPV, 2% discount rate) of the sum of annualized energy-supply system costs from 2020 to 2050 for each scenario. Sunk costs as of 2020 are not included, and costs associated with energy delivery, such as electricity distribution, are also not included in this metric.

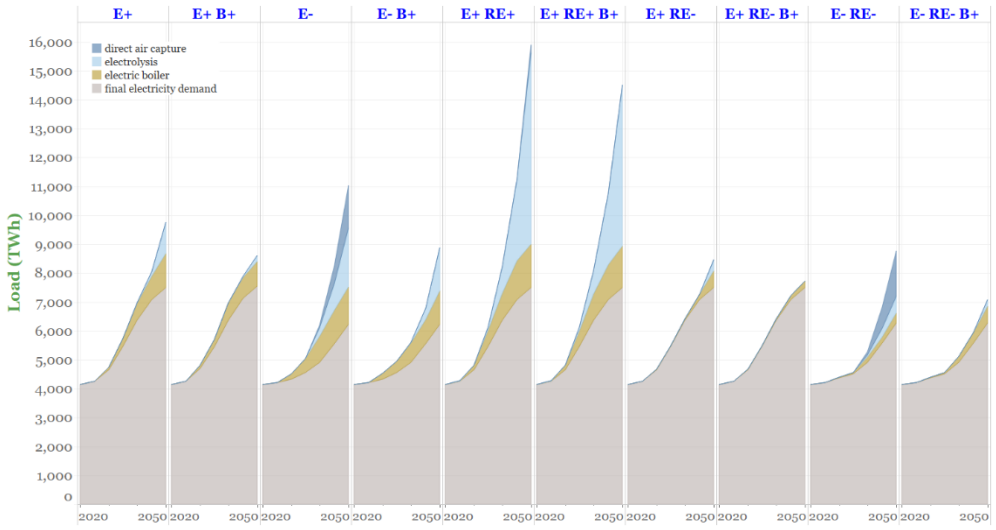

Figure B99. Total electricity load including intermediate, flexibly-operable loads.

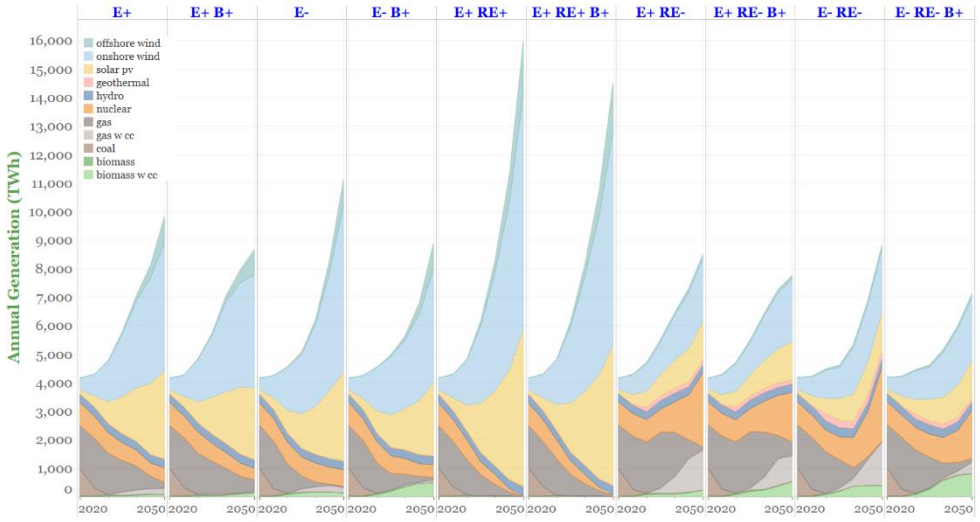

Figure B100. Yearly electricity generation by source.

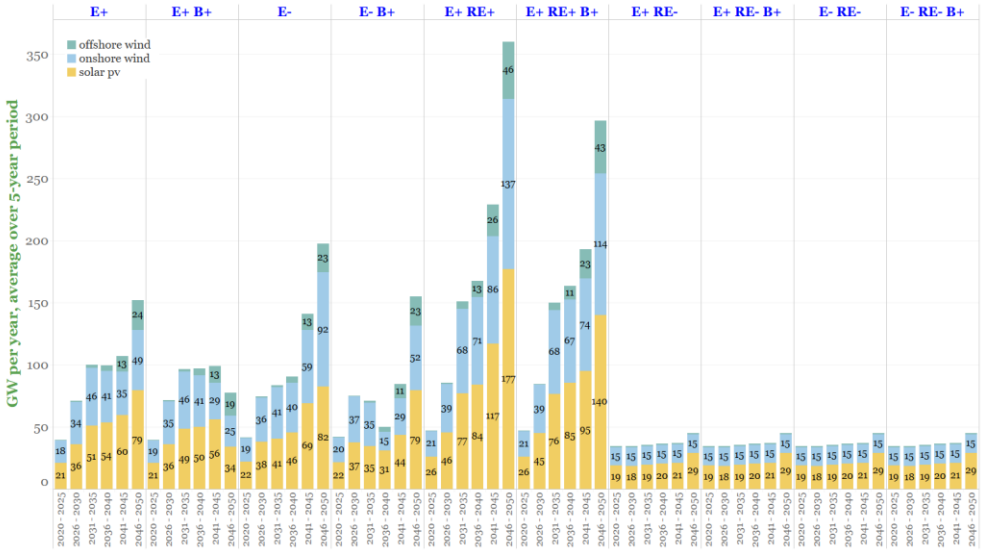

Figure B101. Average annual build rate of solar and wind generating capacity during each five-year period from 2020 through 2050.

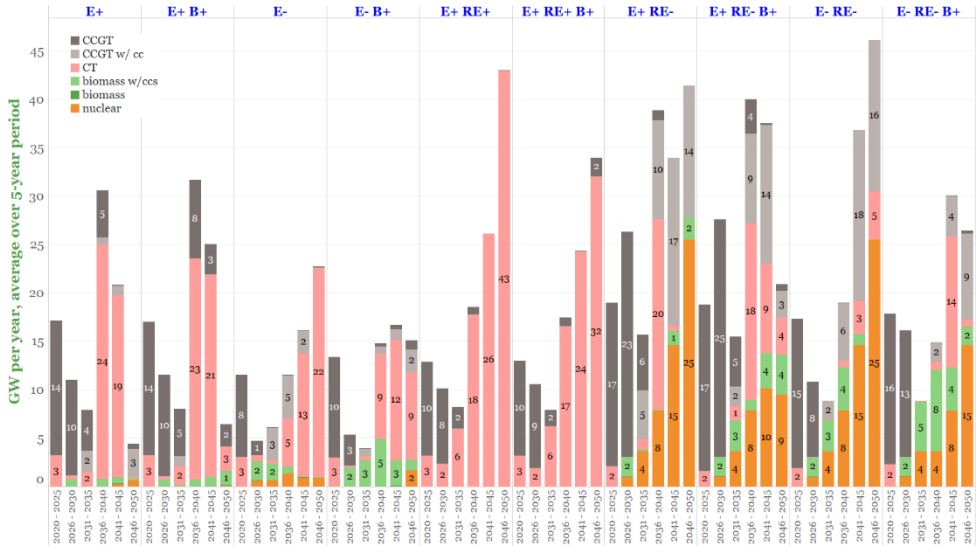

Figure B102. Average annual build rates for dispatchable thermal generating capacity during each five-year period from 2020 through 2050.

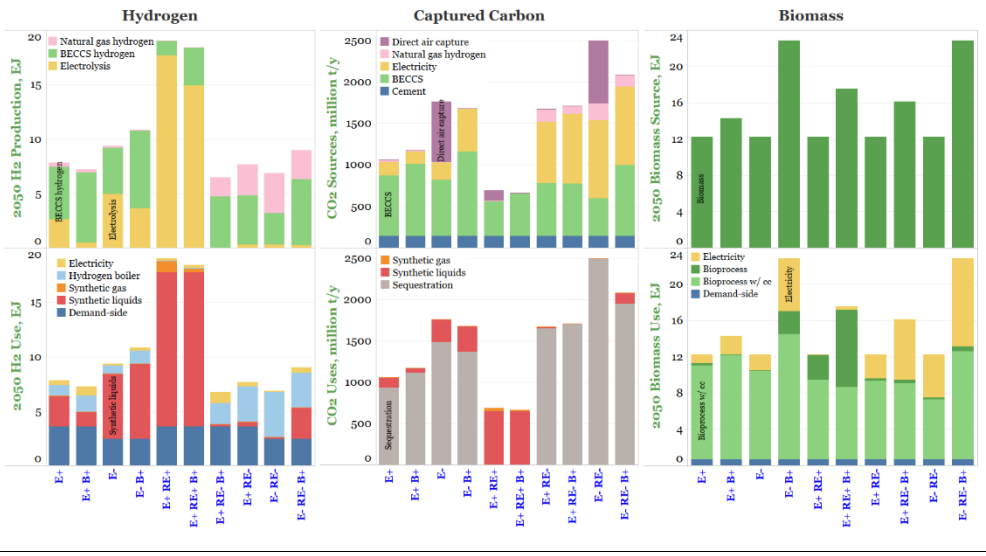

Figure B103. Production (top) and use (bottom) of hydrogen, captured carbon and biomass in 2050.

3.14 CO_2 net-emissions trajectory

The core net-zero pathways were all constrained to meet a linear decline in net CO_2 emissions from the energy/industrial system from 2020 to the 2050 target level of -170 million metric tCO_2/year. Emissions trajectories different from this one, but still meeting the same 2050 target, would result in different modeling outcomes.

To illustrate some possibilities, two sensitivity cases were run for the E+ scenario (Table B1, Group N). In both cases, emissions reductions are assumed to follow the recent historical decline rate up to 2030, which represents a slower start to the transition than in E+. One sensitivity (E+ Slow Start) then assumes a linear decline from 2030 to the 2050 target. The other (E+ S) assumes a sharper linear decline from 2030 until 2040, followed by a less-sharp decline rate to reach the 2050 target. The E+S case is intended to induce an energy-supply expansion that follows a logistics curve approach to market saturation, rather than the exponential expansion

through the full transition period reflected in E+ results. Table B17 shows the assumed annual emissions for each trajectory.

Table B17. Input assumptions that vary between cases in CO_2 net-emissions trajectory sensitivities.

	E+	E+ Slow Start	E+ S
CO_2 net emissions (Gt/y) in 2020, 25, **30**, 35, 40, 45, and 50	5.2, 4.3, **3.4**, 2.5, 1.6, 0.72, -0.17	5.2, 4.8, **4.4**, 3.3, 2.1, 0.97, -0.17	5.2, 4.8, **4.4**, 2.5, 0.50, 0.17, -0.17

Figure B104 shows fossil fuel emissions and geologic CO_2 storage across the sensitivities. With the slower initial decline in net-emissions, fossil fuel use is higher through 2030 in both sensitivity cases and the start of geologic sequestration is delayed relative to the E+ case. After 2030, the two sensitivity cases diverge from each other as explained further below. In aggregate, the NPV of total energy-supply system costs is about 2% lower for E+ Slow Start than for E+ (Figure B105), largely because investments to reduce emissions can be delayed relative to E+. Costs for E+S are about 2% higher than for E+ despite the delay for reasons explained below.

Total electricity demand in 2050 does not change much across all three cases, but there is a large difference in the trajectory of demand to 2050 (Figure B106). In E+ Slow Start demand growth is initially slower than in E+, but is much more rapid in the last decade of the transition. In E+S, there is very rapid demand growth in the 2030s, including an earlier introduction of electrolysis and direct air capture loads, and a slowing of demand growth in the 2040s.

In E+ Slow Start, with slower electricity demand growth initially and with emissions reductions delayed compared with E+, there is less growth in electricity generation from solar and wind to 2030 and an expansion in gas-fired generation (without CO_2 capture) (Figure B107). There are significant gas capacity additions before 2035 (Figure B109), and wind and solar capacity additions are much larger than in E+ after 2035 (Figure B108).

In E+S, growth in solar and wind generation in the 2020s is also slower than in E+ (Figure B107), but because the emissions reduction rate from 2030 is more rapid in E+S than in E+SlowStart, gas-fired generation is rapidly reduced from 2030 to 2040 and nuclear generation is added instead (Figure B107 and Figure B109). Direct air capture plays a role in E+S (Figure B106 and Figure B110). The costs for new nuclear and direct air capture plants contribute to the higher NPV of total energy system costs seen in Figure B105.

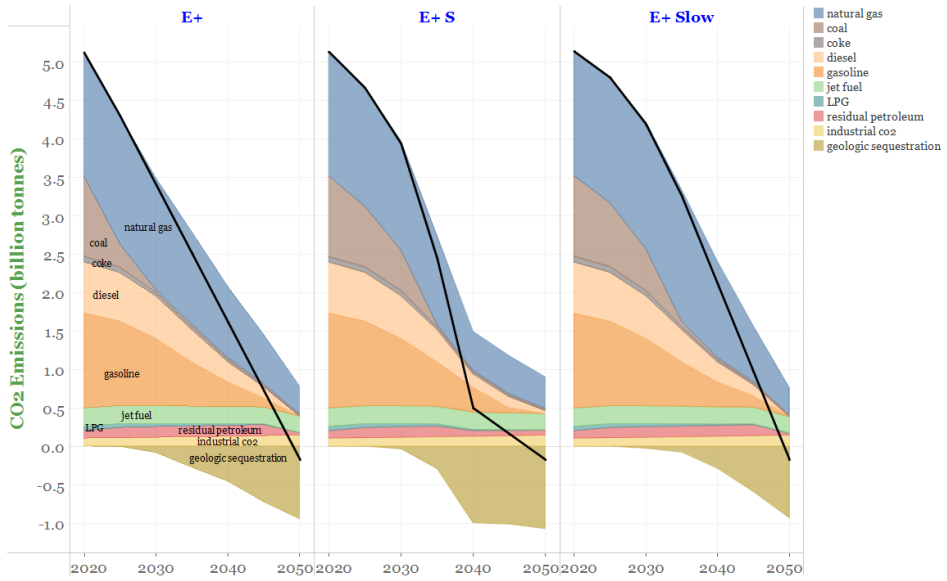

Figure B104. Net-emissions trajectories (black lines) for three net-zero pathways. Fossil fuel emissions (above the x-axis) are partially or fully offset by geologic sequestration of CO2 (below the x-axis) to meet the emissions target at each time step.

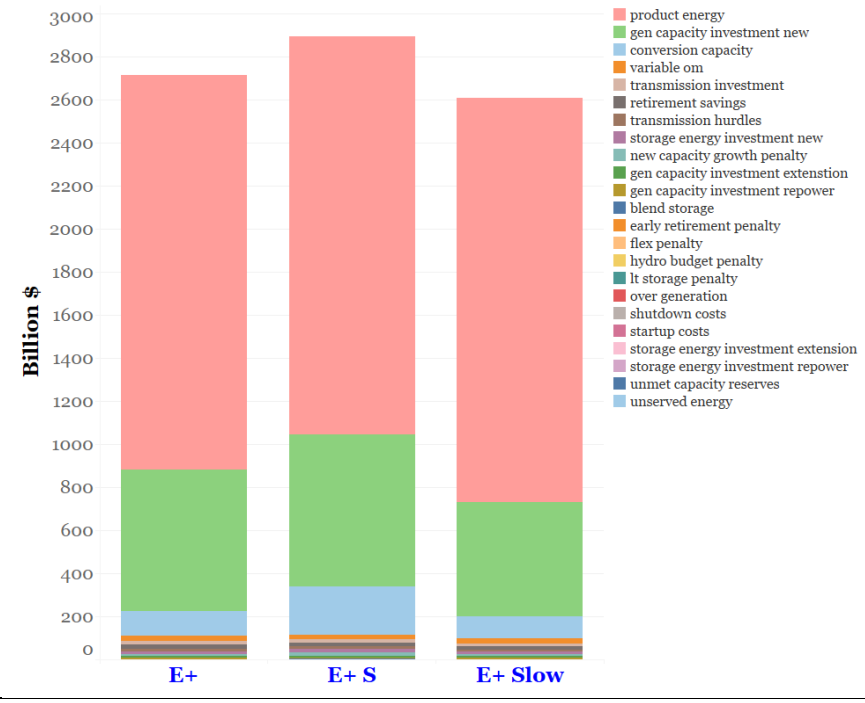

Figure B105. Optimized (minimum) net present value (NPV, 2% discount rate) of the sum of annualized energy-supply system costs from 2020 to 2050 for each scenario. Sunk costs as of 2020 are not included, and costs associated with energy delivery, such as electricity distribution, are also not included in this metric.

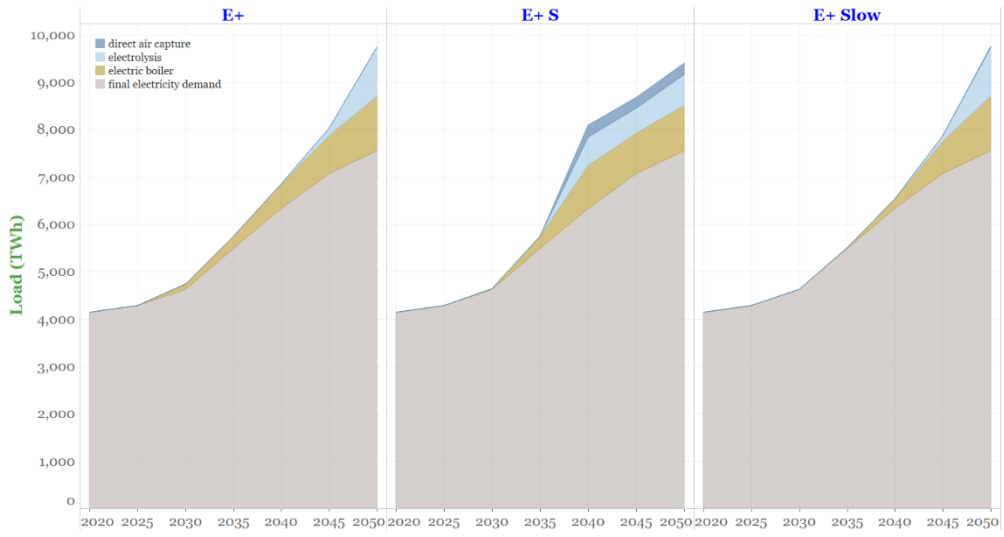

Figure B106. Total electricity load including intermediate, flexibly-operable loads.

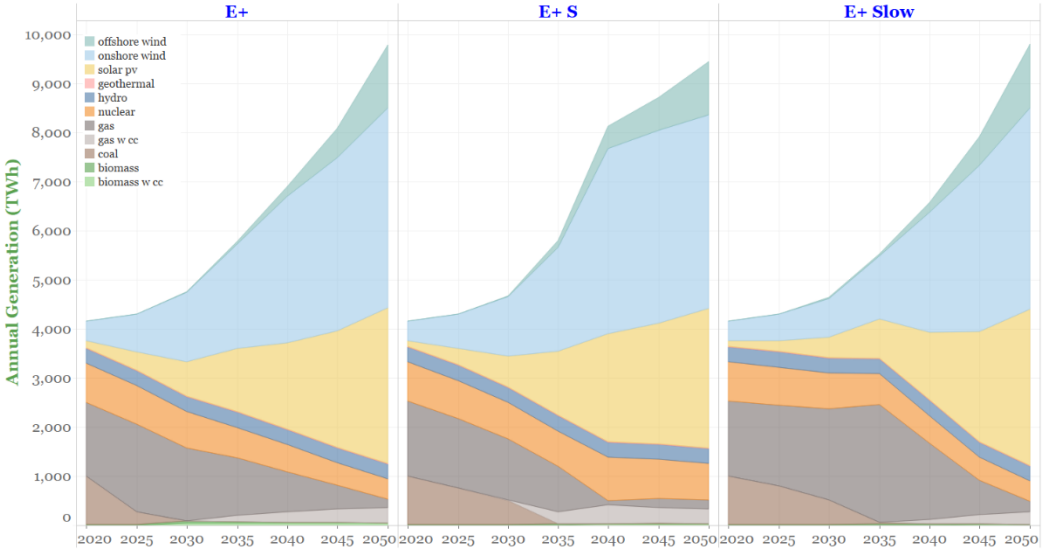

Figure B107. Yearly electricity generation by source.

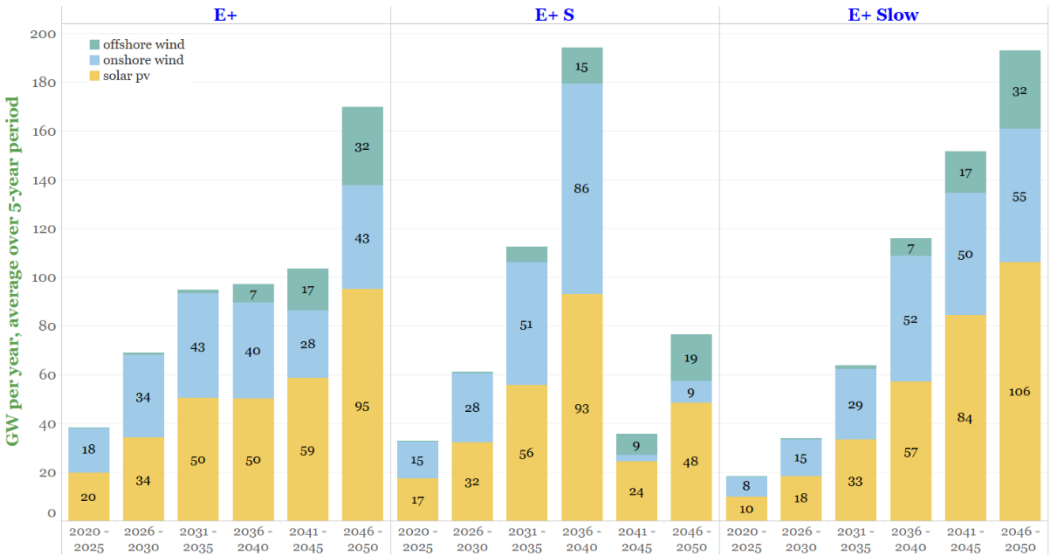

Figure B108. Average annual build rate of solar and wind generating capacity during each five-year period from 2020 through 2050.

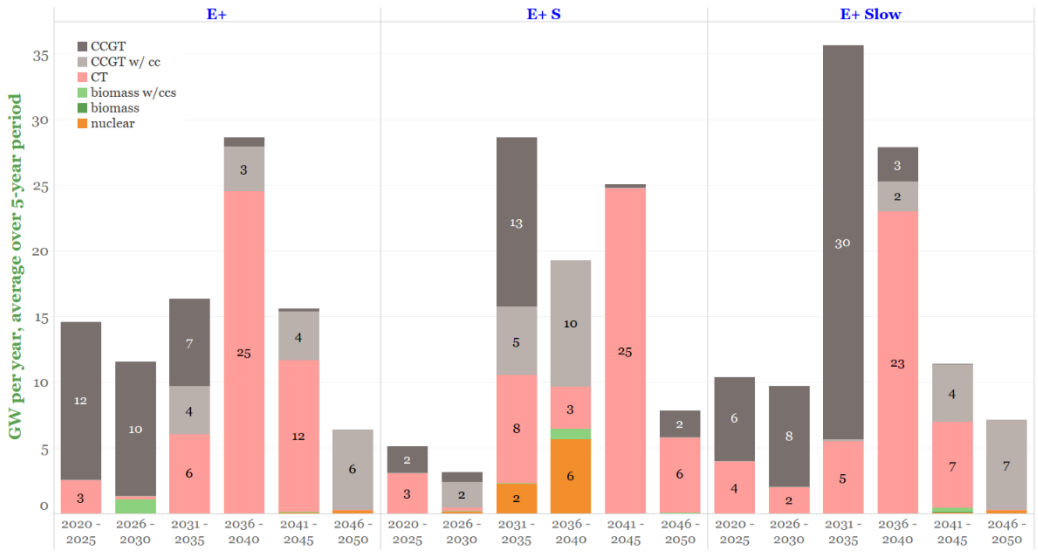

Figure B109. Average annual build rates for dispatchable thermal generating capacity during each five-year period from 2020 through 2050.

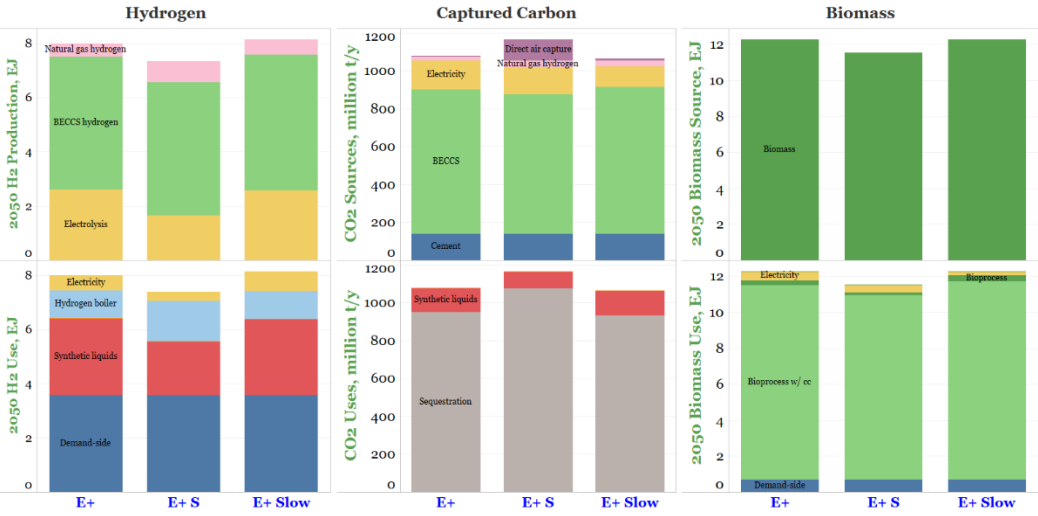

Figure B110. Production (top) and use (bottom) of hydrogen, captured carbon and biomass in 2050.

3.15 Higher social discounting

Two sensitivities cases were run with a 7% "social" discount rate used in calculating the NPV of total energy system costs (Table B1, Group O) instead of the 2% value used in the core scenarios. The E+ and E-B+ cases were selected for these sensitivities (Table B18).

Table B18. Input assumptions that vary between cases in higher discount rate sensitivities

	E+	E+7%	E- B+	E- B+7%
Social discount rate	2%/y	7%/y	2%/y	7%/y

With one large exception, differences in results using a 7% discount rate are generally small compared to using a 2% discount rate. See Figure B111 through Figure B117. The exception is the NPV of total energy-supply system costs across the transition (Figure B111), which is unsurprisingly much lower with the higher discount rate. The subtler differences with the 7% cases are in the delay of some capital investments to later in the transition. For example, thermal capacity additions in the 2040s (Figure B116) and solar and wind capacity additions in the final

five years of the transition (Figure B115) are larger it E+7% than in E+. As well, hydrogen plays a slightly reduced role in the transition (Figure B117).

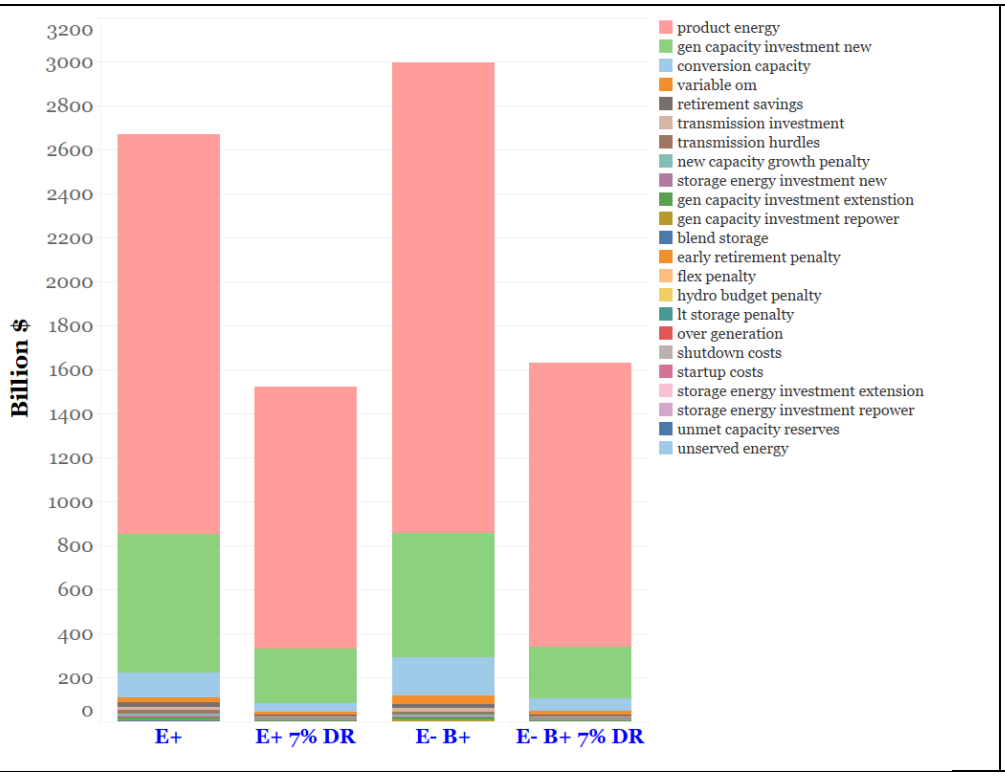

Figure B111. Optimized (minimum) net present value (NPV, 2% discount rate) of the sum of annualized energy-supply system costs from 2020 to 2050 for each scenario. Sunk costs as of 2020 are not included, and costs associated with energy delivery, such as electricity distribution, are also not included in this metric.

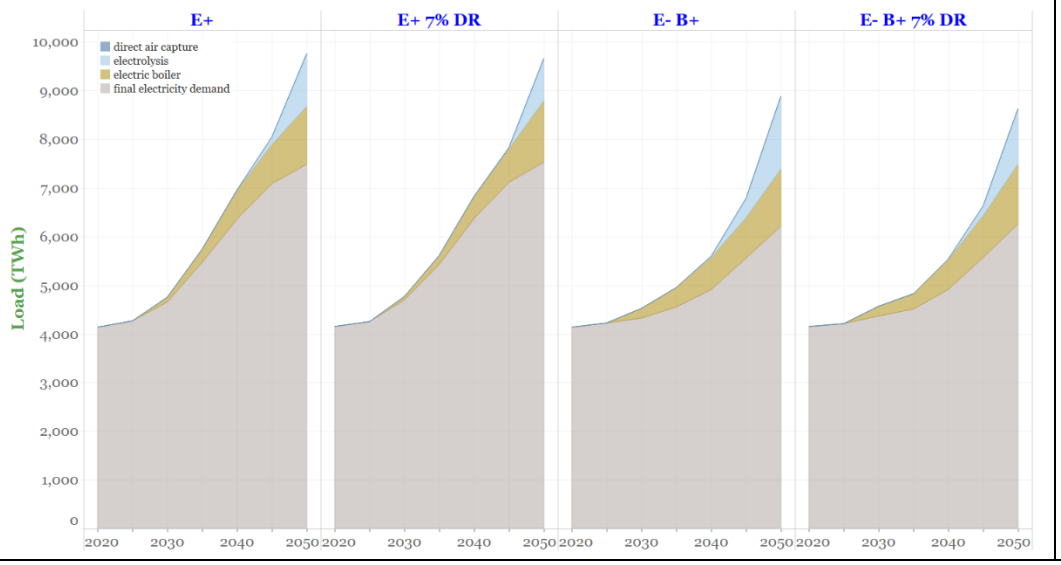

Figure B112. Total electricity load including intermediate, flexibly-operable loads.

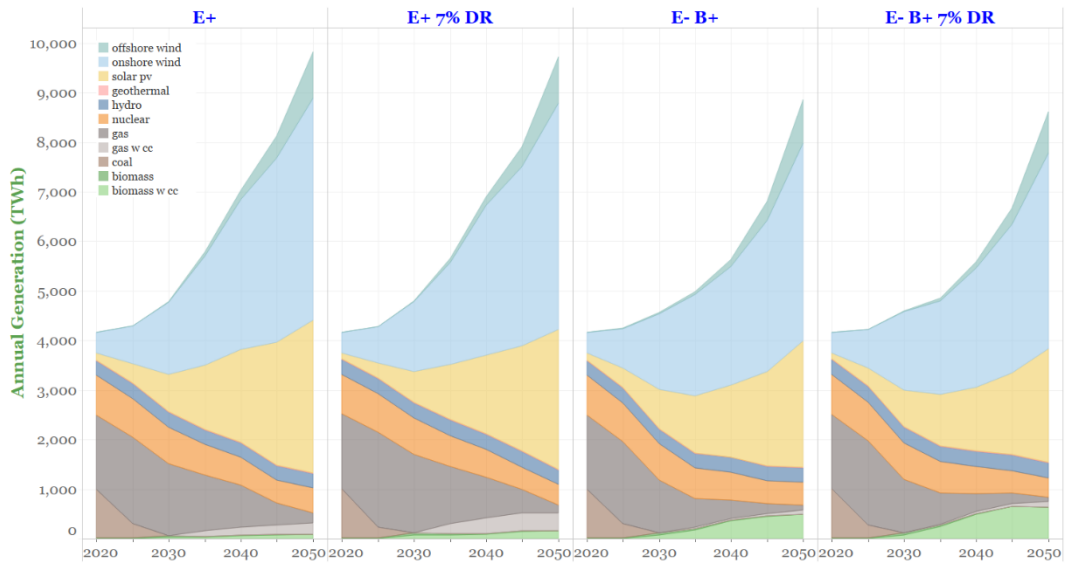

Figure B113. Yearly electricity generation by source.

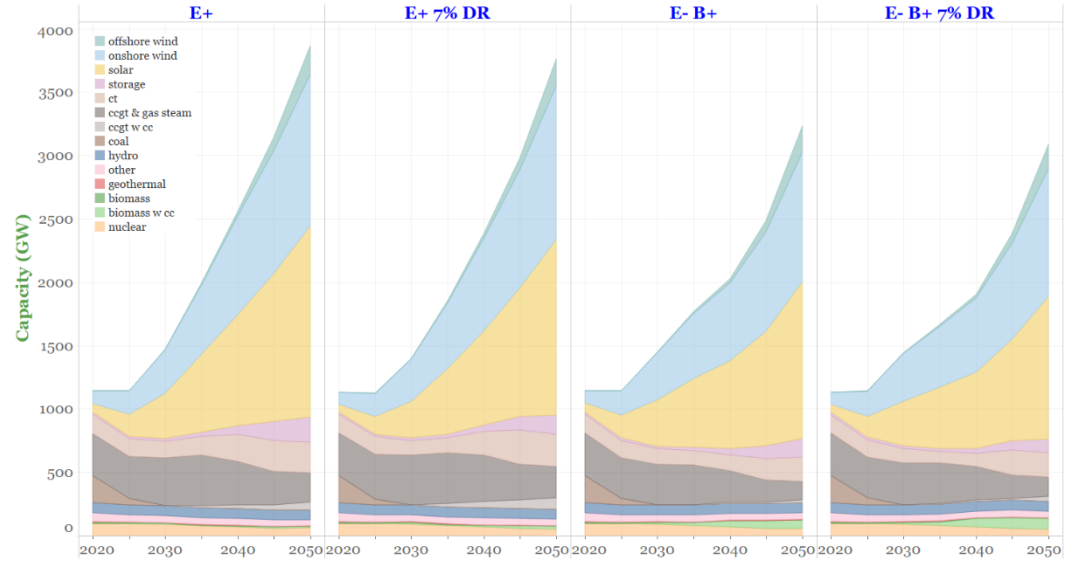

Figure B114. Electricity generating capacity by type of generator.

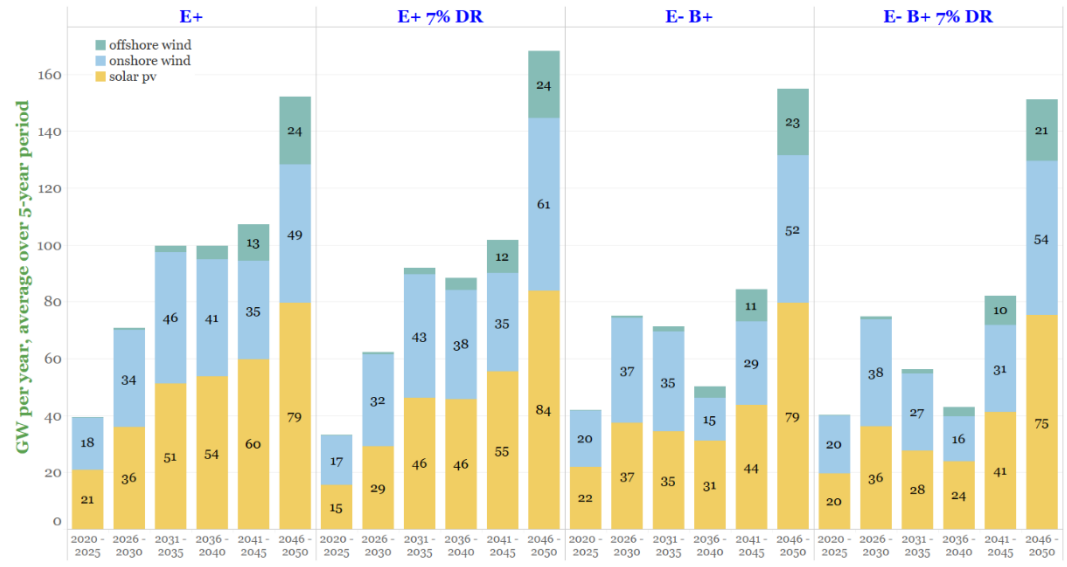

Figure B115. Average annual build rate of solar and wind generating capacity during each five-year period from 2020 through 2050.

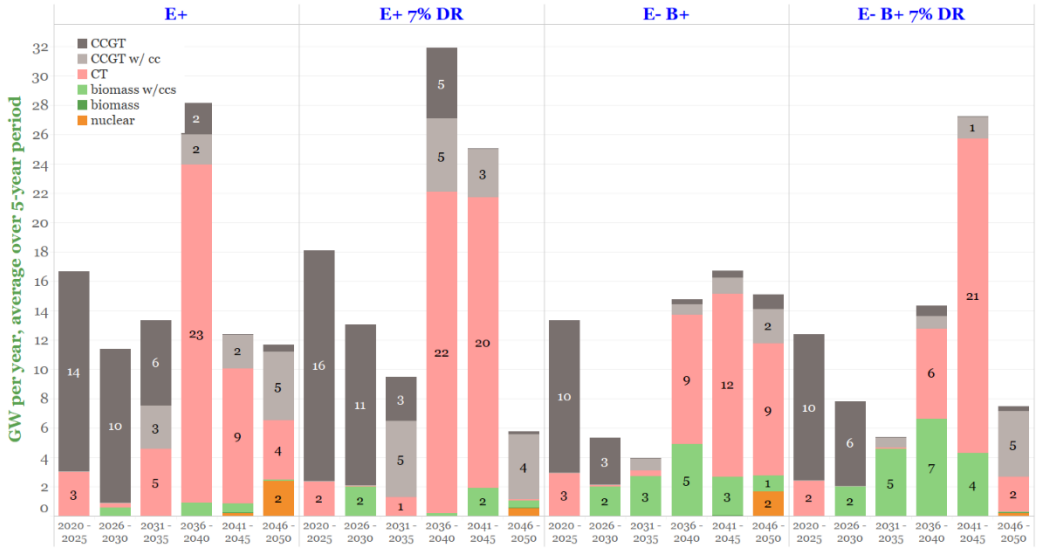

Figure B116. Average annual build rates for dispatchable thermal generating capacity during each five-year period from 2020 through 2050.

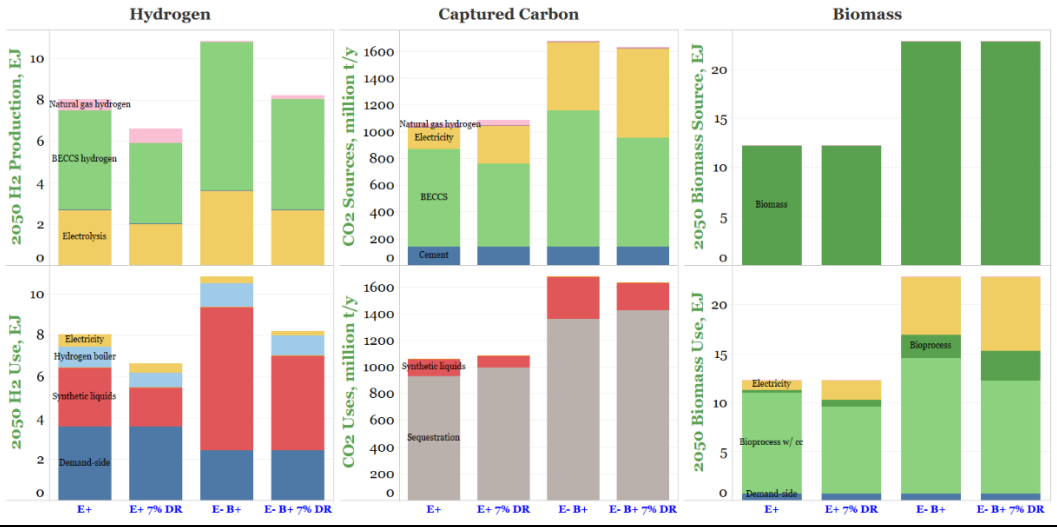

Figure B117. Production (top) and use (bottom) of hydrogen, captured carbon and biomass in 2050.

3.16 No CCUS

To more fully assess the role of carbon capture, utilization and storage, an attempt was made to run a sensitivity case in which no capture, utilization, or geologic storage of CO_2 is allowed ("E+NoCCUS"). No feasible solution was obtained, which suggests that to achieve net-zero emissions economy wide will require some level of CO_2 capture and utilization. CO_2 storage is not necessarily essential, however, as the E+RE+ case demonstrates.

A simple calculation helps illuminate why we obtained no feasible solution for the E+NoCCUS case. Recall that in each of our five core scenarios, net-zero emissions economy wide is achieved when the energy/industrial system contributes negative 170 million tCO_2/y in 2050 to offset residual positive emissions after non-CO_2 emissions and the land sink have been considered. With no CO_2 capture, utilization, or geologic storage allowed, the only way for the energy/industrial system to achieve net-negative emissions is by converting biomass into chemical feedstocks, such as LPG or naphtha, that are then used to make plastics or other long-

lived carbon-containing products. The carbon accounting in our model assumes that the carbon in such long-lived products is permanently sequestered. (Note that chemical feedstocks can also be derived from petroleum or natural gas, but only when made from biomass will carbon storage in long-lived products provide negative emissions.)

Since no combustion of petroleum products or of natural gas would be permissible in 2050 in E+NoCCUS, any liquid or gaseous fuel demand would need to be provided by a carbon-neutral source, e.g., hydrogen made by electrolysis or by biomass gasification. For liquid fuels, the only options available in the model in an E+NoCCUS scenario would be biomass-derived Fischer-Tropsch fuel (BioFT) or biomass pyrolysis liquid products (BioPyr). Total final-energy demand for liquid fuels (LPG, petrochemical feedstocks, gasoline, diesel, jet fuel) in 2050 in the E+ scenario is 12 EJ. If this liquid fuel demand were to be met exclusively using BioFT, a biomass input of 18 EJ would be required (with the energy efficiency for BioFT technology assumed in our model). If the liquid fuel demand were to be met entirely using BioPyr, 23 EJ of biomass input would be required (with the BioPyr technology performance assumed in our model). See Table B19. Since the maximum amount of biomass available to the energy/industrial system in E+NoCCUS is 13 EJ (as in the E+ scenario), one may conclude that there is no feasible solution for the E+NoCCUS case. If additional biomass were available (e.g., as in E+B+, where 23 EJ of biomass are available), it is conceivable that a no CCUS case would be feasible. We did not run such a sensitivity case.

Table B19. Biomass required to meet total liquid fuel demand in 2050 E+, if all the demand were met using one or the other of the two technology options in the model for liquids production from biomass without CO_2 capture.

	Biomass pyrolysis		Biomass to Fischer-Tropsch liquids	
2050 E+ liquid fuel demands (EJ)	Efficiency ($EJ_{bio}/EJ_{product}$)	Biomass needed to make 12 EJ product	Efficincy ($EJ_{bio}/EJ_{product}$)	Biomass needed to make 12 EJ product
12	1.54	18	1.96	23

In addition, our E+ scenario assumes that most of the significant amount of CO_2 generated by cement production would be captured. With no CO_2 capture allowed in E+NoCCUS, the only way to mitigate these emissions would be to deploy entirely new ways to produce cement at scale that involve no CO_2 emissions, or to off-shore US cement production.

4 References

1. P.J. Levi, S.D. Kurland, M. Carbajales-Dale, J.P. Weyant, A.R. Brandt, and S.M. Benson, "Macro-Energy Systems: Toward a New Discipline," *Joule*, 3(10): 2282-2286, 2019. https://doi.org/10.1016/j.joule.2019.07.017
2. R. Jones and B. Haley, "Net-Zero America by 2050, Technical Supplement," Annex A.2 (June 2020) of *Net Zero America: Potential pathways, infrastructure, and impacts*, Dec. 15, 2020.
3. R. Duke, "Non-CO2 Emissions Trends and Abatement Potential," Annex O (December 2020) of *Net Zero America: Potential pathways, infrastructure, and impacts*, Dec. 15, 2020.
4. Anon., *United States Mid-Century Strategy for Deep Decarbonization*, The Whitehouse, Washington, DC, November 2016.
5. A. Swan, K. Paustian, E. Baik, and E.D. Larson, "Potential for Negative Emissions from Carbon Sequestration on US Agricultural Land," Annex Q (January 2021) of *Net Zero America: Potential pathways, infrastructure, and impacts*, Dec. 15, 2020.

6. R. Birdsey, "Past and Prospective Changes in the Net CO2 Flux of U.S. Forests," Annex P (January 2021) of *Net Zero America: Potential pathways, infrastructure, and impacts*, Dec. 15, 2020.
7. Energy Information Administration, *Annual Energy Outlook 2020*, 2020.
8. National Renewable Energy Laboratory, *Annual Technology Baseline*, 2019.
9. AACE International, *Recommended Practice No. 18R-97: Cost Estimate Classification System - As Applied in Engineering, Procurement, and Construction for the Process Industries*, 7 August 2020.
10. Ingersoll, E., Gogan, K. and Locatelli, G., "Managing Drivers of Cost in the Construction of Nuclear Plants," *The Bridge*, 50(3): 32-37, 2020. ISSN 0737-6278
11. Energy Information Administration, "Nuclear Explained: U.S. nuclear industry," (accessed 29 April 2021).
12. Patel, S., "High-Volume Hydrogen Gas Turbines Take Shape," *Power Magazine*, 1 May 2019 (accessed 9 April 2021).
13. E.D. Larson, "Hydrogen and synthetic fuels transition," Annex L (April 2021) of *Net Zero America: Potential pathways, infrastructure, and impacts*, Dec. 15, 2020.
14. The Hydrogen Council, *A Perspective on Hydrogen Investment, Development, and Cost Competitiveness*, 2021. (PDF accessed online 29 March 2021.)
15. Bloomberg New Energy Finance, *Hydrogen Economy Outlook*, March 30, 2020.
16. N. McQueen, M.J. Desmond, R.H. Socolow, P. Psarras, and J. Wilcox, "Natural Gas vs. Electricity for Solvent-Based Direct Air Capture," *Frontiers in Climate*, 27 January 2021.
17. Report Committee, *Direct Air Capture of CO2 with Chemicals: a Technology Assessment*," prepared for the American Physical Society Panel on Public Affairs, 1 June 2011.
18. D.W. Keith, G. Holmes, D. St. Angelo, and K. Heidel, "A Process for Capturing CO_2 from the Atmosphere," *Joule*, 2: 1573–1594, 15 August 2018.
19. R. Socolow (Professor Emeritus, Mechanical and Aerospace Engineering Dept., Princeton University), personal communication, 24 August 2020.
20. Energy Information Administration, *Annual Energy Outlook 2019*, 2019.
21. Energy Information Administration, Industrial Sector Energy Consumption, *Monthly Energy Review*, release date 27 April 2020.
22. Bureau of Economic Analysis, Gross Output by Industry, U.S. Department of Commerce, release date 29 October 2019.
23. C. Zhang, J. Drossman, and E.D. Larson, "Transport and Buildings Sector Transitions," Annex C of *Net Zero America: Potential pathways, infrastructure, and impacts*, August, 2020.
24. E. Baik and E.D. Larson, "Bioenergy supply transition analysis," Annex H (March 2021) of *Net Zero America: Potential pathways, infrastructure, and impacts*, Dec. 15, 2020.
25. U.S. Department of Energy, 2016 Billion-Ton Report: Advancing Domestic Resources for a Thriving Bioeconomy, Vol. 1: Economic Availability of Feedstocks. M.H. Langholtz, B.J. Stokes, and L.M. Eaton (Leads), ORNL/TM-2016/160, Oak Ridge National Laboratory, Oak Ridge, TN, 2016.